universität wien

DIPLOMARBEIT

Titel der Diplomarbeit

„Analyses of the Microdiversity and Physiology of Nitrite-Oxidizing Bacteria in the Genus *Nitrospira*"

Verfasser

Domenico Franco Savio

angestrebter akademischer Grad

Magister der Naturwissenschaften (Mag.rer.nat.)

Wien, 2011

A. Introduction 1

B. Material and Methods 14

Table of contents

A. <u>Introduction</u>

A.1. The role of archaea and bacteria in the biogeochemical nitrogen cycle

The element nitrogen (N) is formed during natural nuclear fusion in suns and is one of the most abundant elements in the universe. On earth, it constitutes the major portion of the atmosphere with 78% by volume. This elemental nitrogen (N_2) is very inert despite it is one of the most electronegative elements besides noble gases, oxygen and fluorine. The reason for that is the very stable intramolecular triple bond between the two nitrogen atoms.

Bound in organic molecules, it appears in the form of nucleic acids, proteins and vitamins and is therefore of enormous importance to all organisms. In the human body, it is the most abundant element after carbon (C), hydrogen (H) and oxygen (O). On average, it accounts for 6.25% of the dry mass of all organisms (Bothe *et al.*, 2007). Thereby, its oxidation state ranges from +5 in nitrate (NO_3^-) to -3 in ammonia (NH_3).

In nature, the conversion of these inorganic compounds is controlled by a reaction cycle called the biogeochemical nitrogen cycle (Bothe *et al.*, 2007). Of particular importance for most steps of the conversion between these states are archaea and bacteria. For instance, nitrogen fixation and anaerobic ammonium oxidation (ANAMMOX) are carried out exclusively by these organisms. The biogeochemical nitrogen cycle is shown in Figure 1.

For a long time, our knowledge of the microbial nitrogen cycle was based on studies from Beijerinck, Winogradsky, Gayon and Dupetit at the end of the 19th century (Beijerinck, 1888; Winogradsky, 1890; Gayon and Dupetit, 1886). But particularly in the last decade new aspects were revealed.
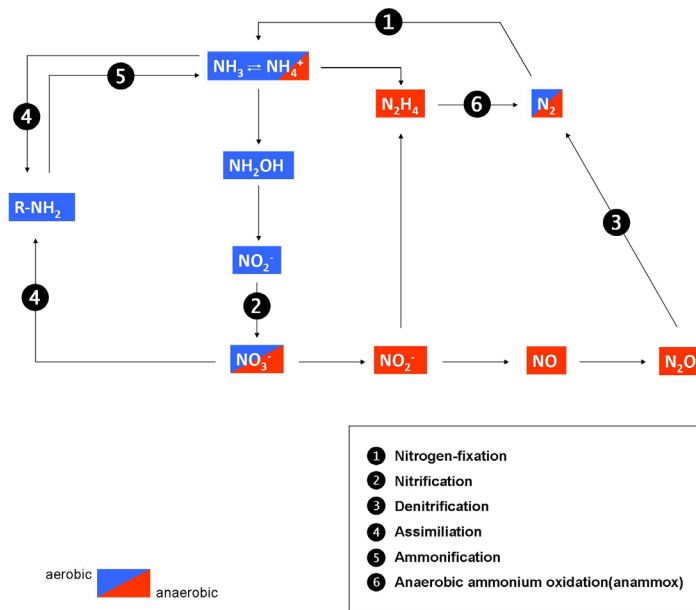
Figure 1: The biogeochemical nitrogen cycle.

The first step of the nitrogen cycle (Figure 1) is the nitrogen fixation which is carried out exclusively by archaea and bacteria (Cabello *et al.,* 2004). Thereby, the inert elemental nitrogen is fixed and reduced to bioavailable ammonia (NH_3). In this state it can be exploited as nitrogen source by many organisms of all domains of life (Kneip *et al.,* 2007; Zehr *et al.,* 2000). During the nitrification process, ammonia or ammonium (NH_4^+) are oxidized via nitrite (NO_2^-) to nitrate (NO_3^-). This two-step process is performed by ammonia-oxidizing archaea (AOA) and bacteria (AOB) which oxidize ammonia or ammonium to nitrite - the rate-limiting step - and by nitrite-oxidizing bacteria (NOB) performing the oxidation of nitrite to nitrate (Könneke *et al.,* 2005; Bock and Wagner, 2001). In these two steps, the respective reduced inorganic nitrogen compound serves as electron donor being the major source of energy, and oxygen (O_2) serves as electron acceptor. In combination with autotrophic fixation of CO_2 this lifestyle is called chemo-lithoautotrophic (Bock and Wagner, 2001). To date, no organism capable of performing ammonia and nitrite oxidation is known.

In the denitrification process, nitrate is reduced to nitrite, nitric oxide (NO) and further via nitrous oxide (N_2O) to atmospheric nitrogen gas (Hayatsu *et al.,* 2008; Cabello *et al.,* 2004). In this stepwise reduction the respective nitrogen compounds serve as electron acceptor under anoxic conditions. Thereby, denitrification is assumed to be one of the major sources of the greenhouse gases nitric and nitrous oxide that are emitted to the atmosphere (Jetten *et al.,* 2008).

Nitrification and denitrification processes have been known for a long time. Only recently, in the year 1999, the process of anaerobic ammonia oxidation (ANAMMOX) was confirmed (Strous *et al.,* 1999). This step of the nitrogen cycle had previously been predicted based on energy calculations (Broda, 1977). Thereby, ammonium is oxidized under anoxic conditions via hydrazine (N_2H_4) using nitrite as electron acceptor. The end product of this energy gaining reaction is elemental nitrogen. All organisms identified to date to be capable of performing this process belong to the phylum *Planctomycetes* (Jetten *et al.,* 2008, Strous *et al.,* 1999).

A.2. Nitrifying microorganisms

Ammonia- and nitrite-oxidizing microorganisms often inhabit the same environments. There, different strains of ammonia-oxidizing bacteria (AOB), ammonia-oxidizing archaea (AOA) and nitrite-oxidizing bacteria (NOB) fill different niches depending on the concentration of ammonia and nitrite, respectively (Schramm *et al.,* 1999; Maixner *et al.,* 2006). Besides these compounds also physiological claims in relation to temperature, pH, oxygen concentration and salinity are influencing the choice of the habitat (Alawi *et al.,* 2007, Santoro *et al.,* 2008; Nicol *et al.,* 2008; Erguder *et al.,* 2009).

A.2.1. Ammonia oxidation

The aerobic oxidation of ammonia to nitrite by AOB is a two-step process with the intermediate compound hydroxylamine (NH_2OH). The chemical reactions of this two-step oxidation are shown in Figure 2. Thereby, the oxidation of ammonia to hydroxylamine is catalyzed by the enzyme ammonia monooxygenase (AMO). The oxidation of hydroxylamine to nitrite is carried out by the enzyme hydroxylamine oxidoreductase (HAO) (Olson and Hooper, 1983; Bock and Wagner, 2006).

$$\text{AMO}$$
$$NH_3 + O_2 + 2H^+ + 2e^- \longrightarrow NH_2OH + H_2O$$

$$\text{HAO}$$
$$NH_2OH + H_2O \longrightarrow HNO_2 + 4H^+ + 4e^-$$
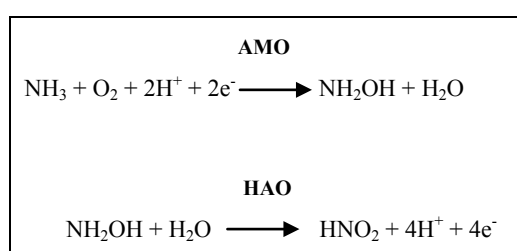
Figure 2: Chemical reactions in biological ammonia-oxidation.

A.2.1.1. Ammonia-oxidizing bacteria (AOB)

Until the year 2005, it was believed that the oxidation of ammonia to nitrite by autotrophic microbes is exclusively performed by aerobic bacteria, the so-called ammonia-oxidizing bacteria (AOB) (Jetten *et al.,* 2008). All yet known genera of AOB (*Nitrosomonas, Nitrosococcus, Nitrosospira, Nitrosovibrio* and *Nitrosolobus*) - characterized by the prefix "*Nitroso-*" - are aerobic chemolithoautotrophic beta- and gammaproteobacteria (Purkhold *et al.*, 2000; Bock and Wagner, *2006;* Bock *et al., 1991*). A common property of all AOB yet known have is their slow growth rate. For example, the maximum growth rate for *Nitrosomonas* in laboratory experiments was 1.7 d^{-1} (Bock *et al.,* 1990; Bock and Wagner, 2006).

A.2.1.2. Ammonia-oxidizing archaea (AOA)

With the isolation of the archaeon "*Candidatus* Nitrosopumilus maritimus" it was shown that aerobic ammonia oxidation is not exclusively performed by bacteria (Könneke *et al.,* 2005). AOA grow chemolithoautotrophically and oxidize ammonia to nitrite. Since this finding, many environments have been screened for the presence of AOA by detecting the alpha-subunit of the putative archaeal ammonia monooxygenase gene (*amo*) *amo*A. The results of these studies suggest that AOA are of enormous importance in the biogeochemical nitrogen cycle since the putative archaeal *amo* genes were found to be more abundant than bacterial *amo* genes in many marine and terrestrial environments (Francis *et al.,* 2005; Leininger *et al.*, 2006; Zhang *et al.*, 2008). A newly-proposed phylum of the archaea, namely Thaumarchaeota, contains species capable of living chemolithoautotrophically by oxidizing ammonia. Cultured representatives are the four species *Nitrosopumilus maritimius*, *Crenarchaeum symbiosum*, *Nitrososphaera gargesis* and *Nitrososphaera viennensis* (Brochier-Armanet *et al.*, 2008; Spang *et al.*, 2010; Tourna *et al.*, 2011).

A.2.2. Nitrite oxidation

The oxidation of nitrite to nitrate is catalyzed by the enzyme nitrite oxidoreductase (Nxr). This enzyme was shown to also be capable of performing the reverse step, the reduction of nitrate to nitrite (Bock and Wagner, 2006; Sundermeyer-Klinger *et al.,* 1984). The chemical reactions for the oxidation of nitrite are cited in Figure 3.

$$NO_2^- + H_2O \longrightarrow NO_3^- + 2H^+ + 2e^-$$

$$2H^+ + 2e^- + \tfrac{1}{2} O_2 \longrightarrow H_2O$$
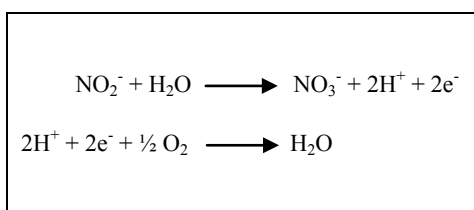
Figure 3: Chemical reactions in biological nitrite-oxidation catalyzed by the nitrite oxidoreductase (Nxr).

A.2.2.1. Nitrite oxidizing bacteria (NOB)

Nitrite oxidizing bacteria (NOB) have a chemolithoautotrophic lifestyle. Thereby, they gain energy by oxidizing the respective reduced nitrogen compound by using O_2 as electron-acceptor. Carbon for the assimilation of organic compounds is provided by fixed CO_2. In their name all NOB include the prefix "*Nitro-*". So far, organisms belonging to only a handful of genera are capable of performing nitrite oxidation. Their phylogenetic affiliation however is diverse. They belong to different subclasses of the phylum *Proteobacteria* as well as to the phyla *Nitrospirae* and *Chloroflexi*. These known genera are namely *Nitrobacter, Nitrococcus, Nitrospina, Nitrotoga, Nitrolancetus* (Teske *et al.,* 1994; Alawi *et al.,* 2007; Sorokin *et al*., unpublished) and *Nitrospira* (Ehrich *et al.,* 1995). All known NOB are highly fastidious concerning their demands on the environment and grow very slowly (Alawi *et al*., 2007).

A.3. The genus *Nitrospira*

The first member of this genus belonging to the phylum *Nitrospirae* was described in the year 1986 with *Nitrospira marina* (Watson *et al.,* 1986). To date, only four species of this genus, namely *Nitrospira marina*, *Nitrospira moscoviensis*, "*Candidatus* Nitrospira bockiana" and very recently *Nitrospira calida* could be cultivated in pure culture (Watson *et al*., 1986; Ehrich *et al.,* 1995; Lebedeva *et al.,* 2008). One further species affiliated to this genus - namely "*Candidatus* Nitrospira defluvii" (*Ca*. N. defluvii) - was isolated from activated sludge and is highly enriched up to 90% (Spieck *et al.,* 2006). One reason for the low number of cultivated members of this genus lies in the difficulties of cultivation. These are their very slow growth on the one hand and for such members growing in colonies the difficulty to separate *Nitrospira* cells from other NOB and heterotrophic contaminants on the other hand (Spieck *et al.,* 2006, Lebedeva *et al.,* 2008). For a long time, little was known about the diversity and environmental distribution of this ge-

nus due to these difficulties in cultivation. A lot of new information concerning the genus *Nitrospira* was revealed with the rise of cultivation-independent molecular methods including the "rRNA approach" (Amann *et al.,* 1995). Members of this genus could be detected in a variety of natural habitats as well as in activated sludge and biofilm samples (Daims *et al.,* 2001, Holmes *et al.,* 2001, Hentschel *et al.,* 2002). Based on these data the genus *Nitrospira* currently is subdivided into six sublineages. The affiliation to a sublineage is based on at least 94.9% sequence identity of two 16S rRNA sequences. The 16S rRNA sequence-similarity of members of different sublineages always has to be below 94% (Daims *et al.,* 2001a). Table 1 shows a list of the six sublineages plus some additional information.

Table 1: Known sublineages of the genus *Nitrospira*.

Sublineage	Isolate or enrichment	Occurrence	Reference(s)
I	*Ca*. N. defluvii	Nitrifying sewage treatment systems	Spieck *et al.,* 2006
II	*Nitrospira moscoviensis*	Wastewater treatment plants (WWTPs), soils, rhizosphere samples, freshwater habitats, drinking water distribution systems, groundwater	Ehrich *et al.,* 1995
III	16S rRNA clones	Nullarbor cave system (Australia)	Holmes *et al.,* 2001
IV	*Nitrospira marina*	Halophilic and marine habitats - planktonic as well as sediments, symbionts of marine sponges	Watson *et al.,* 1986, Hentschel *et al.,* 2002
V	"*Ca.* Nitrospira bockiana"	Urban heating system of Moscow	Lebedeva *et al.,* 2008
VI	*Nitrospira calida*	Garga hot springs	Lebedeva *et al*., 2011

It was shown that members of *Nitrospira* sublineage I are of great importance in wastewater treatment systems since they usually account for 1 to 20% of all detectable bacteria (Daims *et al.,* 2001; Juretschko *et al.,* 1998; Okabe *et al.,* 1999; Müller, 2008). Besides this sublineage, also members of sublineage II of the genus *Nitrospira* are of great importance in wastewater treatment plants (WWTPs) (Maixner *et al*., 2006; Müller, 2008).

Besides the classification of the genus *Nitrospira* in sublineages, a recent study revealed a high microdiversity within this genus (Dorninger *et al*., unpublished). This refers especially to sublineage II of the genus *Nitrospira* and was uncovered by phylogenetic analysis of *Nitrospira* 16S rRNA gene sequences retrieved from the WWTP of the University of Veterinary Medicine Vienna (Vetmed) (Figure 4). Thereby, the co-occurrence of three subpopulations of *Nitrospira* sublineage II (framed red in Figure 4) could be demonstrated by the use of FISH probes specific for each cluster. The abundances of these clusters were analyzed in a semi-quantitative way in samples taken during a six-year period. The obtained results of this study are shown in Table 2.
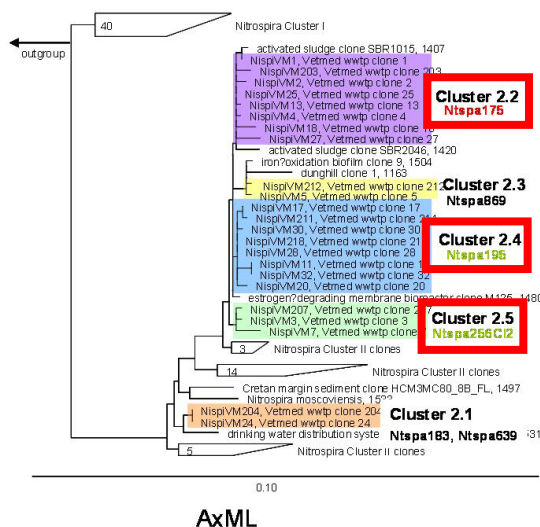
Figure 4: Phylogenetic tree of the subpopulations of *Nitrospira* sublineage II (kindly provided by Christiane Dorninger (Dorninger *et al*., unpublished). Framed in red boxes are those subpopulations (clusters) that were examined semi-quantitatively using FISH.

Table 2: Microdiversity in sublineage II of the genus *Nitrospira* in the WWTP of the University of Veterinary Medicine Vienna (Dorninger *et al*., unpublished).

Sampling date	subpopulation		
	Cluster 2.4	Cluster 2.5	Cluster 2.2
2004-03-04	+	+	++
2004-04-15	++	+++	++
2004-07-13	+	+++	++
2007-05-14	++	++	++
2007-06-28	++	++	++
2008-11-17	+++	++	+
2009-02-03	+++	++	+
2009-10-07	+++	+	-
2010-07-02	+++	+	+

+ few colonies detectable
++ some colonies detectable
+++ many colonies detectable

A.3.1. *Nitrospira* in wastewater treatment plants (WWTPs)

Before the advent of cultivation-independent methods for the detection of microorganisms in environmental samples like the "rRNA approach" (Amann *et al*., 1995), it was believed that species of the genus *Nitrobacter* are mainly responsible for the oxidation of nitrite to nitrate in WWTPs (Coskuner and Curtis, 2002). This assumption was based on studies applying classical methods for investigating microbial communities in activated sludge. However, FISH with rRNA-targeted probes revealed that uncultured *Nitrospira* are highly abundant in sewage treatment systems (Müller, 2008; Daims *et al*., 2001a; Juretschko *et al*., 1998). The dominance of *Nitrospira* in comparison to *Nitrobacter* is due to a better adaptation of *Nitrospira* to the prevailing conditions in WWTPs.

For example, a study with nitrifying biofilms showed that bacteria belonging to the genus *Nitrospira* have a much higher affinity for nitrite compared to cells of the genus *Nitrobacter* (Schramm *et al.,* 1999). Thus, they could be assigned to a K-strategy (Nogueira and Melo, 2006; Andrews *et al.,* 1986). Members of the genus *Nitrobacter* as proposed r-strategists are assumed to need higher nitrite-concentrations (Hunik *et al*., 1993; Prosser, 1989; Andrews *et al.,* 1986).

Differences in the nitrite-affinity between these two genera could also be supported by differences in the localization and orientation of the putative Nxr enzymes in the cell membrane which were extracted from *Nitrobacter* as well as from *Nitrospira moscoviensis* (Spieck *et al.*, 1998). But also a coexistence of these two genera was observed at a certain nitrite-concentration (Bartosch *et al.,* 2002). And also within the genus *Nitrospira* there might be different preferences of different sublineages with respect to their preferred nitrite concentrations. This was shown in a study where two different *Nitrospira* sublineages were examined *in situ*. It was hypothesized that sublineage I prefers higher nitrite concentrations compared to sublineage II, an assumption based on the distances in which these bacteria occur to AOB (Maixner *et al.,* 2006).

However, not only nitrite is determining the occurrence of *Nitrospira* in sewage treatment plants, since there are many other factors affecting the appearance of organisms in certain habitats. For example, the dissolved oxygen concentration can also be a selecting factor, as it was shown in two studies that members of *Nitrospira* dominated cells of the genus *Nitrobacter* when the dissolved oxygen concentration was low (Downing and Nerenberg 2008, Schramm *et al.,* 2000). And again, also for different sublineages of the genus *Nitrospira* differences in terms of preferred oxygen concentrations have been observed. It was shown that sublineage I can deal with lower dissolved oxygen concentrations than sublineage II either due to a higher oxygen affinity or a lower oxygen tolerance of this sublineage (Park and Noguera, 2008). Another factor which might affect the growth of NOB in WWTPs is the abundance and composition of organic compounds.

A.3.2. Nitrite oxidoreductase (Nxr) - key enzyme for energy generation

The nitrite oxidorecductase (Nxr) is the key enzyme responsible for the oxidation of nitrite in chemolithoautotrophic, nitrite-oxidizing bacteria. This enzyme belongs to the DMSO reductase family of molybdopterin-containing enzymes (Lücker *et al.,* 2010). As the name suggests, this enzyme is also capable of performing the reverse step, the reduction of nitrate to nitrite, as shown for the Nxr of *Nitrobacter* (Sundermeyer-Klinger *et al.,* 1984).

The Nxr is built up by at least two subunits - the alpha and beta subunit - where the alpha subunit contains the substrate-binding site and the molybdopterin cofactor (Meincke *et al.,* 1992; Sundermeyer-Klinger *et al.,* 1984). The beta subunit is assumed to perform tasks in the electron transport (Kirstein *et al.,* 1993). *Ca.* N. defluvii contains two copies of the *nxrAB* cluster in its

genome. The same applies to *Nitrobacter winogradskyi* also containing two copies of these two genes (Starkenburg *et al.*, 2006). *Nitrospira moscoviensis*, in contrast, encodes three copies of the *nxr*A subunit (Koch, 2009, unpublished). In *Ca*. N. defluvii, the alpha subunits were shown to be similar to 86.6% on amino acid level while the beta subunits are identical to 100% on amino acid level. The difference between the two predicted alpha subunits could be due to differences in the substrate affinity or specificity. Concerning the expression of these two paralogous *nxrA* genes a former study with biomass from the main WWTP Vienna showed that only the *nxrA2* gene was expressed (Koch, 2009, unpublished). This was examined using RT-PCR. Whether the *nxrA1* gene perhaps is expressed under different environmental conditions is not known yet.

Besides the alpha and beta subunits, for *Ca*. N. defluvii there were four candidates for a putative gamma subunit found with an amino acid identity between 27 to 33%. The gamma subunit could serve as a membrane-anchor for the holoenzyme and channel electrons from the beta subunit to the electron chain as shown for other enzymes of the DMSO reductase family (Lücker *et al.,* 2010).

The biochemistry of Nxr was mainly described on the basis of the Nxr of *Nitrobacter spp*. However, there are differences in the overall arrangement of this enzyme concerning its localization in *Nitrospira* compared to *Nitrobacter*. In comparison to *Nitrobacter*, the Nxr in *Nitrospira* is located on the outer side of the cell membrane reaching into the periplasm and is not located on the cytoplasmic side (Spieck *et al.,* 1996 and 1998). In *Nitrobacter* cells, the oxidation of nitrite is performed on the cytoplasmic side, which requires a transport of nitrite into the cytoplasma. This leads to an enrichment of nitrate within the cell which has to be removed. For *Nitrospira moscoviensis* it was detected immunocytochemically that the Nxr is located on the periplasmic side of the inner cell membrane (Spieck *et al.*, 1998). This is also supposed for *Ca*. N. defluvii since the *nxrA1* as well as *nxrA2* genes contain a motif for the twin-arginine protein translocation (Tat) pathway. All putative *nxrC*-candidates indeed encode a signal peptide for the Sec-pathway while for the *nxrB* subunits a "hitchhiker" mechanism is assumed because signal peptides are missing (Lücker *et al.,* 2010).

The proposed perpilasmic orientation of the Nxr of *Nitrospira* on the basis of biochemical as well as genomic data has two advantages for the organism. On the one hand there is no need for nitrite and nitrate transporters to import nitrite and remove nitrate from the cell which could ac-

cumulate and lead to toxification. On the other hand, the release of protons in the periplasm owing to nitrite oxidation and the concomitant proton-consuming reduction of oxygen in the cytoplasm contribute to the membrane potential and should therefore be advantageous to *Ca*. N. defluvii (Lücker *et al*., 2010).

Electrons from the electron donor nitrite are supposed to be transferred to a cytochrome (cyt.) c and further to a terminal cyt. c oxidase (Lücker *et al*., 2010). The terminal oxidase in *Nitrobacter* belongs to the aa3 type (Starkenburg *et al*., 2008). For *Ca*. N. defluvii indeed no terminal oxidase of the a-type is supposed based on genomic data. Instead, four putative "cyt. bd-like oxidases" are encoded that could transfer electrons from cyt. c to oxygen (Lücker *et al*., 2010).

The regulation of the expression of the two *nxrAB* clusters seems to be different according to genomic data. The *nxrA2B2* expression might be regulated by a two-component signaling system since the gene upstream of the *nxrA2* gene encodes a sigma-54-dependent transcriptional regulator with a CheY-like response regulator receiver region. The sigma-54 dependent transcriptional regulator upstream the cluster *nxrA1B1*, however, differs from the one of *nxrA2B2* (Daims et al., 2010).

Another important property of the Nxr is that it can also perform the reduction of nitrate to nitrite. This was shown for the Nxr of *Nitrobacter hamburgensis* in a former study (Sundermeyer-Klinger *et al.,* 1984). There, reduced methyl- and benzylviologen as well as $NADH^+$ were shown to be suitable electron donors for the Nxr to reduce nitrate. Thus, this enzyme can also play a role in the denitrification process.

A.3.3. Utilization of organic substrates

In general, there are two ways to utilize organic substrates: On the one hand, the use as carbon source and, on the other hand, the use as energy source. *Nitrospira marina* was shown to achieve higher growth yields when pyruvate was present (Watson *et al.,* 1986). Another study showed that uncultered *Nitrospira* in activated sludge assimiliated pyruvate in addition to inorganic carbon under oxic conditions (Daims *et al.,* 2001). Based on this study, *Nitrospira* is assumed to be capable of living mixotrophically - i.e. it incorporates inorganic and organic carbon sources simultaneously. This in turn could facilitate the competitiveness of this genus in sewage treatment plants. For *Ca.* N. defluvii, the possible capability of assimilating organic carbon from

pyurvate and some other simple carbon compounds is also supported by genomic data (Lücker *et al.*, 2010). In the recently published genome of *Ca*. N. defluvii, the complete Embden-Meyerhof-Parnas pathway for the metabolization of hexose sugars, as well as pathways for the catabolic degradation and assimilation of acetate, pyruvate and formate are present. Furthermore, candidate genes for the degradation of branched amino acids were found as well as genes encoding sugar transporters for the utilization of sugars.

Additionally, all enzymes for the oxidative tricarboxylic acid cycle (oTCA) with the exception of the 2-oxoglutarate dehydrogenase complex (ODH) have been encoded. This missing enzyme could theoretically be replaced by the 2-oxoglutarate:ferredoxin oxidoreductase (OGOR). If all these genes were functional, *Ca*. N. defluvii could at least benefit from a mixotrophic lifestyle (Lücker *et al.*, 2010). But still, it is unknown whether bacteria of the genus *Nitrospira* are capable of using organic compounds as energy source.

A.4. Aims of this study

A.4.1. Development of quantitative real-time PCR assays for the detection of the expression of various genes in "*Candidatus* Nitrospira defluvii"

The existence of a sequenced genome of an organism provides lots of interesting information. This in turn raises new questions as, for example, which genes are actually transcribed and which ones are further translated to proteins. The aim of this part of this thesis was to investigate the differences in the expression of several genes of *Ca*. N. defluvii under different environmental conditions. Therefore, assays for the reverse transcription (RT) of mRNA/rRNA and subsequent quantification via qPCR should be developed. The method of combining reverse transcription (RT) and quantitative real-time PCR (qPCR), in the following referred to as RT-qPCR, is a very sensitive tool for this purpose (Nolan *et al.*, 2006). In detail, assays should be developed for the detection of the two paralogous *nxrA* gene copies as well as for the detection of the expression of the *gltA* gene encoding the enzyme citrate synthase. This enzyme is essential and indicative for the oTCA-cycle. In order to normalize the measured expression level of the previously mentioned genes, a fourth qPCR assay should be developed for the expression of the 16S rRNA gene. Since the 16S rRNA is assumed to be stable in its abundance in *Ca*. N. defluvii, its copy number is an indicator for the cell number. This method for normalization was chosen since it is not possible to determine the cell number by simple cell counting due to growth in colonies.

A.4.2. Detection of a possible nitrite-regulated expression of two paralogous copies of the nitrite oxidoreductase enzyme genes

Although members of the genus *Nitrospira* play a significant role in most natural and engineered ecosystems, very little is known about their nitrite oxidizing system. This study was designed to investigate a possible regulation of the expression of the *nxr*A genes by the concentration of the encoded enzyme's substrate. Therefore, *Ca*. N. defluvii cultures should be incubated under different nitrite-concentrations and be examined by the developed RT-qPCR assays for two paralogous of the *nxr*A genes.

A.4.3. Exploration of a possible nitrate reducing activity coupled to organic compound oxidation by "*Candidatus* Nitrospira defluvii"

The Nxr of *Nitrobacter* was shown to be also capable of performing the reduction of nitrate to nitrite (Sundermeyer-Klinger *et al.,* 1984). Therefore, *Ca*. N. defluvii may be able to couple the oxidation of organic compounds to nitrate reduction for energy generation, presumably under oxygen depletion. To date, it is not known yet if *Ca*. N. defluvii can utilize organic compounds for the generation of energy. Therefore, not only the use of nitrate as electron acceptor is uncertain, one also has to find a compatible electron donor which might be used by this organism. For this purpose, pyruvate was chosen since it was shown that uncultured *Nitrospira* in activated sludge were at least capable of assimilating pyruvate (Daims *et al.*, 2001). The choice of pyruvate in this context is moreover obvious since it is not only an energy source for aerobic organisms using the oTCA cycle, but also for some anaerobic organisms capable of fermenting pyruvate to lactate. After incubating *Ca*. N. defluvii cultures under anoxic conditions with pyruvate and nitrate possible differences in the expression pattern of the two *nxrA* genes should be examined applying the developed qPCR assays. Then, the comparison of the expression pattern with the control incubation without pyruvate and nitrate as well could provide a hint for a nitrate reducing activity of one of the two Nxr copies.

A.4.4. Investigation of the coexistence of three subpopulations of *Nitrospira* sublineage II in the wastewater treatment plant of the University of veterinary medicine Vienna applying quantitative FISH

The microdiversity of *Nitrospira* sublineage II in activated sludge of the WWTP of the Vetmed had been investigated in a recent study (Dorninger *et al*., unpublished). A stable coexistence of three closely related subpopulations of *Nitrospira* sublineage II was demonstrated qualitatively and analyzed in a semi-quantitative way during a six-year period. The aim of this study was to quantify the biovolume fraction of the three subpopulations Cluster 2.2, 2.4 and 2.5 relative to the *Nitrospira* sublineage II population, the total *Nitrospira* population and the total bacterial population.

B. <u>Material and Methods</u>

For the preparation of all buffers, media and solutions double distilled and sterile filtered water (ddH$_2$0) was used. This purification was accomplished by using a MQ Biocel-purification facility. To sterilize high-temperature-stable solutions and equipment a waterevapour-high pressure autoclave was used. The autoclavation step was performed for 20 min. at 121 °C and a pressure of 1.013 x 10^5 Pascal. Unstable chemicals were sterile filtered (0.22 μm) instead and added to the solutions afterwards. All used chemicals were of *p.a.* qualitiy.

B.1. Technical equipment

Table 3: Technical equipment.

Equipment	Company
Bead beater Fast Prep FP 120	Savant Instruments Inc., Holbrook, NY, USA
Centrifuges: Mikro 22 R Rotina 35 S Centrifuge Galaxy Mini Centrifuge Centrifuge 5840 R	Andreas Hettich GmbH & Co. KG, Tuttlingen, Germany Andreas Hettich GmbH & Co. KG, Tuttlingen, Germany VWR international, West Chester, PA, USA Eppendorf AG, Hamburg, Germany
Confocal Laser Scanning Microscope LSM 510 Meta	Carl Zeiss MicroImaging GmbH, Jena, Germany
Devices for gelelectrophoresis: Electrophoresis cell (Sub-Cell GT) Electrophoresis power supply (PowerPac Basic) Sub-Cell GT UV-Transparent Gel Tray (15 x15 cm) Gel Dokumentationsystem MediaSystem FlexiLine 4040	Bio-Rad Laboratories GmbH, Munich, Germany Bio-Rad Laboratories GmbH, Munich, Germany Bio-Rad Laboratories GmbH, Munich, Germany Biostep, Jahnsdorf, Germany
DNA Sequencer Applied Biosystems 3130	Applied Biosystems Lincoln, USA
Hybridisation oven UE-500	Memmert GmbH, Schwabach, Germany
Laminar flow hood Safe 2010 Modell 1.2	Holten, Jouan Nordic, Allerød, Denmark
Microbiological incubator KB 115	Binder GmbH, Tuttlingen, Germany
Microwave MD6460 Microstar	
NanoDrop® ND-1000 UV/Vis spectrophotometer	NanoDrop Technologies Inc., Wilmington, DE, USA

PCR thermocyclers: iCycler iQ Real-Time PCR Detection iCycler IQ Thermocycler	Biorad, München, Germany Biorad, München, Germany
pH-Meter WTW inoLab Level 1	Wissenschaftlich-Technische Werkstätten GmbH, Weilheim, Germany
Eppendorf Research® pipettes 1 – 1000 µl	Eppendorf AG, Hamburg, Germany
Platform shaker Innova 2300	New Brunswick Co., Inc., Madison NJ, USA
Scales: OHAUS® Analytical Plus balance Sartorius BL 3100	Ohaus Corporation, Pine Brook, NJ, USA Sartorius AG, Göttingen, Germany
Transilluminator UST-30M-8E (312 nm)	Biostep GmbH, Jahnsdorf, Germany
Ultraviolet Sterilizing PCR Workstation	Peqlab Biotechnology GmbH, Erlangen, Germany
Variomag® Maxi magnetic stirrer	Variomag®, Dayton Beach, FL, USA
Vortex Genie 2	Scientific Industries, New York, USA
Water purification facility: MQ Biocel	Millipore Corporation, Billerica, MA, USA
Water vapour high pressure autoclaves: Varioklav 135S Varioklav 25T	H+P, München, Germany H+P, München, Germany
Waterbaths: DC10 Thermo GFL Typ 1004	Haake, Karlsruhe, Germany Gesellschaft für Labortechnik GmbH, Burgwedel, Germany

B.2. Expendables

Table 4: List of expendables.

Expendable item	Company
Bead-beating-caps	
Cover glasses 24 x 60 mm	Paul Marienfeld GmbH & Co. KG, Lauda-Königshofen, Germany
Cover slips 24×50 mm	Paul Marienfeld GmbH & Co. KG, Lauda-Königshofen, Germany
Eppendorf reaction tubes (ERT), various sizes	Eppendorf AG, Hamburg, Germany
Greiner tubes (15 ml, 50 ml)	Greiner Bio-One GmbH, Frickenhausen, Germany
Microscope slides (76 x 26 mm)	Carl Roth GmbH & Co. KG, Karlsruhe, Germany

Microseal films: Microseal "A" film Microseal® "B" film	MJ Research, Waltham, MA, USA Biorad, München, Germany
Microtiterplates: Microtiterplates Microseal TM 96, V-form Thermo-Fast® 96 QPCR plates U96 MicroWell™ Plates, 0.5 ml	MJ Research, Waltham, MA, USA Peqlab Biotechnology GmbH, Germany Nunc TM Serving life science, Roskilde, Denmark
Needles Sterican® (ø 0.45 x 25 mm, ø 0.90 x 40 mm), single use, sterile	B.Braun Melsungen AG, Melsungen, Germany
Nitrate test strips 0-500 mg L^{-1}	Merck KGaA, Darmstadt, Germany
Nitrite test strips 0-80 mg L^{-1}	Merck KGaA, Darmstadt, Germany
Parafilm® "M"	Pechiney Plastic Packaging, Chicago, USA
PCR tubes (0.2 ml)	Biozym Scientific GmbH, Hessisch Oldendorf, Germany
Petri dishes 94/16	Greiner Bio-one GmbH, Frickenhausen, Germany
Pipette tips (various sizes)	Carl Roth GmbH & Co. KG, Karlsruhe, Germany
Schott DURAN® Erlenmeyer flasks, various sizes	Schott Glas, Mainz, Germany
Schott DURAN® laboratory glass bottles, various sizes	Schott Glas, Mainz, Germany
Sterile filters; 0.22 μm pore size	Qualilab®, Merck Labor und Vertrieb GmbH, Bruchsal, Germany
Syringe (5 ml) Omnifix® single use, sterile	B.Braun Melsungen AG, Melsungen, Germany
Syringe (1 ml) Inject® - F 1ml, single use, sterile	B.Braun Melsungen AG, Melsungen, Germany
Test tubes Assistant	Karl Hecht KG, Sondheim, Germany

B.3. Chemicals and ready-to-use-solutions

Table 5: List of used chemicals.

Expendable item	Company
6x DNA Loading Dye	Fermentas, St. Leon-Rot, Germany
Agar FLUKA	Chemie AG, Buchs, Switzerland
Ammonium chloride (NH_4Cl)	Carl Roth GmbH & Co., Karlsruhe, Germany
Ampicillin (100 mg mL^{-1})	Sigma-Aldrich Chemie GmbH, Steinhausen, Germany
Boric acid (H_3BO_3)	Carl Roth GmbH & Co., Karlsruhe, Germany
Bromphenol Blue	Sigma-Alderich Chemie GmbH, Steinhausen, Germany
Calcium carbonate ($CaCO_3$)	Carl Roth GmbH & Co., Karlsruhe, Germany
Chloroform ($CHCl_3$)	Carl Roth GmbH & Co., Karlsruhe, Germany
Citifluor AF1	Agar Scientific Limited, Essex, England
Di-ethyl-pyrocarbonate (DEPC)	Sigma-Aldrich Chemie GmbH, Steinhausen, Germany
Di-sodium-hydrogenphosphate dihydrate (Na_2HPO_4 x $2H_2O$)	Carl Roth GmbH & Co. KG, Karlsruhe, Germany
Ethanol absolute (EtOH)	Merck KGaA, Darmstadt, Germany
Ethidium Bromide (EtBr) ($C_{21}H_{20}BrN_3$)	FLUKA Chemie AG, Buchs, Switzerland
Ethylene-di-amine-tetra-acetic acid (EDTA), disodium salt	Carl Roth GmbH & Co., Karlsruhe, Germany

Ficoll® 400	Sigma-Alderich Chemie GmbH, Steinhausen, Germany
Fluorescein Calibration Dye	Bio-Rad Laboratories GmbH, Munich, Germany
Formamide (FA) (CH_3NO)	Carl Roth GmbH & Co., Karlsruhe, Germany
GeneRulerTM 100bp Plus DNA Ladder	Fermentas, St. Leon-Rot, Germany
GeneRulerTM 1kb DNA Ladder (KBL)	Fermentas, St. Leon-Rot, Germany
Glycogen	Applied Biosystems/Ambion, Austin, TX, USA
Hydrochloric acid (HCl)	Carl Roth GmbH & Co., Karlsruhe, Germany
Hydrogen Peroxid (H_2O_2), 30%	Carl Roth GmbH & Co., Karlsruhe, Germany
Kanamycin (100 mg mL^{-1})	Sigma-Alderich Chemie GmbH, Steinhausen, Germany
LE Agarose	Biozym Scientific GmbH, Oldendorf, Germany
Magnesium chloride ($MgCl_2$)	Carl Roth GmbH & Co., Karlsruhe, Germany
Magnesiumsulfate heptahydrate ($MgSO_4$ x 7 H_2O)	Merck KGaA, Darmstadt, Germany
N-(1-Naphthyl)-ethylendiamindihydrochlorid (NED)	Carl Roth GmbH & Co., Karlsruhe, Germany
Ortho-phosphorous acid (H_3PO_4)	Carl Roth GmbH & Co., Karlsruhe, Germany
Paraformaldehyde (PFA) ($OH(CH_2O)_nH$)	Carl Roth GmbH & Co., Karlsruhe, Germany
Potassium chloride (KCl)	Merck KGaA, Darmstadt, Germany
Potassium dihydrogen phosphate (KH_2PO_4)	J.T. Baker, Deventer, Netherlands
S.O.C.-Medium	Invitrogen Corporation, Carlsbad, USA
Sodium acetate ($NaC_2H_3O_2$)	Sigma-Alderich Chemie GmbH, Steinhausen, Germany
Sodium chloride (NaCl)	Carl Roth GmbH & Co., Karlsruhe, Germany
Sodium dodecyl sulfate (SDS)	Carl Roth GmbH & Co., Karlsruhe, Germany
Sodium hydroxide (NaOH)	J.T. Baker, Deventer, Netherlands
Sodium nitrate ($NaNO_3$)	Carl Roth GmbH & Co., Karlsruhe, Germany
Sodium nitrite ($NaNO_2$)	Carl Roth GmbH & Co., Karlsruhe, Germany
Sodium pyruvate ($C_3H_3NaO_3$)	FLUKA Chemie AG, Buchs, Switzerland
Sodium-di-hydrogenphosphate (NaH_2PO_4)	Carl Roth GmbH & Co., Karlsruhe, Germany
Sulfanilamid	Carl Roth GmbH & Co., Karlsruhe, Germany
Tris ($(HOCH_2)_3CNH_2$)	Carl Roth GmbH & Co., Karlsruhe, Germany
TRIzol® Reagent	Invitrogen Corporation, Carlsbad, USA
Xylencyanol	Sigma-Aldrich Chemie GmbH, Steinhausen, Germany
Yeast extract	Oxoid Ltd., Hampshire, England

B.4. Kits

Table 6: List of used Kits.

Kit	Company
DNeasy Blood & Tissue Kit	QIAgen
pGEM®-T Easy Vector System I	Promega
Platinum® SYBR® Green qPCR SuperMix UDG	Invitrogen
QIA quick PCR Purification Kit	QIAgen
QIAprep Spin Miniprep Kit	QIAgen
Quant-iT™ PicoGreen® dsDNA Assay Kit	Invitrogen
Quant-iT™ RiboGreen® RNA Assay Kit	Invitrogen
RevertAid™ First Strand cDNA Synthesis Kit	Fermentas
SuperScript® III Reverse Transcriptase Kit	Invitrogen
TOPO® XL PCR Cloning Kit	Invitrogen
TRIzol® Plus RNA Purification Kit	Invitrogen
TURBO DNA-*free*™	Ambion

B.5. Software/Online-Tools

Table 7: List of used software/Online-Tools

Software/Online-Tools	URL	Reference
Basic Local Alignment Search Tool	http://blast.ncbi.nlm.nih.gov/Blast.cgi	Altschul et al., 1990
Copy number calculator	http://endmemo.com/bio/dnacopynum.php	
daime	http://www.microbial-ecology.net/daime/	Daims et al., 2006
Finch TV	http://www.geospiza.com/finchtv/	Geospiza, USA
Molecular weight calculator	http://www.currentprotocols.com/tools/dnarnaprotein-molecular-weight-calculator	
Oligonucleotide Properties Calculator	http://www.basic.northwestern.edu/biotools/oligocalc.html	Kibbe, 2007
Primer Dimer Check	http://mfold.rna.albany.edu/?q=DINAMelt/Two-state-melting	Markham and Zuker, 2005
Primer3	http://frodo.wi.mit.edu/primer3/	Rozen and Skaletsky, 2000
Probe Base	http://www.microbial-ecology.net/probebase/	Loy et al. 2007
Probe Check	http://www.microbial-ecology.net/probecheck/	Loy et al. 2008
Reverse Complementation Tool	http://www.bioinformatics.org/sms/rev_comp.html	

B.6. Buffers, media and solutions

B.6.1. General buffers and solutions

Phosphate buffered saline (PBS) stock solution

NaH_2PO_4	35.6 g L^{-1}
Na_2HPO_4	27.6 g L^{-1}

pH of NaH_2PO_4 solution had to be adjusted to a pH = 7.2 -7.4

1 x PBS

NaCl	7.6 g
PBS stock solution	50 mL
ddH_2O	ad 1000 mL

pH to 7.2–7.4

B.6.2. Buffers for gel-electrophoresis

10 x TBE

Tris	162.0 g
Boric acid	27.5 g
EDTA	9.3 g
ddH_2O	ad 1000 mL

pH to 8.3 – 8.7

1 x TBE

10 x TBE	100 mL
ddH_2O	ad 1000 mL

Loading buffer

Ficoll 25% (w/v)	2.5 g
Bromphenol blue 0.5% (w/v)	0.05 g
Xylencyanol 0.5% (w/v)	0.05 g
EDTA 50 mM	0.15 g
ddH_2O	ad 10 mL

Ethidium bromide solution

EtBr-stock solution (10 mg mL^{-1}) diluted 1:10,000 in ddH_2O

B.6.3. Media for cultivation of microorganisms

Culture medium for „*Candidatus* Nitrospira defluvii"-enrichment

NOB stock solution 10 x

$CaCO_3$	0.1 g
NaCl	5 g
$MgSO_4$ x 7 H_2O	0.5 g
KH_2PO_4	1.5 g
NH_4Cl	0.1 g
ddH_2O	up to 1,000 mL

NOB medium

NOB stock solution	100 mL
trace elements (supplied by Alexander Galushko)	1mL
ddH_2O	up to 1,000 mL

pH to 8.6 before autoclaving, pH should drop to ~ 7.6 within 2-4 days

Culture medium for recombinant *Escherichia coli* TOP10 cells

Luria Bertani (LB) medium

Tryptone	10.0 g L^{-1}
Yeast extract	5.0 g L^{-1}
NaCl	5.0 g L^{-1}
ddH_2O	ad 1000 ml

pH to 7.0-7.5

For the preparation of solid LB medium the addition of 15 gram Agarose per Liter was necessary before autoclaving. Autoclaved LB medium and LB plates were stored at 4°C.

SOC-Medium (content of TOPO® XL PCR Cloning Kit)

Tryptone	2 % w/v
Yeast extract	0.5 % w/v
NaCl	10 mM
KCl	2.5 mM
$MgCl_2$	10 mM
$MgSO_4$	10 mM
Glucose	20 mM

Storage at -20°C

B.6.4. Antibiotics

For LB plates, the antibiotic stock solution (100 mg L^{-1}) was added to the autoclaved medium at a temperature of approximately 50 °C. Into test tubes with 5 mL LB for the growth of *E. coli* strains the respective antibiotic was added immediately before usage for growth of cells.

Kanamycin

    Kanamycin stock solution 100 mg mL^{-1} was diluted to an end concentration of 100 µg $µL^{-1}$

Ampicillin

    Ampicillin stock solution 100 mg mL^{-1} was diluted to 100 µg $µL^{-1}$

B.6.5. Selection solutions

X-Gal (5-brom-4-chlor-3-indolyl-β-D-galactopyranoside) stock solution was dissolved in di-methylformamide (N,N-dimethylmethanamide) to a final concentration of 40 mg mL^{-1}. This solution was filter sterilized and then stored at -20 °C.

B.6.6. Solutions for the measurement of nitrite concentrations

1% Sulfanilamide solution

Sulfanilamide	0.25 g
ortho-Phosphorous acid	1.25 g
H_2O_{dd}	ad 25 mL

0.1% N-(1-Naphtyl-)ethylendiamin-dihydrochloride solution

NED (N-(1-Naphtyl-)ethylendiamin-dihydrochloride)	0.025 g
H_2O_{dd}	ad 25 mL

B.7. Cultivation of microorganisms

B.7.1. Cultivation of recombinant *Escherichia coli* TOP10 cells

For the cultivation of *E. coli* cells two methods were applied. The first one was to cultivate the cells on solid LB agarose medium on plates. To select for cells harboring a vector an antibiotic was added to the LB medium (B.6.4). The vector possesses the appropriate antibiotic resistance. For further growth of selected colonies from plates liquid cultivation was applied. For this, test tubes containing 5 mL liquid LB medium were used. Prior to inoculation, sterile antibiotic-solution was added (B.6.4). Single colonies of interest - in case of pGEM cloning only white colonies containing an insert - were picked from LB plates with toothpicks under sterile condi-tions and taken to inoculate the liquid LB medium in the test tubes.

The plates as well as the test tubes were incubated at 37 °C over night (o/n) and maintained at 4 °C. The test tubes with liquid media were shaken to optimize the supply of oxygen. The liquid cultures were further used for the isolation of plasmid DNA (B.8.2).

B.7.2. Cultivation of "*Candidatus* Nitrospira defluvii"

For the maintenance of enrichment cultures of *Ca.* N. defluvii 200 mL Schott DURAN® flasks containing 150 mL NOB minimal medium were used. Additionally to essential salts and trace elements nitrite (NO_2^-) was added to a final concentration of 3 mM. The nitrite concentration was checked once a week using nitrite test strips (0-80 mg L^{-1}) and adjusted if necessary. The activity of the cultures was assessed by monitoring the consumption of nitrite. When the con-sumption rate decreased this was a hint for the accumulation of nitrate (NO_3^-) in the medium which in higher concentrations inhibits the metabolism of *Nitrospira*. Nitrate arises from the oxidation of nitrite due to the activity of the cells. If such an accumulation of nitrate was observ-able the cultures were split into three 50 mL Greiner tubes and centrifuged at 6,000 rpm for 10(-20) min at room temperature (RT). The supernatant was discarded, the cells resuspended in fresh NOB-medium and decanted into a fresh and sterile 200 mL Schott DURAN® flasks. NO_2^- was added to a final concentration of 3 mM.

B.8. Methods for DNA isolation

B.8.1. DNA isolation from "*Candidatus* Nitrospira defluvii" cultures

Genomic DNA from *Ca.* N. defluvii was isolated using the DNeasy Blood & Tissue Kit. For this, 60 mL of *Ca.* N. defluvii enrichment culture of a chemostat batch reactor-culture were harvested by centrifugation at 8,000 rpm for 10 min at RT. All further steps were performed according to the protocol for the isolation of DNA from gram-negative bacteria provided by the manufacturer. DNA-solutions were stored at -20 °C.

B.8.2. Plasmid isolation from recombinant *E.coli* TOP10 cells

To isolate plasmid DNA from *E. coli* TOP10 cells the QIAprep Spin Miniprep Kit was used. Cells with plasmid containing the right insert were grown o/n in test tubes with 5 mL LB medium. The culture was harvested by centrifugation at 13,000 rpm for 1 and the supernatant discarded. All further steps were carried out according to the manufacturer's instructions. The plasmid DNA was eluted in 50 μL ddH$_2$O.

B.9. Isolation of total RNA

A 100 mL *Ca.* N. defluvii culture was divided into two 50 mL Greiner tubes, centrifuged at 11,000 rpm for 1 min at RT and the supernatant decanted. Aliquots of the supernatant were stored for subsequent analyses. The cell pellets were washed with 40 mL 1 x PBS and centrifuged once again as mentioned above. All these steps have to be conducted as fast as possible since the half-life of mRNA in archaea and bacteria is very short (Seilinger *et al*., 2003; Andersson *et al*., 2006). The washing step increases the yield of RNA since inhibiting substances are removed at this step. The pellets were then transferred to bead-beating-caps whereof each of them contained 1 mL TRIzol® Reagent. Very important at this step is to transfer only lowest possible volumes of medium to the TRIzol® Reagent additional to the pellet in order to not change the pH of the TRIzol® solution. Then the tubes were bead-beated for 45 sec at level 6 in the Bead beater Fast Prep FP 120 and cooled on ice. All these steps were carried out as fast as possible since the transcriptome can change very quickly.

The purification of total RNA was performed using the TRIzol$^®$ Plus RNA Purification Kit. All steps were conducted following the manufacturer's instructions. The RNA was eluted from the spin columns in 30 µL DEPC-treated ddH$_2$O.

B.10. DNase treatment of RNA

Remaining DNA in RNA solutions was digested using the TURBO DNA-*free*™-Kit. All steps were carried out following the manufacturer's instructions. To check if all DNA was digested a PCR was performed with RNA solution as template. In order to detect even smallest residual of DNA the PCR was conducted performing 40 amplification cycles. The primers used were specific for the 16S rRNA gene (16S_814_FW / 16S_911_RV). After PCR 15 µL of the product were loaded onto a 2.5 % agarose gel and an electrophoresis was performed. If no band was visible on the gel the respective RNA solution was assumed to be free of DNA, otherwise the DNA digestion had to be repeated.

B.11. Ethanol precipitation of RNA

Precipitation of RNA was performed to remove substances from the RNA solution that might inhibit the DNase during the digestion of DNA as well as the polymerase during qPCR.

For the precipitation of the RNA 0.1 volume 3 M sodium acetate and 1/50 volume glycogen were added to the RNA solutions. Then 3 volumes 100% ethanol were added to the tubes which then were incubated at -80 °C for 30 min to precipitate the RNA. To recover the RNA the solutions were centrifuged at 14,000 rpm for 30 min at 4 °C before the supernatant was carefully removed. After a further short centrifugation step remaining supernatant was removed. To wash the RNA 1 mL ice cold 70% ethanol was added before vortexing and centrifuging the tubes at 14,000 rpm for 15 min at 4 °C. After removing the supernatant, the washing step was repeated. The RNA pellets were dried for approximately 5 min at RT, resuspended in 30 µL DEPC-treated ddH$_2$0 and stored at -80 °C.

B.12. Synthesis of cDNA applying Reverse Transcription (RT)

For the purpose to synthesize DNA complementary to RNA (cDNA), two different Kits were applied to get information about the reproducibility when applying different enzymes. The first Kit used was the RevertAid™ First Strand cDNA Synthesis Kit (Fermentas). The enzyme performing the reverse transcription supplied in this Kit was isolated from the Moloney Murine Leukemia Virus and is capable of synthesizing cDNA up to 13 kb. The primers used are listed in Table 8. A so-called "multiplexed" reaction was performed where several primers were applied in the same reaction. Between 22.7 and 250.0 ng of total RNA were used for the synthesis reaction which was performed following the manufacturer's instructions. The maximum volume of total RNA solution possible to introduce are 10.5 µL per reaction.

Table 8: Primers used for reverse transcription.

Primer	Sequence (5'-3')	Amount per reaction [pmol]
16S_911_RV	CCG TCA ATT CCT TTG AGT TT	25
gltA_RV	TTG TCC GTC AGT CGC TCA	25
NxrA_RV	CCG ACT TCA ACA TGA CGT C	25

The synthesis step was conducted at 45 °C for 60 min. After the inactivation of the RT-enzyme the cDNA was immediately diluted 1:10, subdivided into aliquots for qPCR analysis and stored at -20 °C.

The second Kit used was the SuperScript® III First-Strand Synthesis System. A "multiplexed" reaction with three different primers (see Table 8) was performed for which 2 pmol of each primer and 250 ng of total RNA were used. The synthesis step was performed for 60 min at 55 °C. All steps were conducted according to the manufacturers' instructions.

B.13. Analyses of nucleic acids

B.13.1. Qualitative analysis of nucleic acids using agarose gel electrophoresis

For a qualitative analysis of nucleic acids agarose gel electrophoresis was performed. This technique allows a separation of nucleic acids according to their mass. The underlying principle is that negatively charged nucleic acids migrate within an electric field in direction to the anode. The longer a fragment, the slower it is migrating through an agarose gel.

For the preparation of agarose gels 1 to 2.5 % w/v agarose - depending on the length of the fragments to be separated - were dissolved in 1 x TBE buffer by heating in a microwave oven. The liquid agarose solution subsequently was cooled to a temperature above the polymerization temperature and poured into a gel tray. The tray previously was prepared with one or more combs to create pockets the samples could be loaded in after the polymerization. The tray with solid agarose was inserted into an electrophoresis cell filled with 1 x TBE buffer. 5-15 μL of nucleic acid solution were mixed with loading buffer and applied to the pockets in the gel. The length of nucleic acid fragments in the samples was determined by comparison to a marker containing nucleic acid fragments of defined lengths which was applied to the adjacent pockets. The nucleic acids were then separated by applying a voltage between 90 to 120 volts for 45 to 100 min. Table 9 shows which agarose gels and DNA ladders were used for certain nucleic acid fragments of different lengths.

Table 9: Agarose gels and DNA ladders used for the separation of fragments of different length via agarose gel electrophoresis.

Fragment length [bp]	% agarose [w/v]	Voltage [V]	time [min]	DNA ladder
> 300	1.0	120	45	GeneRuler™ 1 kb DNA Ladder, 250-10,000 bp or GeneRuler™ 100 bp DNA Ladder, ready-to-use, 100-1000 bp
50-200	2.5	90	80-100	GeneRuler™ 100 bp DNA Ladder, ready-to-use, 100-1000 bp or O'RangeRuler™ 50 bp DNA Ladder, ready-to-use, 50-1000 bp

After the separation step the nucleic acids in the gels were stained in ethidium bromide staining solution (B.6.2) and visualized by UV-transillumination ($\lambda = 312$ nm). The documentation and digitalization was performed using a digital camera-system. The pictures were edited using the software Adobe Photoshop.

B.13.2. Quantitative analysis of nucleic acids

B.13.2.1. Photometric determination of nucleic acid concentrations using a NanoDrop® ND-1000 spectrophotometer

1.5 µL of nucleic acid solution were applied to the end of the fiber optic cable of the device to determine the concentration of the nucleic acid solution at $\lambda = 260$ nm.

B.13.2.2. Quantification of DNA-concentrations using the Quant-iT™ PicoGreen® dsDNA Assay Kit

PicoGreen® is a Fluorescence dye that intercalates into double-stranded (ds) DNA. The advantage of this ultrasensitive Fluorescence dye is that the emission after incorporation is much stronger than unbound to DNA. The dye is excited at $\lambda = 480$ and emits at $\lambda = 520$ nm. The high sensitivity allows an accurate determination of DNA-concentrations of samples with unknown DNA-concentration. Therefore, a DNA-dilution series from a defined λ-phage-DNA-solution (100 µg mL^{-1} in TE buffer) has to be measured for comparison. The obtained linear regression after measurement of the fluorescence of the standards (STD) allows the calculation of the concentrations in the samples. All steps were conducted following the instructions of the manufacturer. The photometrical measurement of the fluorescence was performed in a TECAN Infinite 200 PRO multimode microplate reader where multiple measurements (2 x 2) per well were performed. The excitation wavelength and wavelength of detection were set as mentioned above.

B.13.2.3. Quantification of total RNA-concentrations using the Quant-iT™ RiboGreen® RNA Assay Kit

Quant-iT™ RiboGreen® reagent is an ultrasensitive fluorescence dye binding to single stranded (ss) RNA. Its excitation maximum is at $\lambda = 500$ nm and the emission maximum at $\lambda = 525$ nm. The enormous sensitivity allows an accurate determination of RNA-concentrations based on a comparison with the fluorescence signals of measured RNA standards. The applied standard dilution series was prepared from a standard stock - a mixture of 16S and 23S rRNA from *E. coli* - which is provided in the Kit. All steps were performed according to the manufacturer's instructions. The TECAN Infinite 200 PRO multimode microplate reader was used for photometrical measurement of the fluorescence. Excitation was chosen as mentioned above. The Emission was measured at $\lambda = 525$ nm. Multiple measurements per well (2 x 2) were performed.

B.13.3. Amplification of DNA fragments using Polymerase Chain Reaction (PCR)

The Polymerase Chain Reaction (PCR) allows the specific and exponential amplification of DNA-fragments of interest using the enzyme Taq DNA Polymerase. After melting of the double-stranded DNA at 95 °C specific oligonucleotides ("primers") bind specifically to the single-stranded DNA at a certain annealing temperature (T_a). The Taq DNA Polymerase elongates at the 3' end of the primer at a temperature of 72 °C. These three steps are repeated up to 40 times. In this way up to billions of copies can be amplified from a single template. The used ingredients and volumes are listed in Table 10. Table 11 contains a list of all primers used.

Table 10: Reaction mixture for one standard PCR reaction.

Solution	Volume per reaction [µL]	End concentration [mM]
ddH$_2$O	33.75	
10x buffer	5.00	(1x)
dNTP Mix	5.00	0.2
MgCl$_2$	4.00	2.0
Forward primer	0.50	1.0
Reverse primer	0.50	1.0
MBI Taq DNA polymerase	0.25	
Template DNA	1.00	(~ 100 ng)
End volume	50	

Table 11: List of primers used for qPCR including information on primers designed for RT-qPCR either manually or using the Online-Tool Primer3.

Primer	Sequence (5'-3')	Binding position (5`)	Length of Primer [bp]	GC-content [%]	Length of Primer [bp]	Annealing Temp. [°C]	Length of amplified Fragment [bp]	Specificity gene / product	Reference
16S_814_FW	CTA AGT GTC GGC GGG TTA	1385450[1]	18	56	18	61.4	98	16S rRNA gene of *Ca.* N. defluvii / 16S rRNA	this study
16S_911_RV	CCG TCA ATT CCT TTG AGT TT	1385547[1]	20	40	20				
gltA_FW	GGA CCT CTG CAT GCG TCT	2397165[1]	18	61	18	54.3	99	*gltA* / citrate synthase	
gltA_RV	TTG TCC GTC AGT CGC TCA	2397246[1]	18	56	18				
NxrA1_FW	CGG ATG GCG GAT ACG TAT AAG	3189571[1]	21	52	21	63.9	118	*nxrA1* / putative Nxr, α-subunit	
NxrA2_FW	GCG TGT TCC ACT TCG TGT AC	3218212[1]	20	55	20	66.5	108	*nxrA2* / putative Nxr, α-subunit	
NxrA_RV	CCG ACT TCA ACA TGA CGT C	3189454[1]/ 3218319[1]	19	53	19	63.9/66.5[2]	118/ 108[2]	*nxrA1 + nxrA2* / putative Nxr, α-subunit	
M13 Forward	CAG GAA ACA GCT ATG AC	*	17	47	17	60	depending on insert-length	pCR®-XL-TOPO® Vector / pGEM®-T Easy Vector	TOPO cloning kit (Invitrogen)
M13 Reverse	GTA AAA CGA CGG CCA G	*	16	56	16				

* depending on the used Vector (see in the respective manual)
[1] in *Ca.* N. defluvii
[2] dependend on the used Forward primer
Nxr … nitrite oxidoreducatse

To avoid contaminations with free DNA, the reactions were mixed in a PCR hood. Before preparing the reactions the tubes, H_2O_{dd}, $MgCl_2$ and 10x buffer were exposed to UV-light for 15 min. The master mix was kept on 4 °C whenever possible as well as the reaction tubes.

The PCR Cycler has to be programmed with the respective programs shown in Table 12 depending on the primers used and the length of the fragments to be amplified. This allows an automatic sequence of the different temperature steps.

Table 12: PCR programs for standard PCR.

Step	Temperature [°C]	Duration [min]	Repeats
Denaturation	95	05:00	1 x
Denaturation	95	00:30	
Primer annealing	54.3 - 66.5 [1]	00:30	35-40 x
Elongation step	72	00:20 - 01:00 [2]	
Final elongation	72	10:00	1 x

[1] The annealing temperature is primer-specific.

[2] The elongation time depends on the length of the fragments to be amplified. The Taq polymerase used amplifies approximately 1,000 bp per minute.

B.13.4. Purification of PCR products using the QIAquick PCR Purification Kit

Before PCR products can be used for further applications such as cloning, the amplified DNA fragments have to be purified from primers, genomic DNA, salts and other substances contained in the PCR reaction mixture. The purification was conducted according to the manufacturer's instructions. The DNA was eluted from the spin columns it was bound to with 50 µL ddH_2O and then stored at -20 °C.

B.14. Development of quantitative real-time PCR (qPCR) assays for the detection of the expression of several genes in "*Candidatus* Nitrospira defluvii"

B.14.1. Quantitative real-time PCR

Quantitative real-time PCR allows for the observation of the amount of amplified DNA after each cycle of a PCR in real-time. In general, the amplification of DNA during a PCR reaction is described as a sigmoid curve where the time point, on which the log-linear (exponential) phase of the amplification starts, depends on the initially present amount of template DNA. This information can be used to calculate the original template concentration of a reaction by comparing the amplification curves of tested samples to that of defined standards for which the initial amount of template DNA is known. The detection of the amplified DNA is possible by applying an ultrasensitive fluorescence dye. SYBR Green I is a minor-groove DNA binding dye with a high affinity to double stranded DNA (dsDNA) (Witter *et al*., 1997). When bound to dsDNA the emission at 530 nm increases more than 1,000-fold to its pure form unbound to dsDNA (Real-Time Applications Guide, Bio-Rad Laboratories). The assay relies on measuring the increase in fluorescent signal, which is proportional to the amount of DNA produced during each PCR cycle (Nolan *et al*., 2006).

All qPCR reactions were performed in black 96-well microtiterplates. For the preparation of the reaction mixtures the 2x Platinum® SYBR® Green qPCR SuperMix UDG was used. All reactions were mixed according to the manufacturer's instructions. The volumes used for one reaction are cited in Table 13. 45 µL of the master mix solution containing all ingredients except the template DNA were aliquoted into the wells. Then 5 µL of diluted cDNA and prediluted standard DNA were added respectively. The standards were conducted in duplicate, the unknown samples in triplicate. The plate then was sealed with a transparent film, covered with aluminum foil and centrifuged before the qPCR was run in an iCycler IQ Thermocycler. The fluorescence in this device is measured with the iCycler iQ Real-Time PCR Detection system. The correlation of the fluorescence intensity with the cycle number performed by the software allows the computation of an amplification curve for each sample.

Table 13: Reaction mixture for a standard qPCR.

Solution	Volume per reaction [µL]
ddH$_2$O	17.5
2x Platinum® SYBR® Green qPCR SuperMix-UDG	25.0
Primer FW [1]	1.0
Primer RV [1]	1.0
Fluorescein (1 µM)	0.5
(c)DNA of *Ca.* N. defluvii enrichment	5.0
∑	50.0

[1] The concentration of the primers was chosen between 500 nM and 1000 nM depending on the determination of the optimal primer concentration as stated in B.14.3 and C.1.3.

The flow chart in Figure 5 shows all steps for the development of a qPCR assay.

Development of a qPCR assay

Primer design

⇩

Examination of the optimal annealing temperature (T$_a$)

⇩

Synthesis of standards by cloning and PCR

⇩

Calculation of the copy numbers of the standard solutions

⇩

Determination of the optimal primer concentration

⇩

Evaluation of the specifity of the developed qPCR assay
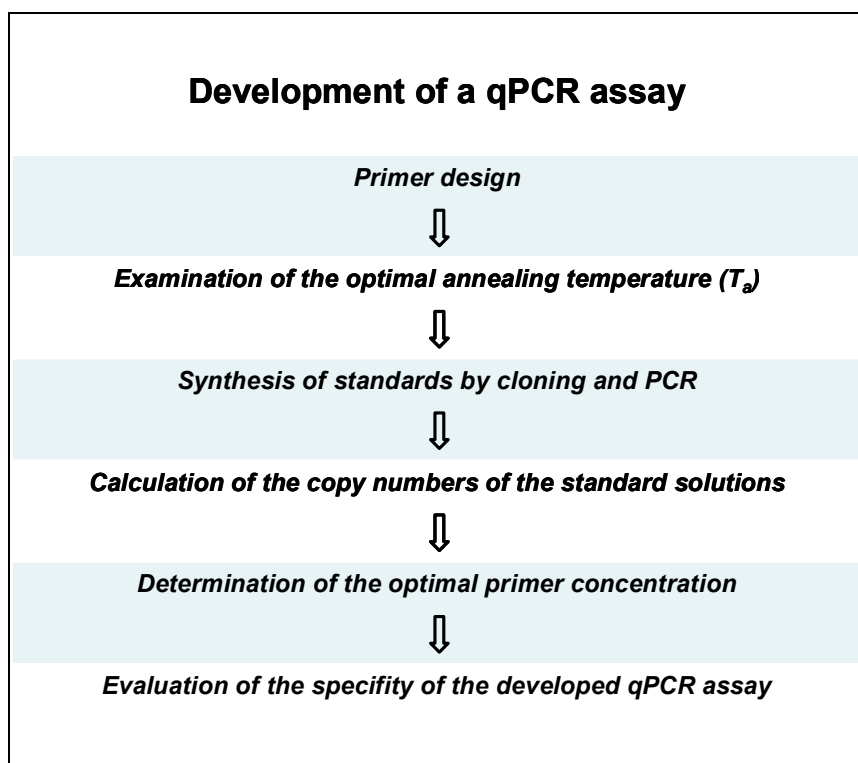
Figure 5: Workflow for the development of a qPCR assay.

B.14.2. Primer design for RT-qPCR

The first step of the development of a RT-qPCR assay is to design specific primers for the regions of interest. Primers for qPCR should possess a length between 15 and 25 bp, a predicted annealing temperature (T_a) of at least 5 °C below the melting temperature (T_m) of the formed primer-DNA duplex, a GC-content between 50 and 80 percent and the amplified fragment should have a length between 80 and 120 bp (Innis *et al.*, 1990; Dorak, 2006). The primers for the 16S rRNA-gene fragment and the *gltA* gene fragments were constructed using the Online Tool Primer3 (see in B.5) using the settings in Table 14. The primers for the two paralogous *nxrA* genes were constructed manually. To compare the different transcription levels of these two putative nitrite-oxidoreductase subunits the efficiency of the primers should be comparable. For this reason, the same reverse primer should capture both paralogous genes. Consequently, the goal was to find an identically region in the alignment of these two gene sequences to find a common reverse primer. A further requirement was to find a variable region 80 to 120 bp upstream of this identical region at which the two sequences differ significantly to set the forward primers within this region (Dorak, 2006). Due to these restrictive requirements only one region in the two *nxrA* genes was of interest for a qPCR assay.

Table 14: Settings for the construction of primers using the Online Tool Primer3 (Rozen and Skaletsky, 2000).

Length [bp]	Min.	16 bp
	Opt.	18 bp
	Max.	24 bp
Primer T_m	Min.	55 °C
	Opt.	60 °C
	Max.	63 °C
GC-content	Min.	50 %
	Max.	80 %
Concentration of monovalent cations	50	
Max. self complementarity	8.00	
3' self compl.	3	
Product size [bp]	80-120 bp	

Since the primer design is of paramount importance for the development of a qPCR assay the designed primers were checked *in silico* for their suitability for qPCR. Therefore, it was checked if they potentially form hairpins or primer dimers. Additionally, the primers where checked for binding sites within 10 kb to the target site in the genome of *Ca*. N. defluvii to rule out unspecific amplification. The final step in the development was to check the primer sequences using the NCBI database to show which organisms could be captured by the respective primer. Thereby, the only primer capturing many 16S rRNA genes of other organisms was the reverse primer specific for the 16S rRNA. Since particularly this primer must be most specific to rule out any unspecific detection, it was additionally checked against 16S rRNA sequences of a clone library from a *Ca*. N. defluvii-enrichment culture provided by Christiane Dorninger. The reverse primer bound to some sequences, but in combination with the highly specific forward primer the detection during qPCR could be ruled out.

B.14.3. Examination of the optimal annealing temperature for the designed primer pairs using Temperature-Gradient PCR

Temperature gradient PCR allows to determine the optimal annealing temperature (T_a) of a primer pair. The reaction mixtures for the PCRs are identical to that of standard PCRs. The determining factor is that different annealing temperatures are applied. To get most specific amplification of the target sequence the highest possible T_a at which a product is obtained is chosen for further applications. This was checked with agarose gel electrophoresis. Thereby, genomic DNA of a *Ca*. N. defluvii enrichment culture served as template for these reactions. The examined annealing temperatures are shown in Table 15.

Table 15: Applied annealing temperatures for gradient PCR.

Row		A	B	C	D	E	F	G	H
Temperature [°C]	[1] **Gradient 1**	48.0	47.6	48.8	63.2	68.0	61.4	63.7	66.0
	[2] **Gradient 2**	46.0	47.7	50.4	54.3	59.9	63.9	66.5	68.0

[1] for 16S rRNA specific primers

[2] for *gltA-*, *nxrA1-* and *nxrA2*-specific primers

B.14.4. Synthesis of standards by cloning and PCR

B.14.4.1. Cloning of DNA fragments for the synthesis of standards for RT-qPCR

For the synthesis of standards for RT-qPCR the target sequences of the four genes of interest (A.4.1) were amplified with the respective primer pair (Table 16) via PCR and purified according to B.13.4. These PCR products were subsequently cloned into plasmids whereof DNA fragments with overhangs could be synthesized by PCR. These pure PCR products containing the respective target site for the qPCR assays served as standards for qPCR. Thereby, on has to consider that the use of linear DNA fragments as templates is preferable because plasmids exist in supercoiled, coiled and linear form. The accessibility for primers and polymerase in coiled state is decreased in comparison to linear state. As the cDNA synthesized from RNA persists in linear state also the template in the standard reactions should be present in linear form to ensure comparability.

The cloning was performed with two different cloning systems, namely pGEM®-T Easy Vector System I and TOPO® XL PCR Cloning Kit.

The pGEM®-T Easy Vector System I works with a T4 Ligase which has to be added to the reaction mixture separately while the TOPO® XL PCR Cloning Kit works with a vector that features a covalently bound Topoisomerase enabling the ligation of the DNA fragments into the vector. The applied cloning systems for the respective gene fragment are cited in Table 16. All steps were conducted following the manufacturers' instructions.

Table 16: Applied cloning system for synthesis of standards for qPCR.

Gene fragment	Applied cloning system
16S rRNA	TOPO® XL PCR Cloning Kit
gltA	pGEM®-T Easy Vector System I
nxrA1	TOPO® XL PCR Cloning Kit
nxrA2	pGEM®-T Easy Vector System I

After heat-shock transformation of the ligated plasmids into recombinant *E. coli* TOP10 cells they were plated on LB agar-plates with kanamycin in case of TOPO® XL vector and ampicillin in case of the pGEM®-T Easy Vector as selection agent and incubated o/n at 37 °C.

The screening for clones harbouring an insert works differently in both applied cloning systems. The pCR®-XL-TOPO® vector is a suicide vector encoding the lethal gene *ccd*B. Inserting a DNA-fragment into the vector disrupts the expression of this gene and allows this organism to grow. Cells without insert die due to the expression of the toxic *ccd*B gene (Bernard *et al.*, 1994). The pGEM®-T Easy vector works with blue/white screening. When inserting a DNA-fragment in this vector the expression of the alpha-peptide coding region of the beta-galactosidase enzyme gets disrupted. Lacking this functional enzyme these cells are not able to cleave X-Gal which is spread on the LB agar plates. X-Gal is a colorless compound that turns blue after cleavage by the beta-galactosidase. Therefore, white cells without functional beta-galactosidase are harbouring an insert and can be used for growth in liquid LB for further analyses.

B.14.4.2. Insert screening for clones containing the correct inserts via PCR

To screen for clones containing an insert of desired length in the transformed vectors insert screening PCRs with M13-primers were performed according to B.14.4.2. Therefore, single colonies were picked with toothpicks from the agar-plates they were grown on and transferred to a LB master plate. The remaining cells on the toothpick served as template for previously prepared PCR-reactions by stirring the toothpicks in the reaction mixtures for some seconds. The colonies on the LB master plate containing an insert of the correct length confirmed by applying the PCR products on an agarose gel then were used for the inoculation of liquid LB medium to grow high amounts of cells containing oodles of plasmids (see B.7.1). From these cultures the plasmid DNA was isolated according to B.8.2.

B.14.4.3. Synthesis of standards for RT-qPCR via PCR

For the synthesis of standards for the developed qPCR assays, PCR applying the M13 primer pair (M13F and M13R) and the accordant plasmid as template was conducted. The PCR products of multiple identical PCR-reactions were pooled and purified using the QIA quick PCR Purification Kit following the manufacturer's instructions (B.13.4). After elution in 50 μL ddH$_2$0 the concentration of the standard stock was determined using the Quant-iT™ Pico-Green® dsDNA Assay Kit as shown in B.13.2. Finally, the standard stocks were diluted in in-

crements of 10 down to a dilution of 10^{-13}. Aliquots of 20 µL were prepared and stored at -20 °C.

B.14.5. Calculation of copy numbers of the synthesized standards

For the calculation of the copy numbers of the synthesized standards, the molecular weights (MW) of the M13-PCR products of the plasmids containing the gene fragments of interest were calculated based on the sequence of the inserts and the amplified M13-overhangs using the Online Tool DNA/RNA/Protein Molecular Weight Calculator (B.5). Based on the calculated molecular weight of the standard fragments and the determined concentration [ng µL^{-1}] of these solutions the calculation of the copy number per µL was performed according to Formula 1.

Formula 1: Calculation of copy numbers.

$$\text{copy number x µL}^{-1} = \frac{c \, [\text{ng µL}^{-1}]}{\text{MW [Da] x 1,66053878283 x } 10^{-15} \, [\text{ng}]}$$

1 Dalton (Da) = 1.66053878283 x 10^{-27} kg

B.14.6. qPCR program

Table 17: qPCR programs for the developed qPCR assays.

Cycle	Step	Temperature [°C]		Time [mm:ss]	Repeats	Data collection
1	1	95.0		05:00	1x	
2	1	95.0		00:40		
	2	16S rRNA *gltA* *nxrA1* *nxrA2*	61.4 54.3 63.9 66.5	00:30	40x	yes
	3	72.0		00:40		yes
3	1	95.0		01:00	1	
4	1	55.0		01:00	1	
5	1	55.0-95.0 (0.5 °C increase after each cycle)		00:10	80x	yes (melt curve + data analysis)

B.14.7. Determination of the optimal primer concentrations for qPCR

To determine the optimal primer concentrations enabling the highest possible efficiency for each qPCR assay reactions with differently concentrated primer solutions were prepared and run in duplicate. The evaluated primer concentrations are shown in Table 18. The optimal primer concentrations for which the lowest threshold cycle (C_t) and the highest fluorescence signal was observed were used for further qPCR analyses. Plasmids harboring the correct insert were used as templates.

Table 18: Evaluated Primer-concentrations for qPCR.

	Concentration Forward-Primer [nM]	Concentration Reverse-Primer [nM]
F250/R250	250	250
F500/R500	500	500
F750/R750	750	750
F1000/R1000	1000	1000
F250/R1000	250	1000
F1000/R250	1000	250

B.14.8. Schematic plate setup for evaluation of the qPCR assays

Figure 6 shows a schematic plate setup for a qPCR run. The standards were run in duplicate. Tested samples with unknown concentration of target DNA were run in triplicate. Each run included at least one negative control with ddH$_2$O as template.

	1	2	3	4	5	6	7	8	9	10	11	12
A												
B		STD 10^{-3}	STD 10^{-4}	STD 10^{-5}	STD 10^{-6}	STD 10^{-7}	STD 10^{-8}	STD 10^{-9}	STD 10^{-10}	STD 10^{-11}	NTC - water	
C		STD 10^{-3}	STD 10^{-4}	STD 10^{-5}	STD 10^{-6}	STD 10^{-7}	STD 10^{-8}	STD 10^{-9}	STD 10^{-10}	STD 10^{-11}		
D												
E		sample 1	sample 2	sample 3	sample 4	sample 5	sample 6	sample 7	sample 8	sample 9	sample 10	NTC - water
F		sample 1	sample 2	sample 3	sample 4	sample 5	sample 6	sample 7	sample 8	sample 9	sample 10	
G		sample 1	sample 2	sample 3	sample 4	sample 5	sample 6	sample 7	sample 8	sample 9	sample 10	
H												

Figure 6: Schematic plate setup for the evaluation of the developed qPCR assays. NTC = negative control

B.14.9. Checking the specificity of the qPCR assays

The specificity of the qPCR assays was checked by analyzing the melting curves after each run as well as by applying the qPCR products to a 2.5% agarose gel to confirm the desired product by length control. Additionally, the primer specificity was checked once by sequencing.

B.14.9.1. Melting curve analysis

Melting curve analysis is an important tool for checking the quality of PCR products. The melting temperature is determined by the length and GC-content of nucleic acid. For measuring the melting curve the fluorescence intensities in the wells were measured within a range of 55 °C to 95 °C in increments of 0.5 °C. The temperature at which the decrease in fluorescence intensity was determined to be highest is defined as melting temperature (T_m) of the respective PCR product. At this temperature the dsDNA-fragments are melted and therefore no fluorescence signal can be detected since the dye emits magnitudes higher fluorescence when intercalated

into double stranded DNA. Ideally, there is one single peak for a PCR product suggesting only one sort of nucleic acid. If there would exist another amplicon with another melting temperature a second peak would be visible. The melting curve was determined immediately after each qPCR run in the iCycler IQ Thermocycler.

B.14.9.2. Direct sequencing of PCR products

To check whether there is no unspecific amplification in PCR with cDNA reverse transcribed from *Ca*. N. defluvii RNA the PCR products were directly sequenced.

The sequencing method is based on the abortion of the amplification due to the use of fluorescently labelled ddNTPs besides common dNTPs lacking the 3' OH group (one colour specific for one base). Thereby, the amplifications stop at an unknown point by accident. These fluorescently labelled PCR products subsequently are separated electrophoretically and the attached dyes are detected. In this way, the DNA sequence can be revealed. To get best possible certainty about the product not only one primer was used but the sequencing was conducted in both directions in independent reactions. This allows an alignment of the sequences obtained with the forward- and the reverse-primer to get the full sequence of the amplicon. For this purpose, the PCR products for all four examined genes were sequenced applying cyclesequencing - a di-deoxy mediated chain termination (Sanger *et al.,* 1977) based PCR (Saiki *et al.,* 1988). The primers used are cited in Table 11. The sequencing was performed by Martina Grill.

The chromatograms obtained by the electrophoretical separation had to be read out manually. A computerized analyzes was not possible for most sequences due to the shortness of the obtained PCR products (~ 100 bp). Afterwards the sequences obtained for sequencing reaction using the reverse primer was reverse complemented and then aligned to the sequence obtained using the forward primer. The overlapping region could be identified and the sequences could be completed.

The obtained sequences were then compared to the NCBI database using the search algorithm BLAST (B.5) (Altschul *et al.,* 1990) to find regions of high similarity to known sequences in the database.

B.15. Gene expression study

B.15.1. Incubation of "*Candidatus* Nitrospira defluvii" under different environmental conditions

To examine changes in the transcription of the *nxrA1* and *nxrA2* genes under different environmental conditions cultures of *Ca.* N. defluvii were incubated at different NO_2^--concentrations under oxic conditions on the one hand and with pyurvate and NO_3^- under anoxic conditions on the other hand. The exact incubation conditions are shown in Table 19. Each incubation was prepared in duplicate and carried out at 30 °C.

Table 19: Incubation conditions for the incubation experiments.

	oxic conditions			anoxic conditions	
e^--Donator Concentration [mM]	NO_2^- 0.3	NO_2^- 3	NO_2^- 15	Pyruvate 0.5	-
e^--Acceptor Concentration [mM]	O_2	O_2	O_2	NO_3^- 2.5	-

For these incubations eight 150 mL enrichment cultures - maintained as described in B.7.2 - were used. They were active up to the start of the incubation experiments and free of detectable nitrite. For the incubation experiments 250 mL Schott bottles airtightly closed with rubber stoppers were used and filled with 100 mL NOB-medium. To adjust the respective incubation flasks to the right environmental conditions (Table 19), sterile filtered $NaNO_2$ solution, anoxic $NaNO_3$ solution and anoxic pyruvate solution were prepared and injected with syringes and needles under sterile conditions next to the Bunsen burner. Additionally, 6 mL N_2CO_2 gas mixture (20% CO_2) were added to the bottles to supply sufficient CO_2. To avoid input of remaining oxygen in the needles into the anoxic bottles when taking samples or adding substances the needles and syringes were flushed with N_2CO_2 gas mixture before injection into the bottles. To ensure that each approach contained approximately the same amount of cells the cultures were pooled in anoxic medium before splitting them up into the different incubation bottles. For each approach the same amount of pooled culture was injected into the Schott bottles.

The concentrations of nitrite and nitrate in the different incubations were controlled regularly by sampling and measuring with nitrite (NO_2^-) and nitrate (NO_3^-) test strips and adjusted if necessary. The samples were centrifuged at 14,000 rpm for 10 min at RT to pellet the cells and the supernatant was stored at -20 °C for later measurements.

B.15.2. Method for accurate measurement of NO_2^--concentrations (Griess Reaction)

For an accurate measurement of nitrite concentrations of taken samples the Griess reaction was applied (Griess, 1879). In this reaction nitrite reacts with sulfanilamide and NED and forms a pinkish compound which is measurable photometrically. Therefore, the absorbance at a wavelength of 545 nm is measured. The method is sensitive for nitrite concentrations up to 100 µM. To calculate the nitrite concentrations of samples the measured values were compared to measured values for a dilution series of a defined nitrite solution. All samples had to be diluted to lie within the range of the standards.

For the preparation of the nitrite standards a 0.1 M nitrite solution was prepared in NOB-medium. This solution was diluted with NOB-medium down to 50, 37.5, 25, 18.75, 6.25 and 3.125 µM. In addition pure NOB-medium was included for the calculation of the standard curve. The thawed samples of the 3 mM nitrite incubations were diluted 1:100 and the samples of the 15 mM nitrite incubation 1:500 to be in the range of the standards. 50 µL of samples and standards were applied in triplicate to a transparent 96-well microtiterplate. Then, 1 µL 1% sulfanilamide solution was added to each well containing sample or standard solution and incubated for approx. 2 min. Subsequently, 1 µL 0.1% N-(1-Naphtyl-)ethylendiamin-dihydrochloride solution was added to each well inducing a color change from transparent to pinkish if nitrite is present. This color change is based on the chemical reaction shown in Figure 7. The intensity of the colour change increases linearly up to a concentration of 100 µM NO_2^-. The photometrical measurement of the absorbance was performed in a TECAN Infinite 200 PRO multimode microplate reader where multiple measurements (2 x 2) per well were performed. The obtained values then where averaged.
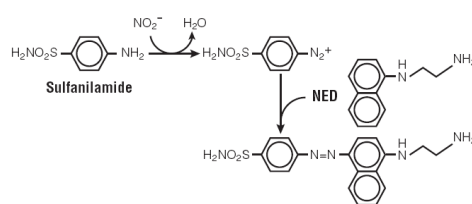
Figure 7: Griess reaction (Griess, 1879;
Griess Reagent System, Promega)

B.16. Investigation of the coexistence of three subpopulations of *Nitrospira* sublineage II in the wastewater treatment plant of the University of veterinary medicine Vienna applying quantitative FISH

B.16.1. Fluorescence in situ hybridization (FISH)

FISH is a method that enables the specific visualization of certain taxa in their natural habitat using fluorescently labeled oligonucleotide probes. These probes are artificially synthesized for the organisms of interest and bind specifically to their 16S or 23S rRNA. Cells are fixed with PFA or Ethanol and then immobilized on a microscope slide. The next step is a hybridization of the specific oligonucleotide probes with the rRNA under stringent conditions. To remove unbound probes a washing step is performed subsequently. The excitation of the fluorescence dye bound to the oligonucleotide probes at a specific wavelength then allows the detection using an epifluorescence or confocal laser scanning microscope.

B.16.1.1. Oligonucleotide probes used targeting the 16S rRNA

Table 20: Properties of applied FISH probes for the quantification.

Probe	Sequence (5'-3')	Binding position*	FA [%]	Specificity	Reference	Competitor sequence (5'-3')
EUB338	GCT GCC TCC CGT AGG AGT	338-355	0-50	Most Bacteria	(Amann *et al.,* 1990)	-
EUB338II	GCA GCC ACC CGT AGG TGT	338-355	0-50	Planctomycetales	(Daims H. *et al.,* 1999)	-
EUB338III	GCT GCC ACC CGT AGG TGT	338-355	0-50	Verrucomicrobiales	(Daims H. *et al.,* 1999)	-
Ntspa662	GGA ATT CCG CGC TCC TCT	662 - 679	35	Genus *Nitrospira*	(Daims H. *et al.,* 2001)	GGA ATT CCG CTC TCC TCT
Ntspa1151	TTC TCC TGG GCA GTC TCT CC	1151 - 1170	35-40	sublineage II of the genus *Nitrospira*	(Maixner F. *et al.,* 2006)	-
Ntspa175	GAC CAG GAG CCG TAT GCG	175 - 193	25	cluster 2.2	(Stoecker *et al.,* 2010)	-
Ntspa195			20	cluster 2.4	(Dorninger *et al.,* unpublished)	-
Ntspa256Cl2			20	cluster 2.5	(Dorninger *et al.,* unpublished)	-

* binding position according to *E.coli* 16S rRNA (Brosius *et al.*, 1981)

Table 21: Properties of used fluorescence dyes.

Fluorescence dye	Absorption maximum [nm]	Emission maximum [nm]	molar extinction coefficient [1/mol*cm]
Fluos	494	518	7.5 x 104
Cy3	554	570	1.3 x 105
Cy5	650	667	≥2 x 105

B.16.1.2. Cell fixation with paraformaldehyde (PFA)

For the fixation of sludge samples three volumes 4% PFA solution were added to one volume of sludge and incubated for approximately 2 h at 4 °C. Subsequently, the sludge was centrifuged at 11,000 rpm for 15 min and the supernatant was discarded. By resuspending the pellet in 1x PBS and subsequent centrifugation as mentioned before the pellet was washed. The supernatant was discarded and the sludge pellet resuspended in a mixture of one volume 1x PBS and one volume EtOH$_{abs.}$. These PFA-fixed samples were stored at -20 °C.

B.16.1.3. Cell immobilization

3 x 10 µL of fixed activated sludge were successively pipetted onto a microscope slide and dried at 46 °C. For quantifications with probes giving very weak signal the amount of sludge was decreased down to at least 1.5 µL to reduce the autofluorescence (AF) signal.

B.16.1.4. Dehydration of the cells

To further dehydrate the samples after drying in the immobilization step and to increase the permeability of the cells an ethanol series was performed. For this, the slides were immersed for 3 min into 50%, 80% and 96% ethanol in this sequence and subsequently air-dried.

B.16.1.5. Hybridization

The hybridization has to be performed under stringent conditions. Since all hybridizations are carried out at 46 °C the adjustment of stringency is not ensured by change of temperature but by addition of formamide (FA). FA acts as destabilizer of hydrogen bonds between two strands and increases the stringency in this way. NaCl on the other hand acts stabilizing and facilitates the formation of duplexes between rRNA and DNA-probes. In this way the stringency can be decreased. This is made possible by a masking of the negatively charged nucleic acid backbone by Na^+ ions and thereby a reduction of the repulsion between the two strands. The composition of the hybridization buffer (HB) according to the required FA concentration is shown in Table 22.

Table 22: Composition of hybridization buffer (HB) depending on the desired FA concentration.

FA [%]	0	5	10	20	25	30	35	40	45	50
5 M NaCl [µL]	180	180	180	180	180	180	180	180	180	180
1 M Tris/HCl pH 8 [µL]	20	20	20	20	20	20	20	20	20	20
ddH$_2$0 [µL]	800	750	700	600	550	500	450	400	350	300
FA [µL]	0	50	100	200	250	300	350	400	450	500
10% SDS (w/v) [µL]	1	1	1	1	1	1	1	1	1	1

10 µL of HB were pipetted onto each well. 1 µL of each probe was added to the applied HB and mixed by pipetting up and down carefully. The rest of the 1 mL of HB was emptied into a 50 mL Greiner tube prepared with a piece of paper tissue. The slide was inserted into this Greiner tube taking care that the slide lies horizontally. The tube then was closed and placed into an hy-

bridization oven set to 46 °C and incubated for 15 hours. The reason for this long incubation time was that especially the probes specific for subpopulations of *Nitrospira* sublineage II give very weak signals and therefore have to be hybridized for longer times to improve the binding. To ensure comparability of all applied probes all of them had to be hybridized for the same period of time.

B.16.1.6. Washing step

After the hybridization step the slides had to be washed to remove unbound probes. The stringency in the washing buffer is determined by the addition of NaCl. To guarantee that only Na^+ ions stabilize the nucleic acid-duplexes, EDTA is added to bind bivalent cations which also could affect the stringency. The composition of the washing buffer (WB) depending on the FA concentration used in the HB is shown in Table 23.

Table 23: Composition of washing buffer (WB) depending on the introduced FA concentration in the hybridization buffer (HB).

FA [%] in HB	0	5	10	20	25	30	35	40	45	50
5 M NaCl [µL]	9000	6300	4500	2150	1490	1020	700	460	300	180
1 M Tris/HCl pH 8 [mL]	1	1	1	1	1	1	1	1	1	1
0.5 M EDTA pH 8 [µL]	0	0	0	500	500	500	500	500	500	500
ddH₂0	ad 50 mL									
10% SDS (w/v) [µL]	50	50	50	50	50	50	50	50	50	50

In the washing step the slides were washed in pre-heated, 48 °C warm WB for 10 min. To wash away all remaining probes and salt, an additional washing step followed under hyper-stringent conditions by dipping the slide shortly into ice cold ddH₂0. In order not to wash away correctly bound probes this hyperstringent washing step had to be really short. Afterwards the slides were dried immediately with compressed air and could then be analysed or stored at -20 °C in the dark.

B.16.2. Analyzed activated sludge samples

All samples analyzed in this study were obtained from Christiane Dorninger. The samples were taken in the WWTP of the Vetmed within the years 2004 and 2010 and PFA-fixed for the stabilization of the bacterial cell morphology of especially garm-negative bacteria. All sampling times are shown in Table 24.

Table 24: Analyzed activated sludge samples of the WWTP of the University of Veterinary Medicine Vienna.

03/04/04	04/15/04	07/13/04	05/14/07	06/28/07	11/17/08	02/03/09	10/07/09	07/02/10	08/16/10

B.16.3. Confocal laser scanning miscroscopy (CLSM)

This special microscope type allows one to take pictures only of single planes of a sample. This is made possible by the application of an adjustable pinhole in the beampath which excludes light emitted from planes out of the focus. The objects are scanned with different lasers of specific excitation-wavelength which is depending on the applied fluorescence dye. After detection of the emission the signals are converted into digital images by the microscope software.

B.16.4. Detection of labelled cells using the CLSM

Before microscopic inspection the slides were covered with Citifluor AF1 and a cover slip. Citifluor AF1 reduces bleaching effects on the fluorescence dye during the application of very intense laserbeams. For microscopy, two He-Ne-lasers were used with excitation-wavelengths at 453 and 633 nm for the excitation of the fluorescence dyes Cy3 and Cy5, respectively. For the quantification an oil-objective with a 40x magnification in combination with a 10x magnifying ocular were used.

B.16.5. Quantification of labelled cells using daime

The biovolume fraction of a subpopulation labelled with a Cy3-labelled probe was quantified relative to the biovolume of a higher order population labelled with a Cy5-labelled probe. This was done for 30 two-dimensional pictures taken at randomly selected positions on the microscopic slide by searching for thick layer of biomass when visualized under transmitted light were. The biovolume fraction then was determined by using the software *daime*.

The settings for recording of most pictures are listed in Table 25. In case of the probe specific for cluster 2.5 of *Nitrospira* sublineage II the settings had to be adjusted by increasing the diameter of the pinhole due to the extremely weak signal.

Table 25: Settings for image recording.

Pinhole diameter	1.1 μm
Picture number	2
Resolution	512 x 512
Objective	400 x
Zoom	1 x
Scanspeed	8
Pixel time	2.56 μs

The analysis of the pictures was carried out using the software daime. The first step of the analysis is to segment the images to distinguish between objects and background signals. This has to be done for both levels - the superordinate and the subordinate probes. These automatically defined objects can furthermore be edited by hand for applications such as the removal of artefacts which have been observed during the recording of the images. This is particularly important when an artefact gives signals in both channels (Cy3 and Cy5) or only in Cy5. If there are artefacts only in the subordinate level - here always the Cy3 channel - there is the possibility of removal by the software automatically. The congruency threshold was set to 50% to eliminate all signals from the subordinate level which are not covered by the superordinate probes at least to 50%.

The recorded images were evaluated using the software daime. The biovolume fractions calculated for each picture were then cumulated. The cumulative curves can be exported from the software and show the change of the average biovolume fraction after adding each further picture to the analysis. Observing the development of the cumulative curve provides information about the sufficiency of the number of pictures taken. If there is no visible change in the total biovolume fraction after a certain number of pictures taken this number can be assumed to be accurate.

Important information about the quality of the assay is also revealed by the standard deviations for each examined samples. This standard deviation is calculated for each examined sample out

of 30 pictures. The standard deviation then provides information about the consistence of the distribution of the quantified cells. This information is especially important when quantifying cells growing in colonies because thereby the variations from picture to picture are assumed to be high.

C. <u>Results</u>

C.1. Development of quantitative real-time PCR assays for different genes of "*Candidatus* Nitrospira defluvii"

C.1.1. Primer design for RT-qPCR

Table 11 shows all primers designed for the reverse transcription and subsequent qPCR to amplify fragments of four different genes of *Ca.* N. defluvii. The length of the amplified fragments was between 98 and 118 bp. As mentioned in B.14.2 the two paralogous *nxrA*-copies should be captured by the same reverse primer which was possible in the 3'-region of the genes.

C.1.2. *In-silico* check for primer specificity

To ensure the specificity of the designed primers, they were additionally checked *in silico* against the NCBI-database. Thereby, all primers were shown to be specific with the exception of the reverse primer specific for the 16S rRNA. This one, however, was shown to be specific in combination with the designed forward primer after checking this primer pair against the 16S rRNA contaminant clone library of the *Ca*. N. defluvii enrichment culture.

C.1.3. Examination of the optimal annealing temperature (T_a) for the developed primer pairs

The optimal annealing temperatures (T_a) for the examined primer pairs were found to range between 54.3 and 66.5 °C (Table 26). The selection of the optimal T_a was carried out by selecting the highest temperature at which specific amplification was observed. Thereby, the risk of unspecific binding of the primers to other, similar regions can be reduced. The selected temperatures are framed with black rectangles in Figure 8 and Figure 9. Especially for the gene *nxrA2* the T_a is quite high but still applicable.
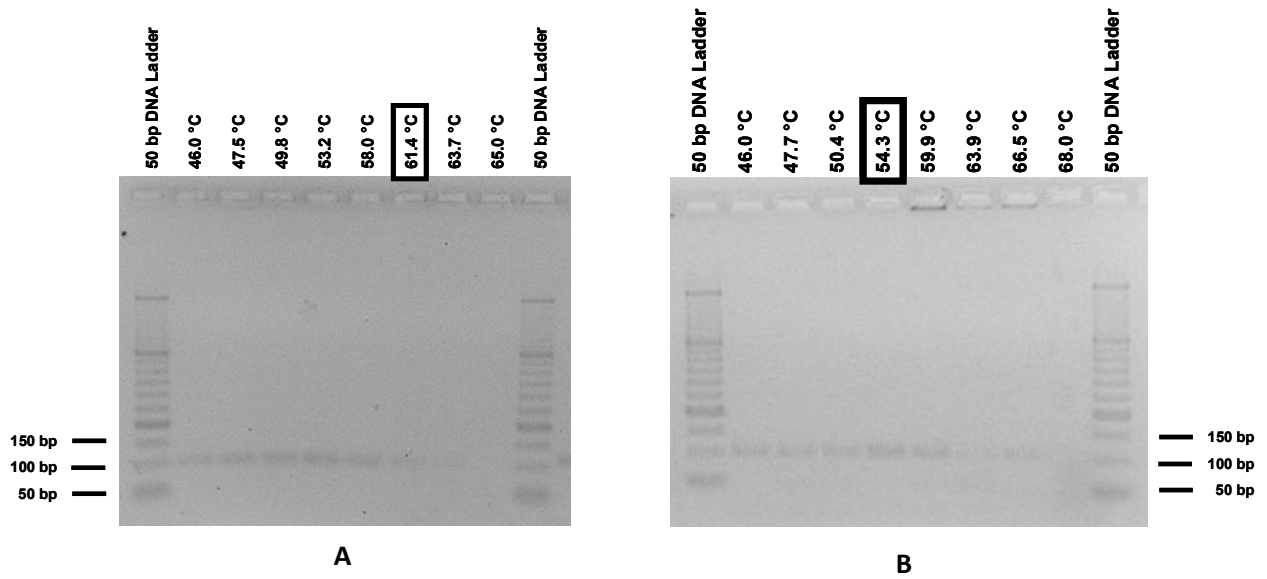
Figure 8: Gel pictures of gradient-PCRs for the evaluation of the optimal annealing temperatures for two different primer pairs. A: 16S rRNA-specific primers. B: *gltA*-specific primers.
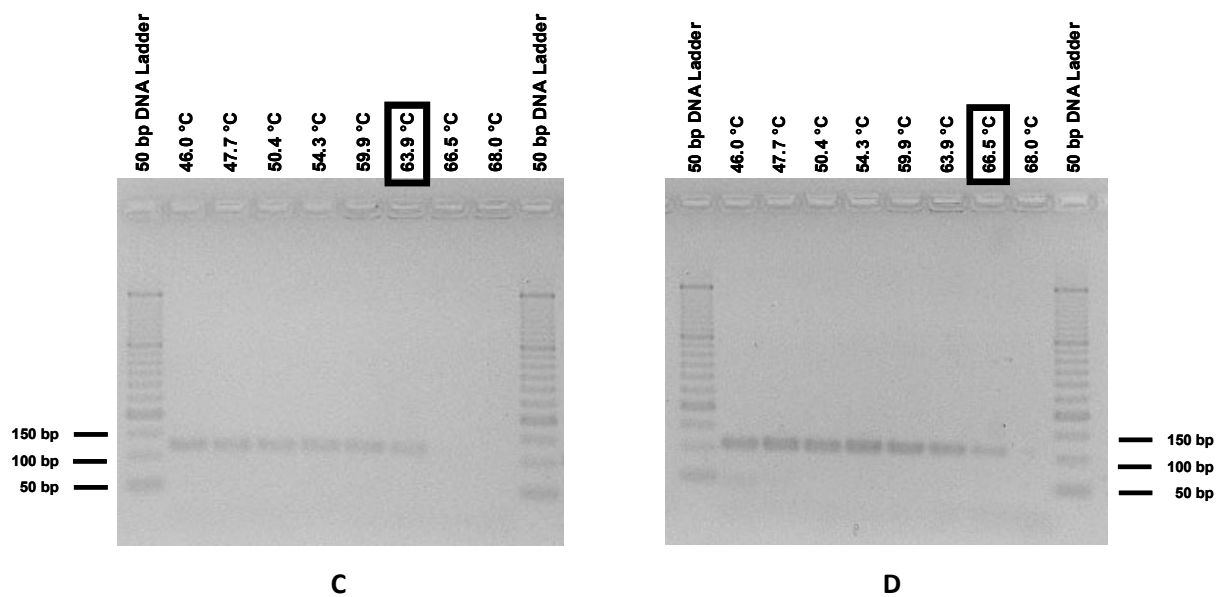

Figure 9: Gel pictures of gradient-PCRs for the evaluation of the optimal annealing temperatures for two different primer pairs. C: *nxrA1*-specific primers. D: *nxrA2*-specific primers.

Table 26: Selected primer annealing temperatures for the designed primer pairs.

Primer Pair	Optimal T_a [°C]
16S_814_FW / 16S_911_RV	61.4
gltA_FW / gltA_RV	54.3
NxrA1_FW / NxrA1_RV	63.9
NxrA2_FW / NxrA1_RV	66.5

C.1.4. Synthesis of standards for qPCR by cloning

For the synthesis of standards for qPCR the target gene fragments were amplified via PCR with the respective specific primers and purified. The obtained PCR products then were cloned into vectors. After growing of cultures containing these vectors and isolation of the plasmids via miniprep the desired plasmid solutions were obtained. All information concerning the applied cloning systems and the concentrations of the plasmid solutions are listed in Table 27.

Table 27: Plasmids containing the target-gene-fragments for the synthesis of qPCR-standards.

Target gene	Length of target fragment [bp]	Used vector	Concentration of plasmid DNA [ng µL^{-1}]*	Molecular weight of amplified vector-overhangs [kDa]	Molecular weight of vector-overhangs + insert [kDa]
16S rRNA	98	pCR®-XL-TOPO®	326.5	150.33	211.19
gltA	99	pGEM®-T Easy Vector	209.1	143.46	204.91
nxrA1	118	pCR®-XL-TOPO®	233.9	150.33	223.42
nxrA2	108	pGEM®-T Easy Vector	169.4	143.46	210.23

* measured with NanoDrop® ND-1000 spectrophotometer.

The actual synthesis of the standards was done by performing PCR using the M13F/R primer pair and 1:100-dilutions of each plasmid listed in Table 27 as template. To get more PCR product five PCRs per target-gene were performed in parallel and pooled afterwards. All information concerning the PCR products is listed in Table 27.

These PCR products were purified according to B.13.4 and used as standards for qPCR by diluting them 1:10 in several steps. Aliquots of 20 µL were prepared and stored at -20 °C to prevent degradation by repeated thawing.

C.1.5. Calculation of copy numbers of the synthesized standards

To calculate the copy numbers of the standards the concentrations of the purified M13-PCR products were measured using the Quant-iT™ PicoGreen® dsDNA Assay Kit. The copy numbers of the undiluted standard stocks (STD 10^0) have been calculated according to B.14.5. The measured concentrations of the standard stocks as well as the calculated copy number per µL are listed in Table 28.

Table 28: Information on synthesized standards concerning their MW, concentration and copy number.

Target gene	DNA-concentration* [ng µL^{-1}]	Length of amplified fragment [bp]	MW of amplified fragment [kDa]	Copy number x µL^{-1} (of STD 10^0)
16S rRNA	62.2	342	211.19	1.77×10^{11}
gltA	5.4	331	204.91	1.58×10^{10}
nxrA1	18.2	362	223.42	4.90×10^{10}
nxrA2	64.9	340	210.23	1.86×10^{11}

* calculated using the Quant-iT™ PicoGreen® dsDNA Assay Kit
MW = molecular weight

C.1.6. Determination of the optimal primer concentrations for qPCR

For the determination of the optimal primer concentration for the qPCR assays identical reactions with the exception of the primer concentration were prepared. 5 µL of standard solution - ranging between 0.1 and 10.0 pg µL^{-1} for the different assays - served as templates. The optimal primer concentration for each assay was selected on basis of the threshold-cycle (C_t) and the fluorescence intensity. A combination of a low C_t-value and high fluorescence intensity was desired. An example of the selection based on these requirements is shown in Figure 10 A for the *nxrA2* qPCR assay where the primer concentration of 750 nM for the forward as well as for the reverse primer gave the lowest C_t-value for the reaction in combination with the highest fluorescence signal (Figure 10 B). The results of all primer evaluations are shown in Table 29.
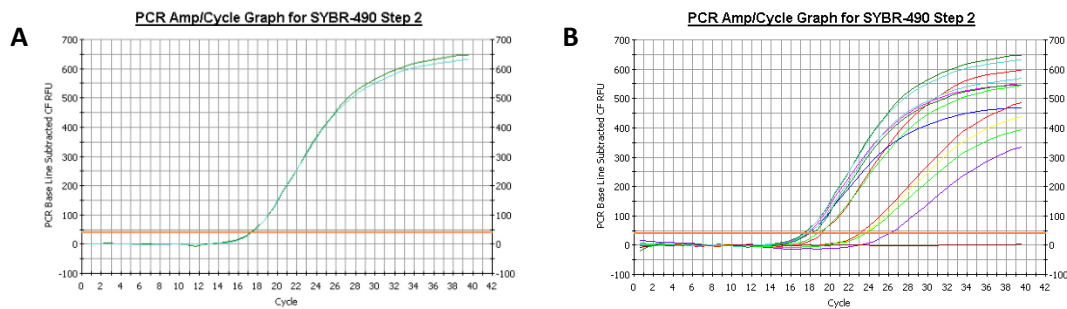
Figure 10: Example for the evaluation of the optimal primer concentration based on the evaluation for the *nxrA2* qPCR assay. A: Amplification curves of the reactions with the optimal primer concentration of 750 nM for the forward (FW) and reverse (RV) primer, respectively showing the lowest C_t-value. B: Amplification curves of all reactions with different primer-concentrations.

Table 29: Optimal primer concentrations for the four developed qPCR assays.

Target gene	Primer pair	Optimal annealing temperature [°C]	Optimal primer concentrations [nM]	
			FW-primer	RV-primer
16S rRNA	16S_814_FW/RV	61.4	**750**	**1000**
gltA	gltA_FW/RV	54.3	**500**	**500**
nxrA1	NxrA1_FW/NxrA_RV	63.9	**750**	**750**
nxrA2	NxrA2_FW/NxrA_RV	66.5	**750**	**750**

C.1.7. Evaluation of qPCR assays with cDNA from "*Candidatus* Nitrospira defluvii"

For each qPCR assay a test run with cDNA synthesized by reverse transcription (RT) of total RNA from *Ca*. N. defluvii enrichment culture with the respective reverse-primer was performed. The total RNA was isolated from an enrichment culture of *Ca*. N. defluvii according to B.9. For the synthesis of cDNA two different RT-Kits were used to get also information about the influence of the used Reverse Transcriptase on the efficiency and comparability of the assay. The RT reactions with the two different Kits from Fermentas and Invitrogen (Table 6) were performed as described in B.12. Thereby, 250 ng of total RNA were used per reaction. For the qPCR runs 5 µL of different dilutions (10^{-1}, 10^{-2} and 10^{-3}) of the RT-products were used as templates to get an assessment of how much cDNA is necessary to get evaluable results. Also the efficiencies of the qPCR assays and thus the efficiencies of the amplifications depending on the quality of the primers were evaluated in this way.

C.1.7.1. 16S rRNA qPCR assay

The first qPCR assay that was tested was specific for the 16S rRNA of *Ca*. N. defluvii. Figure 11 shows that the duplicates of standards fit very well and also the distances between the different standard solutions are very similar. This proves accurate pipetting. Detection was possible for the standards diluted to 10^{-3} to 10^{-9}. Therefore, there is the possibility to detect between 886 and 8.86×10^8 copies of 16S rRNA with this assay based on the calculation in C.1.5.

Figure 11: Amplification curves of standards and negative controls of the 16S rRNA qPCR test run.

Figure 12 A and B show the calculated standard curve with a quite high correlation coefficient of 0.998 and a PCR efficiency of about 80%. Thereby, there were no conspicuous outliers. Dis-

played in A are the dilutions (10^{-1}, 10^{-2} and 10^{-3}) of cDNA synthesized using the RevertAid™ First Strand cDNA Synthesis Kit (in the following referred to as Fermentas-Kit). Figure 12 B shows the results for the applied cDNA synthesized with the second applied reverse transcriptase (SuperScript®, Invitrogen) which was compared to the one of Fermentas. One can see that there are nearly the same results obtained for the two different RT-Kits. The 1:10 dilutions of cDNA synthesized from 250 ng total RNA are detected in the upper range of the applied standards. Therefore, also the 1:10 dilution of cDNA transcribed from 100 ng total RNA which is recommended as minimal amount of total RNA per reaction should be easily detectable with this assay.
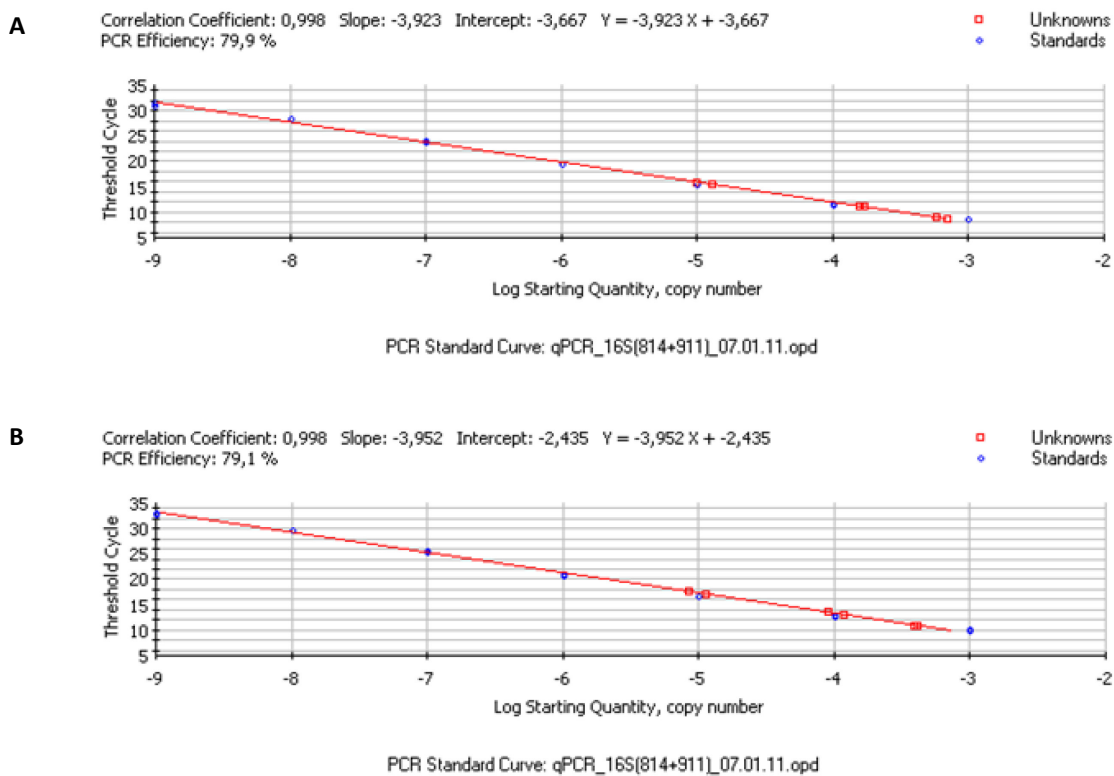
Figure 12: Standard curves and concentrations of tested samples of the 16S rRNA qPCR. A: Standard curve with tested samples reverse transcribed with RevertAid™ First Strand cDNA Synthesis Kit. B: Standard curve with samples reverse transcribed with SuperScript® Reverse transcriptase.

C.1.7.2. *gltA* qPCR assay

The expression of the mRNA of the *gltA* gene encoding the enzyme citrate synthase was de-tected with the *gltA* qPCR assay. Figure 13 shows the amplification curves of the standards 10^{-3} to 10^{-11} and of the negative controls - all in duplicates. The amplification curves of the negative controls show amplification after approximately 36 cycles similar to that of STD 10^{-11} (see Figure 13, additionally marked with an arrow). The duplicates are very consistent. The distances between the different standard dilutions at the interface with the threshold line show similar lenghts. Detection of *gltA* copies was possible for the standards 10^{-3} to 10^{-10} allowing the detection of *gltA* mRNA copies in samples between 8 and 7.89 x 10^7 copies.
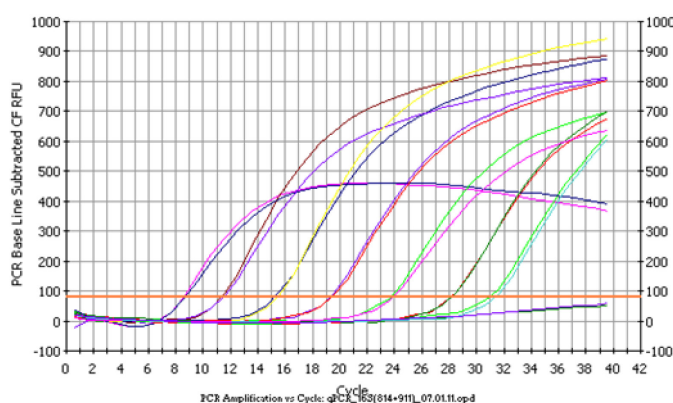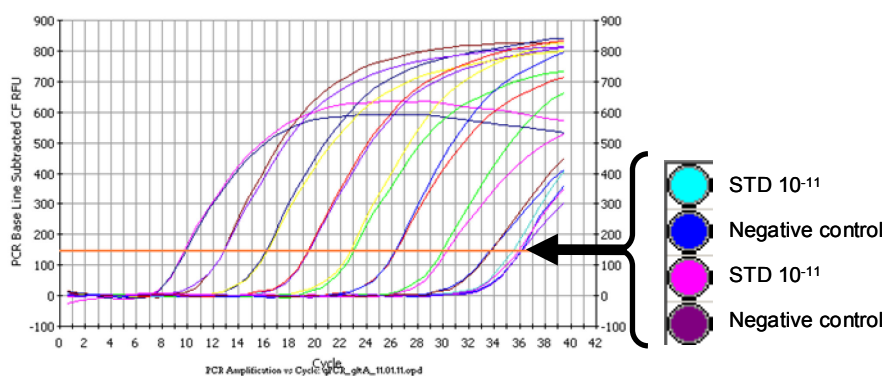

Figure 13: Amplification curves of standards and negative controls of the *gltA* qPCR test run.

Figure 14 A and B show the calculated standard curve. The PCR efficiency of about 99% and a correlation coefficient of 0.999 are almost perfect and confirm a high efficiency of this assay. Furthermore, the measured samples reverse transcribed with the two different RT-Kits are shown. The obtained results are comparable for the different dilutions of samples (1:10, 1:100, 1:1000). The expression of the citrate synthase seems to be very low since the 1:10 dilutions are detected near standard 10^{-7} and therefore contain only approximately 8,000 copies. This is more than four orders of magnitude lower than the expression of the 16S rRNA.

Figure 14: Standard curves of the *gltA* qPCR. A: Standard curve with samples reverse transcribed with RevertAid™ First Strand cDNA Synthesis Kit: B: Standard curve with samples reverse transcribed with SuperScript® Reverse transcriptase.

C.1.7.3. *nxrA1* qPCR assay

For the *nxrA1* qPCR the standard dilutions from 10^{-3} to 10^{-11} (shown here from 10^{-3} to 10^{-9}) were detectable (Figure 15). Similar distances between the amplification curves of the different standards applied in duplicate show an accurate dilution of the standards. With the standards diluted to 10^{-3} to 10^{-11} a detection of 3 to 2.53×10^{8} copies of the *nxrA1* gene is possible.
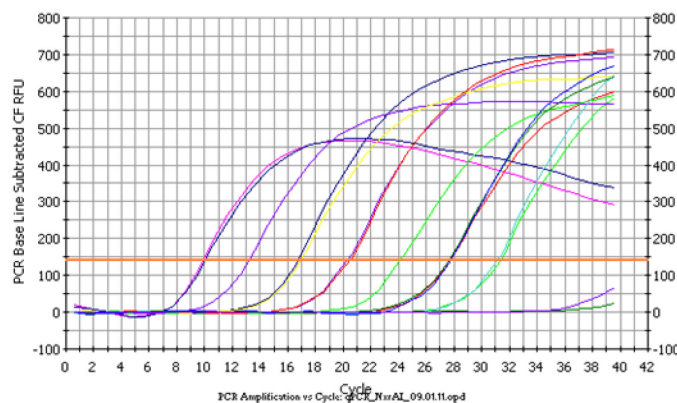
Figure 15: Amplification curves of standards and negative controls of the *nxrA1* qPCR test run.
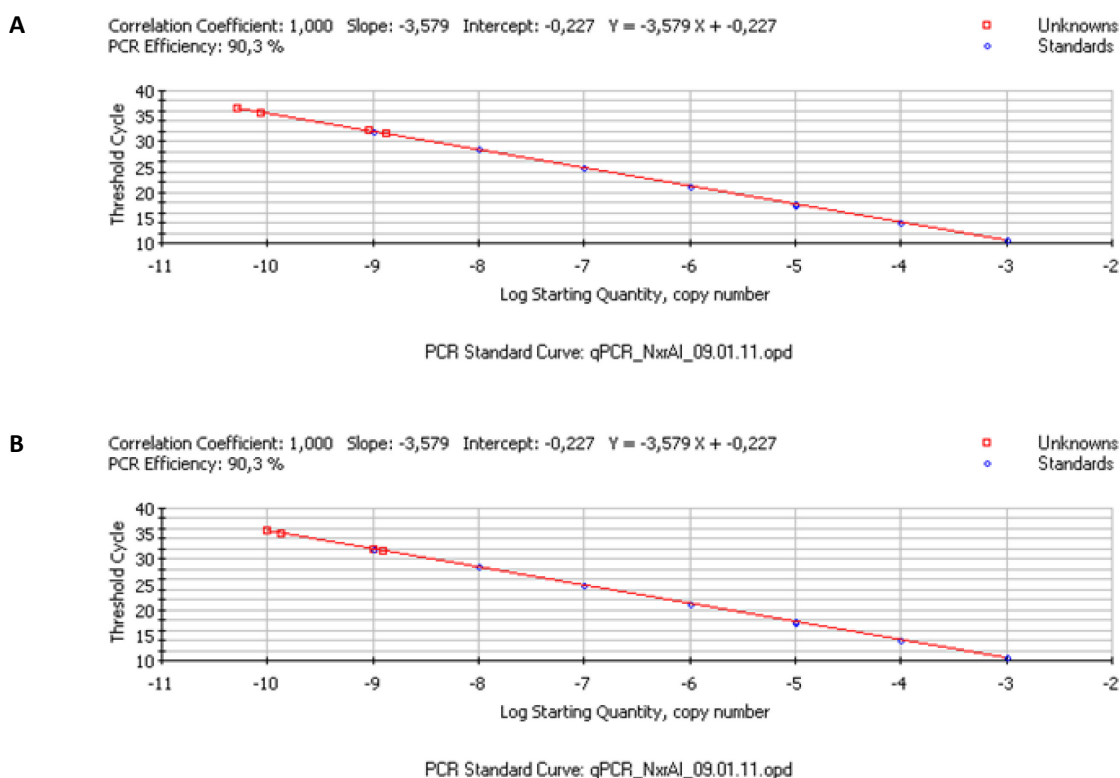
Figure 16: Standard curves of the *nxrA1* qPCR evaluation. A: Standard curve with samples reverse transcribed with RevertAid™ First Strand cDNA Synthesis Kit: B: Standard curve with samples transcribed with SuperScript® Reverse transcriptase.

The calculated standard curve for this qPCR is displayed in Figure 16 A and B. The PCR efficiency of 90.3% is very high and shows that the applied primer pair is well-suited for a qPCR assay. The correlation coefficient was perfect with 1.000.

The results for the samples synthesized with the two different reverse transcriptase enzymes are displayed in Figure 16 A and B, respectively. The *nxrA1* gene is expressed at a very low level. Therefore, standards diluted to 10^{-10} and 10^{-11} were included in further qPCR assays investigating this gene. The comparison of the two different RT enzymes shows similar results for the two first dilutions of the RT-product (1:10, 1:100). The 1:1000-dilution was not detectable.

C.1.7.4. *nxrA2* qPCR assay

Figure 17 shows the amplification curves for the standards of the *nxrA2* gene diluted to 10^{-4} to 10^{-9}. The range of detectable copy numbers of the *nxrA2* gene in an unknown sample therefore is between 930 and 9.3 x 10^7 copies. The duplicates of the standards fit very well and also the distances between the amplification curves of the different standards are similar showing accurate dilution.
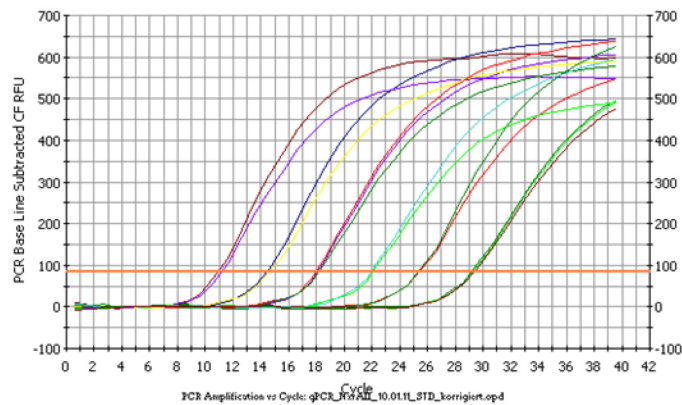
Figure 17: Amplification curves of standards and negative controls of the *nxrA2* qPCR test run.

The standard curves shown in Figure 18 show a high PCR efficiency of 88.0%. The correlation coefficient of 1.000 confirms accurate pipetting. The unknown samples transcribed with different RT-enzymes show similar results. This again confirms the same efficiency of the applied RT-enzymes. The expression of the *nxrA2* gene in comparison with the *nxrA1* gene is much higher.
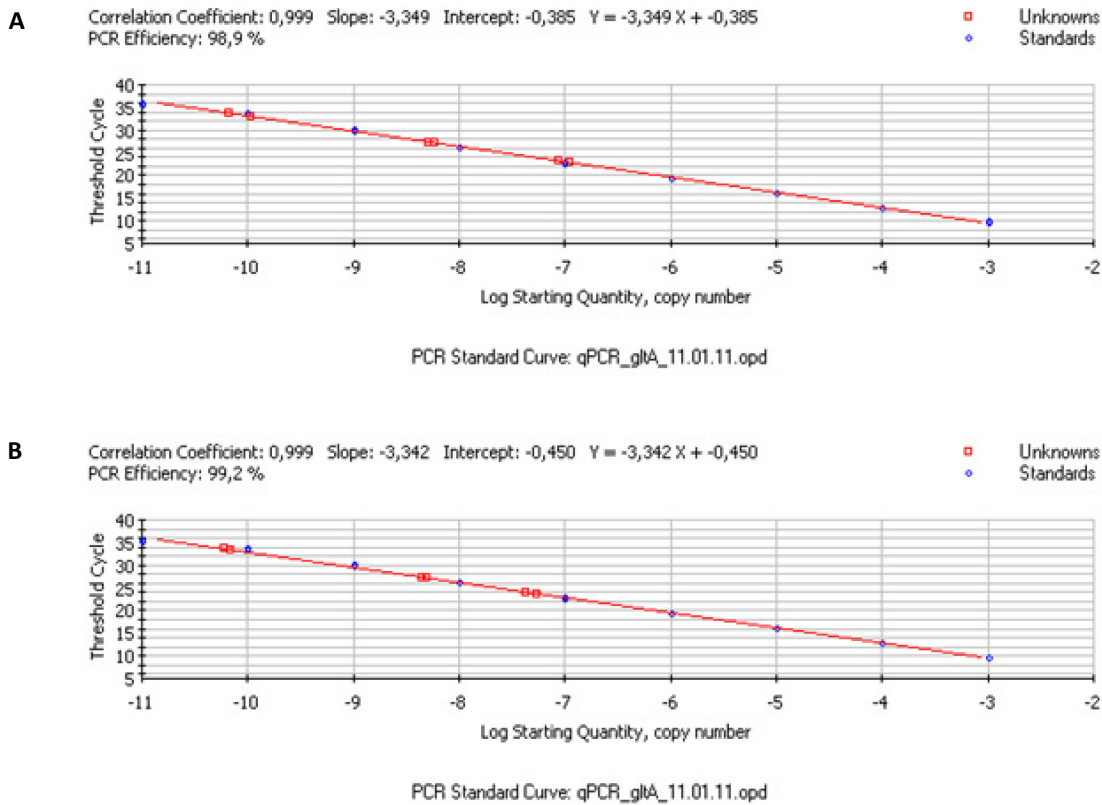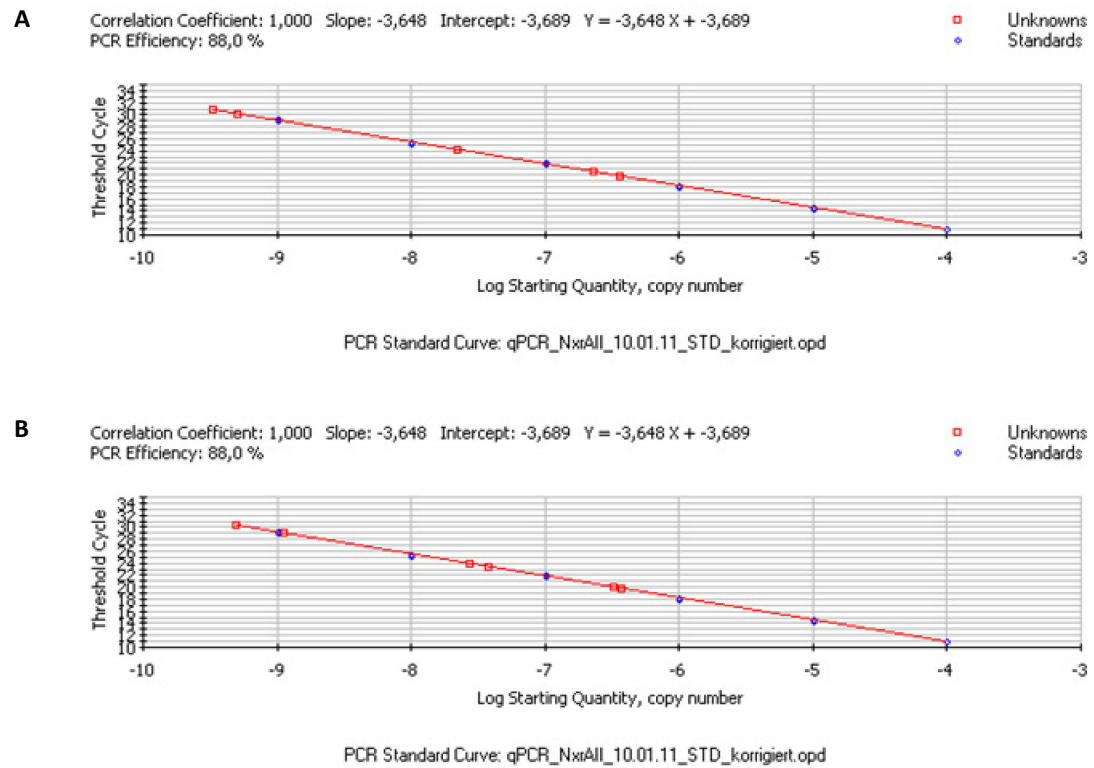
Figure 18: Standard curves of the *nxrA2* qPCR. A: Standard curve with samples reverse transcribed with RevertAid™ First Strand cDNA Synthesis Kit: B: Standard curve with samples transcribed with Super-Script® Reverse transcriptase.

C.1.8. Evaluation of the specificity of the qPCR assays by melting curve analyses

C.1.8.1. 16S rRNA qPCR assay

Figure 19 shows the melting curves of the evaluation of the 16S rRNA assay. All tested samples and standards showed similar melting curves. The negative controls show clearly that there was no product and therefore no amplification.
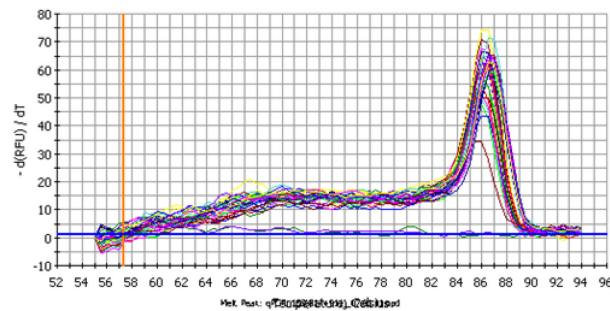
Figure 19: Melting curves of standards, negative controls and tested samples of the 16S qPCR evaluation.

C.1.8.2. *gltA* qPCR assay

Figure 20 A shows the melting curves of all standards and the negative controls of the *gltA* qPCR test run. The higher concentrated standards (10^{-3} to 10^{-9}) and the 1:10 and 1:100 dilutions of the samples show one peak at about 88 °C. The standards 10^{-10} and 10^{-11} as well as the 1:1000 dilutions of the samples and the negative controls in contrast show a second peak at about 78 °C.

Second peak of the standards 10^{-10} and 10^{-11}, the negative controls and the 1:1000 diluted unknown samples.
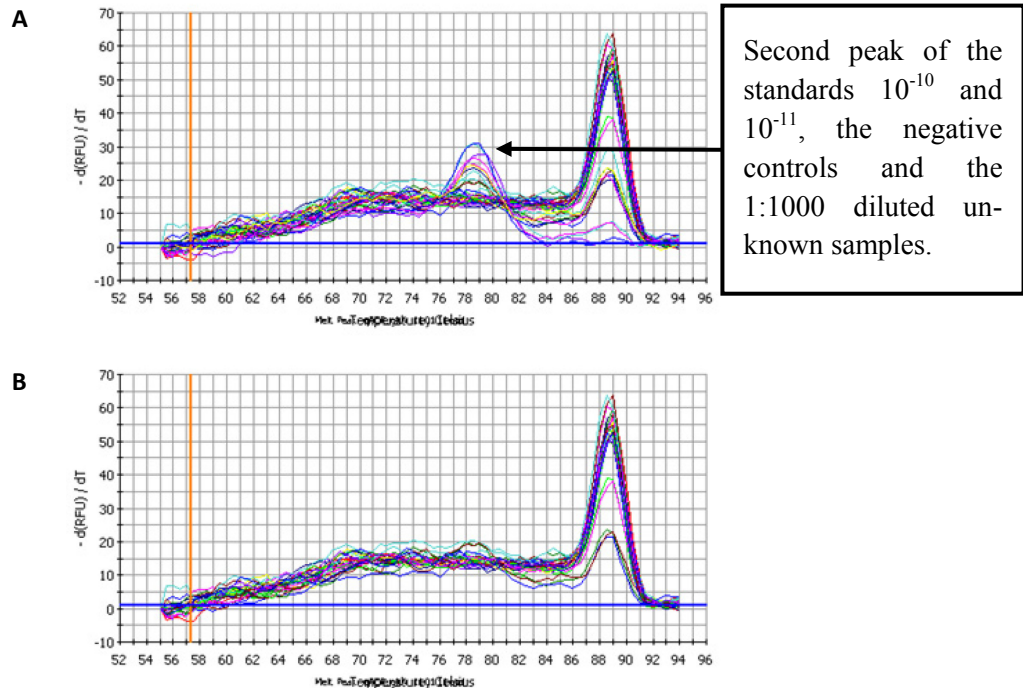
Figure 20: Melting curves of standards, negative controls and samples of the *gltA* qPCR evaluation. A: Melting curves of all reactions. B: Melting curves of all reactions without the negative controls, standards 10^{-10} and 10^{-11} and 1:1000 dilutions of the tested samples.

C.1.8.3. *nxrA1* qPCR assay

All melting curves of the qPCR assay specific for the *nxrA1* gene shows one sharp peak at about 85 °C for all standards (Figure 21). No primer dimer formation and no detectable peaks for the negative controls were observable.
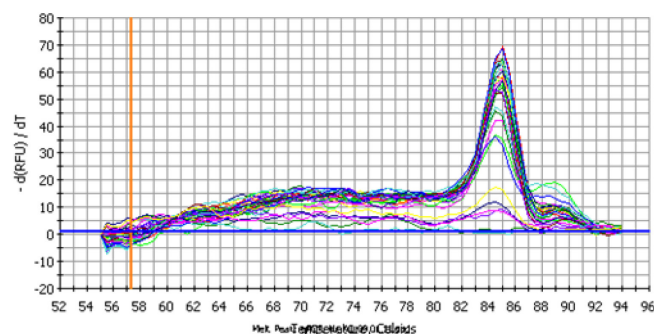
Figure 21: Melting curves of standards, negative controls and samples of the *nxrA1* qPCR test run.

C.1.8.4. *nxrA2* **qPCR assay**

Figure 22 shows the melting curves of all standards, tested samples and negative controls of the *nxrA2* qPCR evaluation. All standards have a peak at about 87 °C and no peaks are visible for the negative controls.
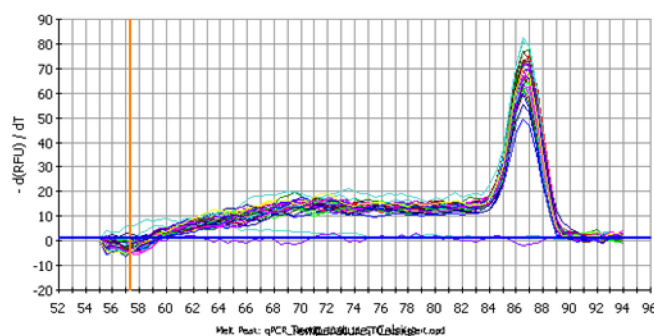
Figure 22: Melting curves of standards, negative controls and samples of the *nxrA2* qPCR test run.

C.1.9. **Evaluation of the specificity of the primers developed for qPCR by sequencing of RT-PCR products**

The same cDNA as applied in the qPCR test runs was used as template for end-point PCR. The primer pairs and PCR programs applied for these reactions were identical to the qPCR runs. The PCR products were sequenced to get more information about the specificity of the developed primers. The obtained sequences are shown in Table 30. The primer-targeting sites are marked grey at the beginning and end of the sequences. For the *gltA*- and *nxrA2*-specific primers the amplified fragments were 100% identical to the respective region in the target genes. In the obtained sequences for the 16S rRNA- and *nxrA1*-specific primers there were gaps (indicated as "-" in Table 30) in the obtained sequences when aligned against the gene sequences of the genome of *Ca*. N. defluvii. For the amplicon obtained by applying the 16S rRNA targeting primers three gaps were detected in the sequence and for the *nxrA1* targeting primers one gap was observed. The chromatograms for all sequences did not show any background signal suggesting that there was no unspecific amplification.

Table 30: Sequences obtained for direct sequencing of RT-PCR products for the examination of the primer-specificity. The grey region in the middle of the sequences is the overlapping part of the sequences obtained by using the the forward- and reverse-primer for the sequencing reaction, respectively.

Primer pair	Sequence	Alignment (BLAST)	
		Identities	Gaps
16S_814_FW / 16S_911_RV	CTAAGTGTCGGCGGGTTACCGCCGGTGCCGCAGCTAACGCATTAAGTATCC-GCCTGGGA-GTACGGCCGCAAGGTTGAA-CTCAAAGGAATTGACGG	95/98 (97%)	3/98 (3%)
gltA_FW / gltA_RV	GGACCTCTGCATGCGTCTCTTCAACGTCTGCGGAACGTCCCCGCTGTATGAGGTGGCCGTGGCGGTGGAGCAACTCGCGGGTGAGCGACTGACGGACAA	99/99 (100%)	0/99 (0%)
NxrA1_FW / NxrA_RV	CGGATGGCGGATACGTATAAGTTTGTCTATCACAACCGGG-GGATATTTACGTGCAGCGCATTCTCGATGCGTCGACCACGTTTTTCGGCTACAGCGCCGACGTCATGTTGAAGTCGG	117/118 (99%)	1/118 (0%)
NxrA2_FW / NxrA_RV	GCGTGTTCCACTTCGTGTACATGAACCGCGTCGATGTTTATCCGCAGCGGATGCTGGATGCCAGCGCCACCTGCTACGGATACAGCGCTGACGTCATGTTGAAGTCGG	108/108 (100%)	0/108 (0%)

C.1.10. Summarized results of the qPCR assay evaluations

Table 31: Summarized results of the qPCR evaluations including copy numbers of the tested samples.

Gene	Dilution of cDNA	Calculated copy number in original sample (multiplied with dilution factor)		Standards used	PCR Efficiency [%]	Correlation Coefficient (R2)	Melting temperature [° C]
		Fermentas	Superscript				
16S	10	5,6E+09	3,97E+09	10^{-3} - 10^{-9}	79%	0.998	86
	100	1,45E+10	9,29E+09				
	1000	1,02E+10	9,82E+09				
gltA	10	8,44E+04	4,19E+04	10^{-3} - 10^{-11}	98,9%	0.999	89 / 78*
	100	4,87E+04	4,20E+04				
	1000	8,52E+03	6,35E+03				
NxrA1	10	2,72E+03	2,70E+03	10^{-3} - 10^{-9}	90,3%	1.000	84
NxrA2	10	2,75E+06	3,25E+06	10^{-4} - 10^{-9}	88%	1.000	86
	100	2,03E+06	3,02E+06				
	1000	3,94E+05	7,45E+05				

* melting temperature of the second peak in the negative controls and standards 10^{-10} and 10^{-11}

C.2. Gene expression study

C.2.1. Incubation of „*Candidatus* Nitrospira defluvii" under different environmental conditions

Five different incubations of *Ca.* N. defluvii cultures were performed in duplicate. During the incubation time of 53 hours in case of the oxic incubations and 69 hours in case of the anoxic incubations repeatedly samples of 1 mL were taken to check the concentrations of nitrite in the oxic incubations and nitrate in the anoxic incubations. The concentrations were checked with nitrite (0-80 mg x L^{-1}) and nitrate (0-500 mg x L^{-1}) test strips. The timepoints at which samples were taken or nitrite or nitrate was added are listed in Table 32.

Table 32: Time points of sampling for checking concentrations of nitrite, nitrate or pyruvate.

sampling time [h]	oxic incubations			anoxic incubations	
	0.3 mM	3 mM	15 mM	NO_3^- + pyruvate	control (without NO_3^- and pyruvate)
2.5	+	+	+	+	+
5.0	+	+	+	+	+
12.0	+	-	-	-	-
19.0	+	+	+	+	+
22.0	+	-	-	-	-
23.5	+	-	-	-	-
25.0	+	+	+	+	+
29.0	+	+	+	+	+
35.0	+	+	-	-	-
43.0	+	+	+	+	+
45.5	+	-	-	-	-
47.0	-	-	-	+	+
47.5	+	-	-	-	-
49.0	+	+	+	-	-
51.0	+	-	-	+	+
52.0	+	-	-	-	-
53.0	+	+	+	-	-
69.0	-	-	-	+	+

+ sample taken   - no sample taken

  nitrite/nitrate concentration adjusted.

Furthermore, nitrite measurements via Griess reaction were performed to determine the exact nitrite concentration of the samples taken during the incubation. These measurements were performed for the 3 mM and 15 mM nitrite incubations. The nitrite concentrations are illustrated in Figure 23 A and B. For the 0.3 mM nitrite incubations this measurement was not performed because nitrite was added in very short intervals. The concentration ranged between 0 and 0.3 mM nitrite.
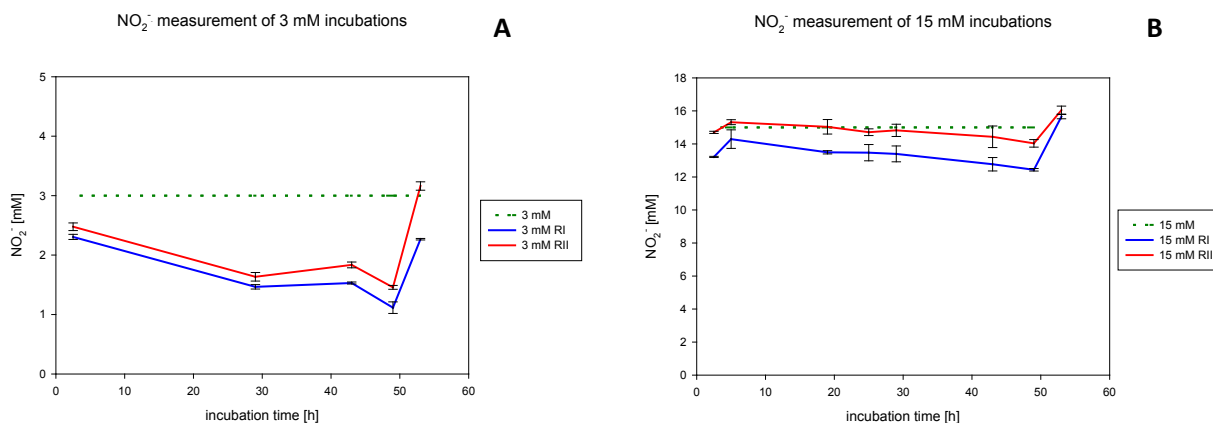
Figure 23: A: Nitrite concentrations during 3 mM incubations. B: Nitrite concentrations during 15 mM incubations.

For the oxic incubations with 3 mM nitrite the actual concentrations were in a range between 1.5 and 3 mM nitrite during the incubation. Nitrite was added twice, once after 35 hours and once four hours before harvesting of the cells.

In case of the oxic incubations with 15 mM nitrite the concentrations were always in a range between 12.5 and 16 mM nitrite. Here, nitrite was added once after 49 hours. The measurement revealed that the nitrite concentration in replicate II was always higher than in replicate I by about 1.5 mM. For the oxic incubation with 0.3 mM nitrite consumed nitrite was replaced 12 times.

In the anoxic incubations there was no nitrate-consumption visible during the whole incubation period. However, a consumption of pyruvate was observable. This was measured qualitatively by Bela Hausmann with capillary electrophoresis (method not shown). Therefore, anoxic pyruvate solution was added twice.

C.2.2. Isolation of total RNA from "*Candidatus* Nitrospira defluvii" cultures

Table 33 shows the determined concentrations of isolated nucleic acids after the isolation of total RNA performed according to B.9. To check for the quality of the RNA an agarose gel electrophoresis was performed (Figure 24). The upper band represents the 23S rRNA, the lower one the 16S rRNA. The 5S rRNA is not visible because due to its length of approximately 120 bp (Szymanski *et al.*, 2002) it gets lost during the purification on a column. The 23S and 16S rRNA is visible due to its high abundance. Other RNA forms like mRNA are also present in the gel but not visible due to their low abundance. On the gel only the samples containing high concentrations of RNA were applied. Lowly concentrated RNA solutions contained insufficient RNA to be visible on a gel. Since all samples were treated the same way the quality of the more highly concentrated samples should be representative for the quality of all samples.

Table 33: RNA concentrations measured with NanoDrop® ND-1000 spectrophotometer. RI = replicate I; RII = replicate II; marked grey = anoxic incubation; control: incubations without substrate;

Sample	nucleic acid concentration [ng x µL^{-1}]
0.3 mM NO$_2^-$ RI	27.06
0.3 mM NO$_2^-$ RII	35.76
3 mM NO$_2^-$ RI	33.68
3 mM NO$_2^-$ RII	80.46
15 mM NO$_2^-$ RI	44.84
15 mM NO$_2^-$ RII	38.12
NO$_3^-$ + pyruvate RI	13.17
NO$_3^-$ + pyruvate RII	103.22
control RI	21.60
control RII	60.18
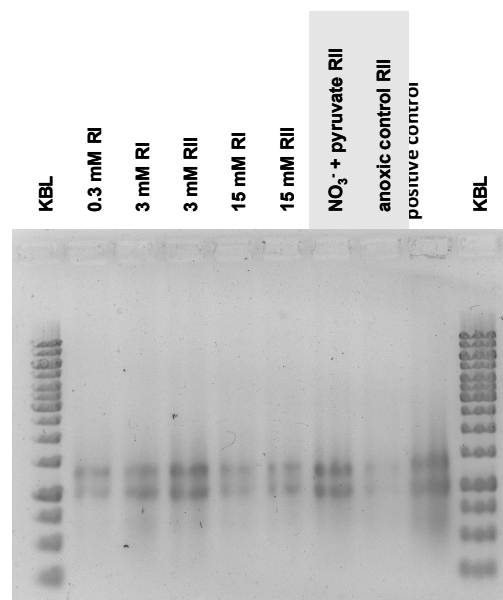
Figure 24: Agarose gel eclectrophoresis photo of isolated RNA. Lane 1-7: isolated RNA of the incubation experiments. Lane 8: positive control - *Ca.* N. defluvii RNA from bioreactor culture provided by Christiane Dorninger. marked grey = anoxic incubation;

C.2.3. DNase treatment

In Figure 25 A-C the PCR products of reactions using DNase treated RNA solution as template are shown. In this way the RNA solutions were checked for remaining DNA. The treatment was performed several times until there was no band visible on the gel anymore. The samples shown in Figure 25 C were not free of DNA after five DNA digestions for which reason the RNA was precipitated and once again treated with DNase. After this step the RNA was free of DNA. To use always the same amount of RNA for each RT reaction the concentrations were measured using the Quant-iT™ RiboGreen® RNA Assay Kit (B.13.2). The measured concentrations are shown in Table 34.
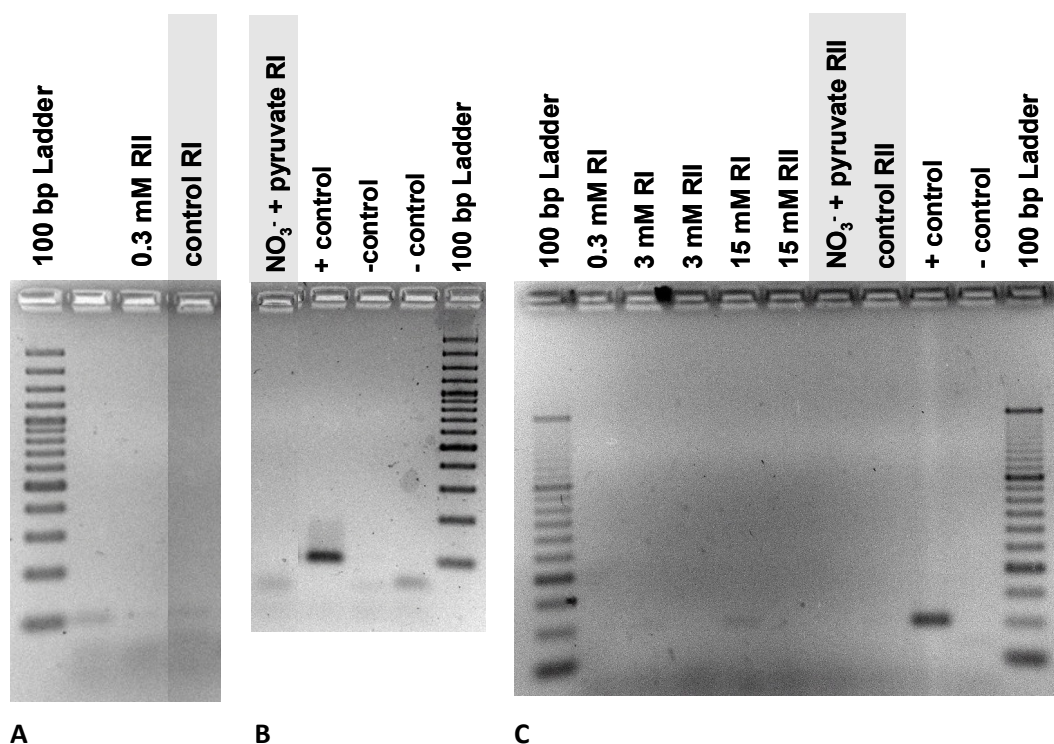
Figure 25: A-C: Gel picture of PCRs performed on DNase treated RNA solutions. Pictures were modified by splicing together with Adobe Photo Shop-software. marked grey = anoxic incubation;

C.2.4. cDNA synthesis applying reverse transcription (RT)

The cDNA synthesis was performed as described in B.12. The use of the minimum recommended amount of 100 ng total RNA per RT reaction was based on the low concentrations of total RNA after isolation and DNase-treatment. For all samples 100 ng were used with one exception. For the incubation with NO_3^- + pyruvate replicate I only 23 ng could be used due to its extremely low concentration. The concentrations of the RNA solutions as well as the actually used amounts of RNA are shown in Table 34 for each sample.

Table 34: Measured RNA concentrations after isolation of RNA using the Quant-iT™ RiboGreen® RNA Assay Kit. P = pyruvate, control = no nitrate or pyurvate added;

Sample	0.3 mM NO_2^-		3mM NO_2^-		15 mM NO_2^-		NO_3^- + P		control	
	RI	RII	RI	RII	RI	RII	RI	RII	RI	RII
Concentration of isolated total RNA [ng μL^{-1}]	10.57	22.90	14.87	26.69	10.52	13.36	2.16	29.31	17.28	16.69
Volume to-use for 100 ng total RNA [μL]	9.46	4.37	6.73	3.75	9.51	7.48	46.38	3.41	5.79	5.99
Actually used volume of total RNA [μL]	9.46	4.37	6.73	3.75	9.51	7.48	10.50	3.41	5.79	5.99
Actually used amount of total RNA [ng]	100	100	100	100	100	100	27.3	100	100	100

Following, a PCR for each examined gene and each sample was conducted to check if the reverse transcription was successful. Figure 26 shows the results of the gelelectrophoretical analysis of the PCR products. It shows that the multiplexed RT reactions worked out well for all examined samples confirmed by single bands. Furthermore, different gene expression patterns were observable for the *gtlA* as well as for the *nxrA1* gene depending on the incubation conditions. To reveal the observed differences in the gene expression levels in more detail, qPCR was performed.
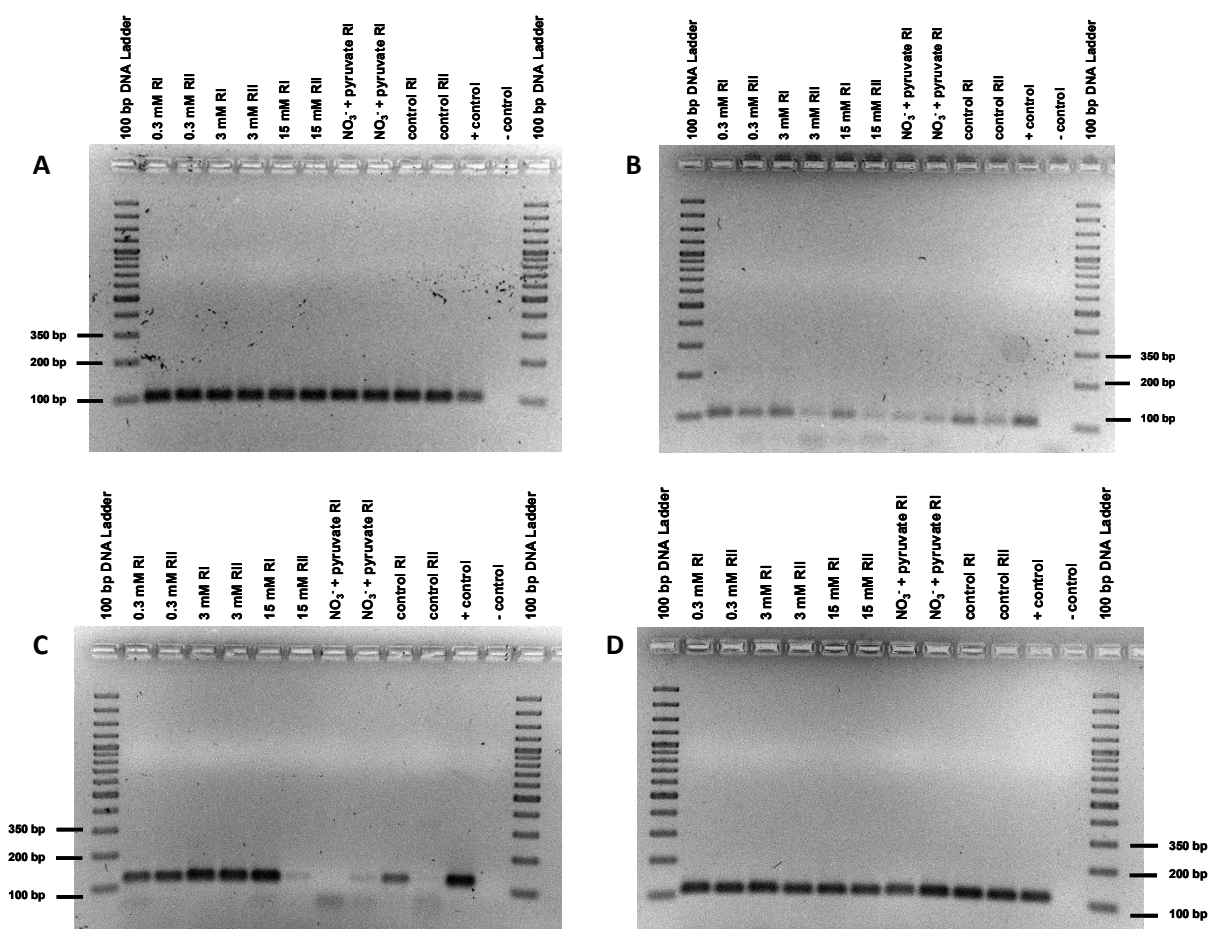
Figure 26: Gel pictures of RT-PCRs for each examined gene. A: 16S rRNA; B: *gltA*; C: *nxrA1*; D: *nxrA2*;

C.2.5. Quantitative real-time PCR

In Table 35 the PCR efficiency as well as the correlation coefficient for each performed qPCR run is shown. The efficiencies were all above 80%. An efficiency of 100% would be desirable meaning a doubling of the PCR products after each cycle. This, however, is unlikely due to the presence of inhibitory substances in the reaction mixture. Therefore, a minimal efficiency was set with 75%. The correlation coefficients were all above 0.997 indicating a high pipetting accuracy. The calculation of the copy numbers of the tested samples was performed using the iCycler iQ Real-Time PCR Detection system and the included software.

Table 35: PCR Efficiencies and correlation coefficients of the performed qPCR runs.

qPCR assay	PCR efficiency [%]	Correlation coefficient (R^2)
16S rRNA	81.6	0.999
gltA	95.6	0.999
nxrA1	82.8	0.999
nxrA2	84.1	0.997

The calculation of the copy number of each transcript in each sample was performed for all replicates according to B.14.5. The results of this calculation are shown in Table 36, whereby the copy numbers of the triplicates where averaged.

Table 36: Calculated copy numbers of examined samples. Triplicates were averaged.

Sample	16S rRNA		*gltA*		*nxrA1*		*nxrA2*	
	copy number*	sd	copy number*	sd	copy number*	sd	copy number*	sd
0.3 mM RI	3,18E+08	6,83E+07	2,85E+03	5,21E+02	1,17E+03	2,09E+02	1,75E+05	5,64E+04
0.3 mM RII	4,93E+08	2,57E+07	1,74E+03	1,58E+01	2,61E+03	3,46E+02	2,74E+05	3,41E+04
3 mM RI	2,12E+08	3,35E+07	3,14E+03	5,45E+02	3,11E+04	1,23E+04	1,86E+05	8,32E+04
3 mM RII	2,40E+08	3,18E+07	1,45E+03	9,30E+01	3,22E+04	3,38E+03	6,30E+04	2,41E+04
15 mM RI	1,90E+08	9,46E+06	6,61E+02	1,07E+02	3,62E+04	4,92E+03	1,29E+04	5,46E+03
15 mM RII	1,90E+08	2,75E+07	1,29E+02	5,96E+00	2,71E+01	1,16E+01	3,35E+04	1,66E+04
$NO_3^- + P$ RI	2,14E+07	2,60E+06	5,19E+01	1,06E+01	6,68E+00	1,24E+00	1,22E+04	4,03E+03
$NO_3^- + P$ RII	1,02E+08	1,51E+07	1,24E+02	2,54E+00	1,13E+01	3,09E+00	7,47E+04	3,08E+04
control RI	4,35E+08	3,74E+07	1,65E+03	9,93E+01	1,97E+02	2,69E+01	3,21E+05	2,43E+04
control RII	2,01E+08	1,59E+07	7,48E+02	2,36E+02	5,56E+01	9,70E+00	9,27E+04	2,59E+04

* arithmetic average out of three replicates

sd … standard deviation

C.2.5.1. Expression of the 16S rRNA gene

Figure 27 shows the expression levels of the 16S rRNA gene in copy numbers for all incubations. The expression levels between the biological replicates were consistent since they were always within one order of magnitude. The similar copy numbers of all incubations except one is due to the fact that the same amounts of total RNA were used for the RT reactions. Only for incubation NO_3^- + pyruvate replicate I a lower amount of total RNA was used resulting in a considerably lower copy number than replicate II. These values were adducted for the standardization of the expression of the other genes.

Expression of the 16S rRNA gene

Figure 27: Expression of the 16S rRNA gene. Oxic incubations: Concentration of nitrite used for the respective incubation shown in mM; Anoxic incubations (marked grey): NO_3^- + P = incubation with 0.5 mM pyruvate and 2.5 mM nitrate; control = incubation without nitrate and pyruvate added; RI = replicate I; RII = replicate II;

C.2.5.2. Expression of the *gltA* gene

Figure 28 shows the copy numbers of the *gltA* mRNA relative to the copy number of the 16S rRNA of the respective incubation. The replicates were all within one order of magnitude. For the expression levels of the 3 mM nitrite incubations a slightly higher expression of the *gltA* gene was observable. However, obvious differences between the different incubations could not be observed.

Figure 28: Expression of the *gltA* gene relative to the expression of the 16S rRNA gene multiplied by 10^7. Oxic incubations: Concentration of nitrite used for the respective incubation shown in mM; Anoxic incubations (marked grey): NO$_3^-$ + P = incubation with 0.5 mM pyruvate and 2.5 mM nitrate; control = incubation without nitrate and pyruvate added; RI = replicate I; RII = replicate II;
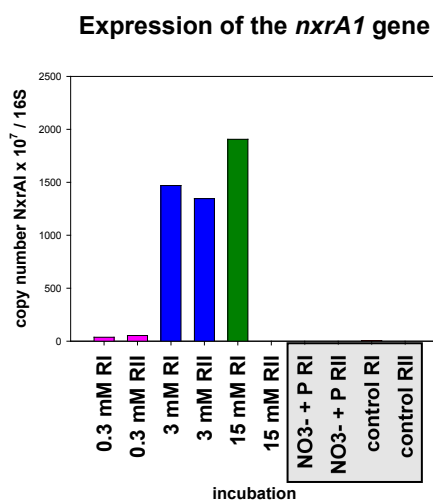
Figure 29: Expression of the *nxrA1* gene relative to the expression of the 16S rRNA gene multiplied by 10^7. Oxic incubations: Concentration of nitrite used for the respective incubation shown in mM; Anoxic incubations (marked grey): NO$_3^-$ + P = incubation with 0.5 mM pyruvate and 2.5 mM nitrate; control = incubation without nitrate and pyruvate added; RI = replicate I; RII = replicate II;

C.2.5.3. Expression of the *nxrA1* gene

The expression of the *nxrA1* gene was considerably different between the different incubations as shown in Figure 29. Again, the expression of this gene relative to the 16S rRNA gene expression is shown. The expression of the *nxrA1* gene was about 30 times higher in the incubations with 3 mM nitrite than in the incubations with 0.3 mM nitrite incubations. Replicate I of the 15 mM nitrite incubation exhibited a similarly high expression level as the 3 mM incubations. Interestingly, replicate II of the 15 mM incubation did not behave similar to replicate I and showed a pretty low expression level of the *nxrA1* gene. The anoxic incubations showed no detectable expression of this gene. To completely rule out DNA contamination, especially for the confirmation of the results obtained for the 15 mM incubations, untranscribed RNA of all samples was applied to an *nxrA1*-specific qPCR run showing no amplification at all. Therefore, the possibility of DNA-contamination could be ruled out.

C.2.5.4. Expression of the *nxrA2* gene

The obtained numbers for the expression of the *nxrA2* gene relative to the expression of the 16S rRNA gene are visualized in Figure 30. The expression levels are within one order of magnitude both for the oxic and anoxic incubations. Only for the 15 mM incubations there seems to be a little lower expression level.

Expression of the *nxrA2* gene

Expression of the *nxrA1* / *nxrA2* gene
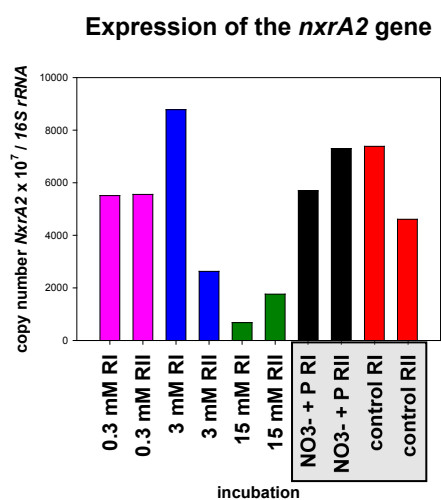
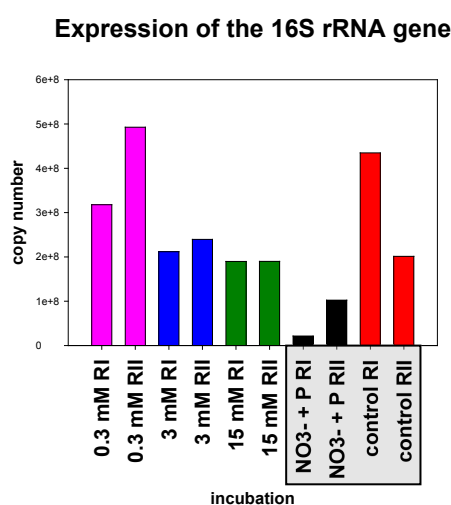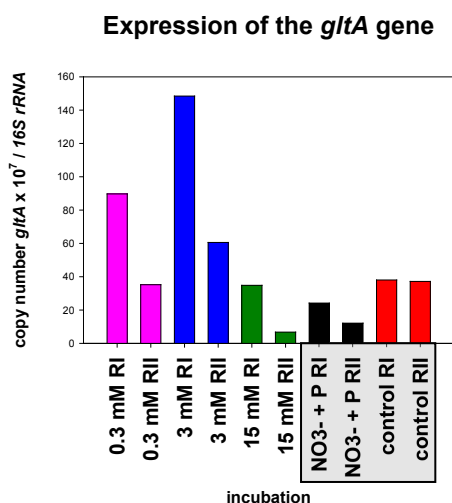**Figure 30: Expression of the *nxrA2* gene relative to the expression of the 16S rRNA gene. Oxic incubations: Concentration of nitrite used for the respective incubation shown in mM; Anoxic incubations (marked grey): NO_3^- + P = incubation with 0.5 mM pyruvate and 2.5 mM nitrate; control = incubation without nitrate and pyruvate added; RI = replicate I; RII = replicate II;**
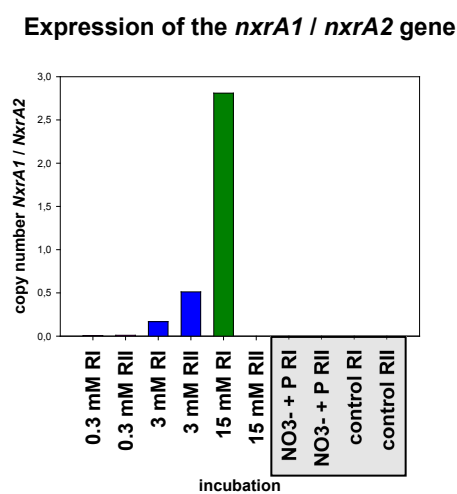
Figure 31: Comparison of the expression levels of the *nxrA1* gene and *nxrA2* gene. Oxic incubations: Concentration of nitrite used for the respective incubation shown in mM; Anoxic incubations (marked grey): NO_3^- + P = incubation with 0.5 mM pyruvate and 2.5 mM nitrate; control = incubation without nitrate and pyruvate added; RI = replicate I; RII = replicate II;

C.2.5.5. Expression of the *nxrA1* gene compared to the *nxrA2* gene

Figure 31 shows that the *nxrA2* genes show a much higher expression in the incubations with 0.3 mM nitrite as well as in the anoxic incubations. There the proportion of the *nxrA1* transcript makes up only a small fraction of all *nxrA* transcripts. In the incubations with 3 mM nitrite the expression of the *nxrA1* gene is considerably higher but still not exceeding the expression of the *nxrA2* expression level. The highest *nxrA1* / *nxrA2* ratio was observed for the 15 mM nitrite replicate I incubation where the expression of *nxrA1* exceeds the expression of the *nxrA2* gene by about three times. This data does not fit with the obtained data for replicate II. There, the expression of the *nxrA1* in comparison to the expression of *nxrA2* is negligible.

C.3. Investigation of the coexistence of three subpopulations of *Nitrospira* sublineage II in the wastewater treatment plant of the University of veterinary medicine Vienna applying quantitative FISH

C.3.1. Quantification of the abundance of the genus *Nitrospira*

Cells belonging to the genus *Nitrospira* made up between 7.8 and 20.2 percent of the whole bacterial biomass during the examined period between 2004 and 2010 (Figure 32). Figure 33 shows the cumulative curves calculated for each sample. Here the change of the biovolume fraction after each further included picture in the analysis is visible. If the biovolume fraction is not changing anymore the number of pictures taken can be assumed to be sufficient for giving significant results. This is the case for all examined samples.
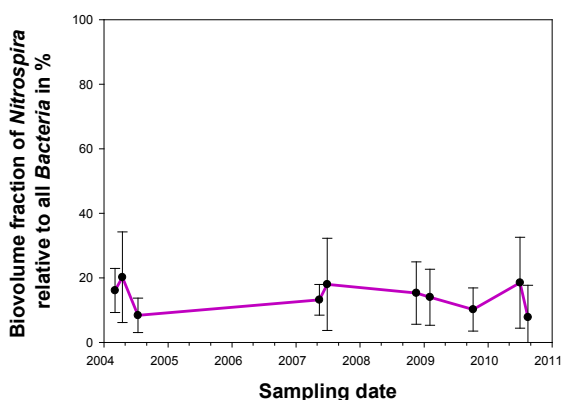
Figure 32: Biovolume fractions of the genus *Nitrospira* (Ntspa662) relative to all bacteria (EUB338Mix). The error bars show the standard deviation for 30 pictures.
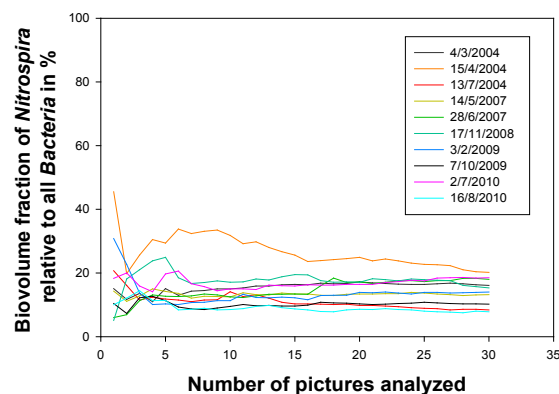
Figure 33: Cumulative curves of the quantification of the biovolume fractions of the genus *Nitrospira* (Ntspa662) relative to all bacteria (EUB338Mix).

C.3.2. Quantification of the biovolume fraction of *Nitrospira* sublineage II relative to the genus *Nitrospira*

Figure 34 shows the biovolume fraction of *Nitrospira* sublineage II of all *Nitrospira* cells in the examined samples. The biovolume fractions were relatively constant over time ranging between 63.9 and 75.1 percent during the sampling period. This is also confirmed by the standard deviations shown in Figure 34. Additionally, the cumulative curves are visualized in Figure 35 where all calculated biovolume fractions can be assumed to be stable after approximately 15 pictures taken.
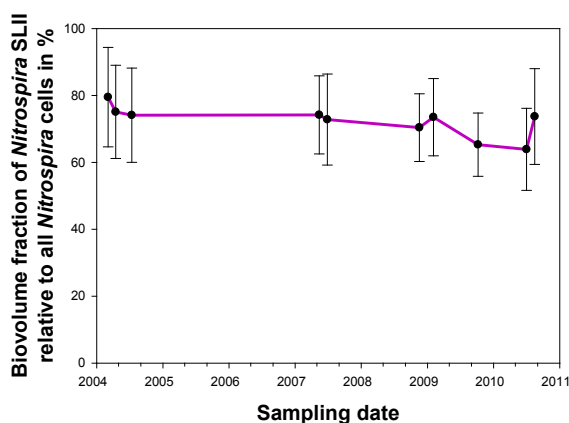
Figure 34: Biovolume fractions of *Nitrospira* sublineage II (Ntspa1151) relative to all *Nitrospira* (Ntspa662) cells. The error bars show the standard deviation for 30 pictures.
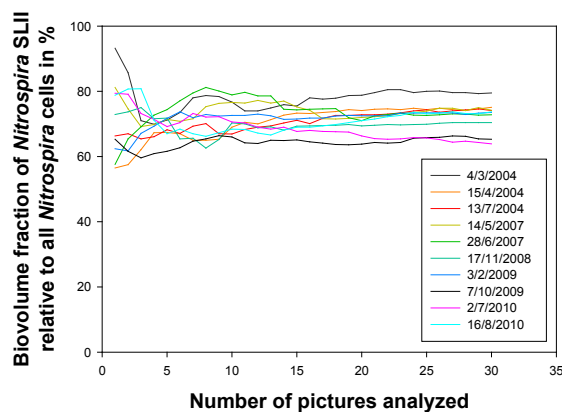
Figure 35: Cumulative curves of the quantification of the biovolume fractions of *Nitrospira* sublineage II (Ntspa1151) relative to all *Nitrospira* (Ntspa662) cells.

C.3.3. Quantification of the cluster 2.4 of *Nitrospira* sublineage II

For cluster 2.4 labelled by probe Ntspa195 a clear shift in their abundance was visible over the examined period (Figure 36). In the beginning of the sampling period in the year 2004 cluster 2.4 made up only about 20 percent of all sublineage II cells. A sharp increase of the biovolume fraction occurred between 2007 and 2010 up to a biovolume fraction of 76.6 percent. The cumulative curves in Figure 37 show more or less constant biovolume fractions from picture number 15 on for all samples, assuring the validity of the calculated biovolume fractions.
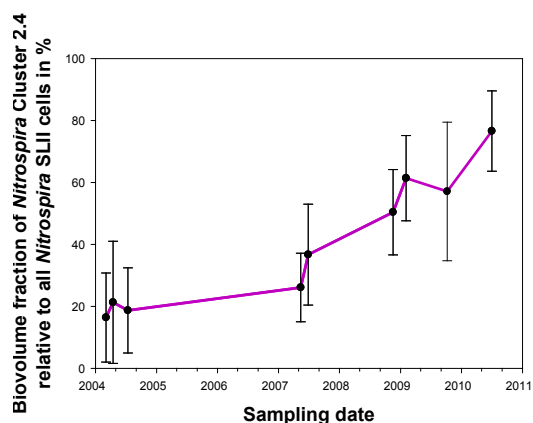
Figure 36: Biovolume fractions of *Nitrospira* cluster 2.4 (Ntspa195) relative to *Nitrospira* sublineage II (Ntspa1151). The error bars show the standard deviation for 30 pictures.
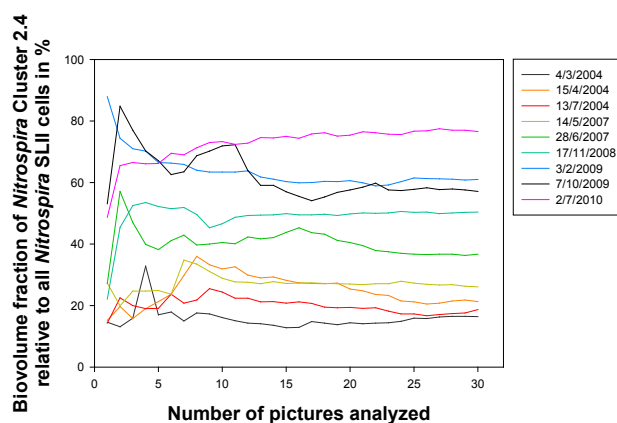
Figure 37: Cumulative curves of the quantification of the biovolume fractions of *Nitrospira* subpopulation Cluster 2.4 (Ntspa195) relative to all *Nitrospira* SLII (Ntspa1151) cells.

C.3.4. Quantification of the cluster 2.5 of *Nitrospira* sublineage II

Cluster 2.5 showed a more or less stable abundance in all samples (Figure 38). In the beginning cells of this subpopulation made up about 30 percent of the whole *Nitrospira* sublineage II bio-mass while in the end only about 10 percent were assignable to this subpopulation. However, considering the large standard deviations, a statement about a slightly decreasaing shift in the abundance over the examined period would not be reliable. The cumulative curves in Figure 39 show that the number of pictures taken was sufficient.
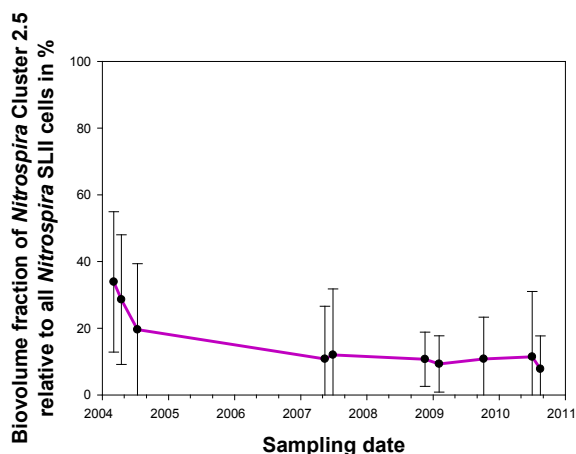
Figure 38: Biovolume fractions of *Nitrospira* cluster 2.5 (Ntspa256Cl2) of *Nitrospira* sublineage II (Ntspa1151). The error bars show the standard deviation for 30 pictures.
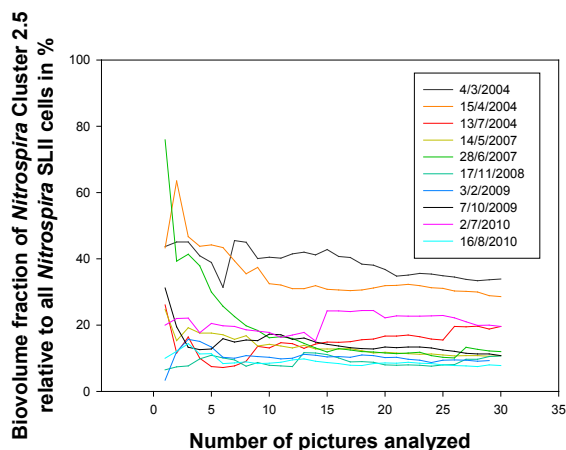
Figure 39: Cumulative curves of the quantification of the biovolume fractions of *Nitrospira* subpopulation cluster 2.5 (Ntspa256Cl2) relative to all *Nitrospira* sublineage II (Ntspa1151) cells.

C.3.5. Quantification of the cluster 2.2 of *Nitrospira* sublineage II

This subpopulation could not be quantified due to the very weak signal of the used probe. The signal of this probe was detectable in the microscope by eye but it was not possible to take pictures of sufficient quality of these colonies. An upregulation of the signal gain to improve the recording of the FISH-labelled cells also led to increased detection of aufofluorescence (AF) signal which covered the signal of the cells. Another fact disabling the quantification was that cells belonging to this subpopulation were extremely rare which would call for taking much more pictures to get statistically significant results. This was impaired by the AF problem mentioned before.

Summarizing all obtained results, a list of all quantified biovolume fractions of the different examined taxa is shown in Table 37.

Table 37: Biovolume fractions of all quantified groups in all examined samples.

sampling date	Biovolume fraction of the genus *Nitrospira* relative to all bacteria [%]	Biovolume fraction of *Nitrospira* sublineage II relative to the genus *Nitrospira* [%]	Biovolume fraction of *Nitrospira* cluster 2.4 relative to *Nitrospira* sublineage II [%]	Biovolume fraction of *Nitrospira* cluster 2.5 relative to *Nitrospira* sublineage II [%]
2004-03-04	79,5	16,1	16,4	33,9
2004-04-15	75,1	20,2	21,3	28,6
2004-07-13	74,1	8,4	18,7	19,6
2007-05-14	74,2	13,2	26,1	10,8
2007-06-28	72,8	18,0	36,7	12,0
2008-11-17	70,4	15,3	50,4	10,7
2009-02-03	73,5	14,0	61,4	9,3
2009-10-07	65,3	10,2	57,1	10,8
2010-07-02	63,9	18,5	76,6	11,4

D. <u>Discussion</u>

D.1. Development of a quantitative real-time PCR assay for the detection of the expression of several genes in "*Candidatus* Nitrospira defluvii"

D.1.1. Advantages and disadvantages of the used SYBR®Green chemistry for qPCR

Quantitative real-time PCR in combination with foregoing reverse transcription of mRNA targets (RT-qPCR) is a very sensitive method for the quantification of expression levels of genes (Nolan *et al*., 2006). To date, there are several qPCR applications available, all having their advantages and disadvantages (Wong and Medrano, 2005). The applied method in this study was the SYBR®Green chemistry with the big advantage that any primer pair can be used as long as a certain product length is not exceeded. Thereby, no additional probes have to be designed in contrast to quantification using the TaqMan™ chemistry (Holland *et al*., 1991).

Like every molecular method, also the SYBR®Green chemistry has its disadvantages. The first drawback of this method is an inhibiting effect of the SYBR®Green fluorescence dye on the PCR-reaction if it is too highly concentrated (Monis *et al*., 2004). In this study this problem was circumvented by the use of a ready-to-use Kit from Invitrogen. Another disadvantage is that it is not possible to detect multiple target genes in a single (multiplex) reaction, contrary to TaqMan™ chemistry where several probes labelled with different fluorescence dyes can be applied simultaenously (Nolan *et al*., 2006).

The main drawback of SYBR®Green chemistry, however, is the co-detection of unspecific amplicons such as primer dimers. Therefore, it is of greatest importance to make sure that the primers are highly specific in order to rule out any unspecific amplification (Dorak, 2006). By contrast, in case of TaqMan™ chemistry, the fluorescence dye is only released if all three oligonucleotides bind correctly, and therefore co-detection of unspecific amplicons is not an issue.

D.1.2. Methods for the normalization of gene expression levels

An important challenge when designing a RT-qPCR assay is to develop an appropriate method for the normalization of the measured gene expression. Under ideal conditions, for example for planktonic cells, mRNA expression levels can be normalized against cell numbers. This is difficult when working with tissue samples or cultures where the cell number is not determinable (Wong and Medrano, 2005). For *Ca*. N. defluvii cultures, cell counting is not feasible due to their growth in dense flocs. In such cases, control genes are often used to normalize the expression levels of the genes of interest. Thereby, the ideal control gene should be expressed constitutively regardless of the experimental conditions (Wong and Medrano, 2005). For this purpose, so-called "housekeeping" genes are often used (Schmittgen and Zakrajsek, 2000).

Another possibility is to normalize against the total RNA amount which has to be measured applying an accurate method like RiboGreen® (Bustin, 2000). However, this method is not as reliable as reference genes, since total RNA levels are affected by cellular processes, RNA quality and the reverse transcription efficiency (Wong and Medrano, 2005).

According to the current opinion, the best solution for the normalization is the employment of multiple housekeeping genes (Vandesompele *et al*., 2002). In this study, the development of multiple assays for different housekeeping genes was not feasible since to date little is known about the expression stability of certain genes in *Ca*. N. defluvii.

Therefore, in this study, the 16S rRNA was chosen for the normalization of the gene expression levels of the other examined genes. This decision was based on earlier studies which had observed that the ribosome content and consequently the amount of rRNA in nitrifying bacteria is stable, also during periods of starvation (Wagner *et al.,* 1995; Morgenroth *et al.,* 2000).

D.1.3. Methods for the evaluation of the specificity of a qPCR assay

D.1.3.1. Agarose gel electrophoresis

The first step in the evaluation of the primer specificity was to perform agarose gel electrophoresis. This quick method provides first information concerning the correct length of the products. The possibility of unspecific amplification leading to a product with the same length as the desired amplicon was unlikely concerning the *Ca*. N. defluvii genome, since the primers were additionally checked for primer binding sites in the genome. Still, contaminants in the enrichment-cultures could also possess binding sites for the primers.

D.1.3.2. Melting curve analysis

Melting curve analysis was performed to investigate the amplicons not only by their length but also by their properties concerning their nucleotide compositions. In case of one single amplicon type, the melting curve should show one peak at the temperature, at which the majority of the double stranded nucleic acids is melted. At this point, the difference in fluorescence before and after melting of the double stranded DNA fragments is highest. Ideally, all PCR reactions with a specific primer pair should show the same peak in the melting curve, whereas the negative controls should show no peak at all. This was the case for all reactions of the 16S rRNA, *nxrA1* and *nxrA2* assay. In the case of unspecific amplification, a second peak would be visible with high probability. This occurred with the standards 10^{-10} and 10^{-11} and with the negative controls in the *gltA*-specific qPCR assay, probably due to primer dimer formation. This explanation is supported by the observation that the melting curves for the standard dilutions 10^{-3} to 10^{-9} showed only one single peak. Based on this information concerning the melting curves, the 16S rRNA, *nxrA1* and *nxrA2* assays can be assumed to be highly specific. The same is true for the *gltA* assay as long as the template concentrations of the tested samples were within the range of the standards where no primer dimer formation occurred.

However, there is a chance that two or more different amplicons possess the same melting temperature based on their length and GC-content and consequently would show one single peak in the melting curve. Such amplicons could not be distinguished by melting curve analysis alone. Therefore, the combination of both, agarose gel electrophoresis and melting-curve-analysis, is of great importance.

D.1.3.3. Sequencing of RT-PCR products

Besides the two methods mentioned above, the specificity of the developed qPCR assays was also checked by rDNA-sequencing. Therefore, PCR products obtained from RT of total *Ca*. N. defluvii RNA and subsequent end-point-PCR were directly sequenced. Despite some gaps in two of the four obtained sequences the chromatograms suggested only specific amplification and therefore confirmed the assays to be highly specific. One possible reason for the observed gaps could have been the formation of deletion mutants during RT-PCR. This assumption is based on the observation that PCR templates containing stable secondary structures as typical for rRNA can lead to deletion mutagenesis in PCR products (von Wintzingerode *et al*., 1997). Point-mutations, deletions and insertions during the RT-reaction thereby are amplified during PCR and a mix of slightly different amplicons is obtained. Furthermore, ambiguities in the obtained sequences can result from direct-sequencing of the PCR products.

D.1.4. Methods for the synthesis of standards

The synthesis of standards for the calculation of the copy number in unknown samples is another very important point besides all previously mentioned considerations when developing a qPCR assay. In general, there are several possibilities for the synthesis of standards. They can either be PCR products, circular plasmids or linearized plasmids containing the target fragment (Dhanasekaran *et al*., 2010). PCR products used as standards have the disadvantage to be of lower stability against freezing and thawing compared to plasmids. The disadvantage of plasmids is that they can also exist in coiled and supercoiled form which can reduce the accessibility of the template for the primers as well as for the polymerase enzyme. Consequently, the use of plasmids as standards can lead to an underestimation of the copy number of supercoiled plasmids (Suzuki *et al*., 2000). PCR products are present in linearized form and thus are better comparable with the cDNA targets in the unknown samples. For this reason, in this study, the standards were amplified with M13-primers from plasmids containing the correct insert to obtain linearized DNA. The drawback of increased susceptibility to degradation of linearized PCR products was circumvented by aliquoting them to prevent multiple freezing and thawing steps.

D.1.5. Factors influencing the efficiency of a qPCR assay

The last step in the development of a qPCR assay is to check the assay for sufficient efficiency, which is determined by the designed primers as well as other factors like inhibitory components. To evaluate the efficiency of the qPCR assays test runs were performed. A PCR efficiency of

100%, meaning the doubling of the PCR products during each cycle, would be desirable. For all assays conducted in this study a PCR efficiency between 80 and 100% was achieved. An efficiency of above 100% is also possible and indicates the formation of primer dimers which are co-detected and bias the calculations. This might be suspected for the *gltA* qPCR assay with its conspicuously high efficiency. However, this is unlikely since there was no primer dimer formation observed for the applied standards.

The already mentioned inhibiting compounds have to be removed as thoroughly as possible since they can lead to a reduction of the sensitivity and the kinetics of the qPCR (Radstrom *et al.*, 2004). In this study, this risk was reduced by precipitating and washing the RNA to remove these compounds. Furthermore, it should be noted that the issue of inhibitory compounds is more of a problem for absolute quantification, but should not interfere with relative quantification since the inhibitors hamper the amplification of reference genes to the same extent.

Another factor influencing the efficiency of a qPCR assay is RNA quality. Degradation of transcripts during processing can also lead to distortions in their quantification (Bustin, 2002). In this study, RNA quality was checked by applying the RNA to an agarose gel. Special devices like the Agilent Bioanalyser or the BioRad Experion microfluidic capillary electrophoresis system would allow better assessments of the RNA quality by measuring the RNA quality more objectively based on several characteristics (Nolan *et al.*, 2006).

Furthermore, the efficiency of the reverse transcription of RNA to cDNA influences the reliability of the RT-qPCR assay. Here, it would be desirable to get one cDNA copy per transcript. The use of target-specific primers is recommended because they are most specific and sensitive and therefore achieve the highest possible efficiency (Nolan et al., 2006).

Summing up, these qPCR assays developed for four genes of *Ca*. N. defluvii were shown to be highly specific and provide powerful tools for the further investigation of the energy metabolism of *Ca*. N. defluvii.

D.2. Gene expression study

D.2.1. Incubation setup

The aim of this experiment was the detection of possible physiological responses of *Ca*. N. defluvii to changing environmental conditions on a transcriptome-level. Thereby, we focused on three genes for which a RT-qPCR assay was developed.

D.2.1.1. Oxic incubation with different nitrite concentrations

Ca. N. defluvii possesses two copies of the *nxrAB* gene cluster encoding a putative nitrite oxidoreductase. There is evidence that the expression of these two gene clusters is regulated differently (Lücker *et al.*, 2010; Koch, 2009, unpublished). Furthermore, the nitrite concentration is suspected to be a regulating factor for the expression of these genes. Therefore, *Ca*. N. defluvii cultures were incubated at three different nitrite concentrations. One nitrite concentration was set to 3 mM, which is the optimal concentration for nitrite oxidation by *Ca*. N. defluvii (Spieck *et al.*, 2006). A considerably lower concentration was chosen with 0.3 mM - a concentration *Ca*. N. defluvii still can grow with (Spieck *et al.*, 2006). This concentration was also shown to be optimal for the growth of a member of sublineage II of the genus *Nitrospira*, namely *Nitrospira moscoviensis* (Ehrich *et al.*, 1995). Apart from that, this low concentration better reflects the ambient nitrite concentrations in WWTPs. Besides these two different nitrite concentrations, an additional rather high concentration of 15 mM was chosen which is close to the upper maximum of 20-25 mM of nitrite *Ca*. N. defluvii can deal with (Lebedeva *et al.*, 2008).

The main issue concerning the implementation of the incubations was to keep the nitrite concentrations constant. Since the used nitrite test strips are very inaccurate and insensitive, changes in the nitrite concentrations were difficult to detect. This led to fluctuations in the nitrite concentrations measured after the incubation applying the Griess reaction (Griess, 1879). In the end, the expression of genes was not examined at certain nitrite-concentrations but rather at different ranges of nitrite concentrations. But still, these ranges were never overlapping and clearly distinguishable from each other. For further studies, an alternative method to keep the concentrations more stable would be a chemostat continuous culturing system. However, accurate devices for this purpose are very expensive and their operation is laborious.

D.2.1.2. Anoxic incubation with nitrate and pyruvate

The Nxr of *Nitrobacter* was shown to be capable of performing the reduction of nitrate to nitrite (Freitag *et al*., 1987; Bock *et al*., 1988). Moreover, also *Nitrospira moscoviensis* was capable of reducing nitrate when using hydrogen as electron donor under anoxic conditions (Ehrich *et al*., 1995). Based on this knowledge, it should be tested if also *Ca*. N. defluvii might be able to reduce nitrate under anoxic conditions. To answer this question for *Ca*. N. defluvii, anoxic incubations were performed with 2.5 mM nitrate as possible electron acceptor. As possible electron donor pyruvate was added to an end concentration of 0.5 mM. Pyruvate was chosen because it was shown that uncultered *Nitrospira* in activated sludge assimilated pyruvate in addition to inorganic carbon under oxic conditions (Daims *et al.,* 2001). However, there was no visible consumption of nitrate during the incubation suggesting that there was no denitrification. However, consumption of pyruvate was observed. This might be explained by the activity of heterotrophic contaminants, which could have used pyruvate as carbon source. Furthermore, heterotrophic contaminants could have used pyruvate as electron donor in the fermentation of extracellular polymeric substances (EPS) leaching from *Ca*. N. defluvii cells.

D.2.2. Gene expression analyses

D.2.2.1. Expression of the 16S rRNA gene under oxic conditions with different nitrite concentrations

The expression of the 16S rRNA gene was examined for the normalization of the expression levels of the other examined genes since the amount of 16S rRNA is an indicator for the cell number. The analysis of the obtained qPCR results showed that the expression levels of the 16S rRNA gene were similar in all but one of the incubations despite differing environmental conditions. The calculated copy numbers were within one order of magnitude. Only for replicate I of the anoxic incubations with nitrate and pyruvate a lower number of 16S rRNA copies was detected. This most probably results from the fact that a smaller amount of total RNA was used for the RT for this sample as compared to the other samples. Consequently, the proportion of 16S rRNA relative to total RNA seems to be more or less stable, also under different environmental conditions at least for short incubation times as performed in this study. Therefore, the 16S rRNA was shown to be suitable for the normalization of the expression levels of other genes. However, to test the 16S rRNA for its suitability as reference gene for *Ca*. N. defluvii in more detail, a study applying lots of different environmental conditions and incubation times would have to be conducted.

D.2.2.2. Expression of the *gltA* gene under oxic conditions with different nitrite concentrations

The expression of the *gltA* gene encoding the citrate synthase enzyme was examined to prove the potential use of organic compounds by *Ca*. N. defluvii. This enzyme is indicative for the oxidative tricarboxylic acid cycle (oTCA). This metabolic pathway generates reduced electron carriers like $NADH^+$ which are partially used for the conservation of energy in the form of ATP during respiration. Although in *Ca*. N. defluvii one enzyme complex of the oTCA cycle, namely the 2-oxoglutarate dehydrogenase complex (ODH), is missing, this complex could be replaced by the enzyme 2-oxoglutarate:ferredoxin oxidoreductase (OGOR) which is included in the reverse tricarboxylic acid cycle (rTCA-cycle) and also encoded in *Ca*. N. defluvii (Lücker *et al*., 2010). OGOR usually is very O_2-sensitive but it was shown to be also functional in some microaerophilic autotrophs such as *Hydrogenobacter thermophilus* where it is included in the rTCA-cycle (Campbell *et al*., 2006; Shiba *et al*., 1985). Interestingly, the one of the two encoded OGOR-copies in *H. thermophilus* tolerating higher concentrations of O_2 is highly similar to the one of *Ca*. N. defluvii (Yamamoto *et al*., 2006; Lücker *et al*., 2010).

In this study, the expression of the *gltA* gene showed a similar pattern in all incubations, the oxic as well as the anoxic ones. Therefore, a basic constitutive expression is assumed for this gene. However, it was not expected for the anoxic incubations to show any upregulation of the expression of this gene since a decrease of TCA cycle function during anaerobic growth with nitrate was observed for *E. coli* as well as for *Pseuudomonas fluorescens* and is suggested to be a broadly distributed regulatory mechanism. In *E. coli,* the synthesis of most enzymes of the TCA cycle were shown to be partially repressed and the synthesis of two enzymes - 2-oxoglutarate dehydrogenase and succinate dehydrogenase - was repressed nearly completely when growing on glucose and using nitrate as electron acceptor under anoxic conditions (Prohl *et al*., 1998). In the oxic incubations, however, no pyruvate or similar potential electron donor was supplied since the main focus in this study was on the investigation of the *nxrA* genes. Due to biomass limitation it was not possible to investigate the expression of the *gltA* gene under oxic conditions when supplying pyruvate. The only possible upregulation would have been expected if *Ca*. N. defluvii had used their own storage compounds or organic compounds leaching from contaminants.

In general, the necessity to use organic compounds could arise in case of environmental conditions where energy generation by oxidizing nitrite is inhibited or decreased due to nitrite-limitation. Therefore, for further studies it would be of interest to test *Ca*. N. defluvii for the use

of pyruvate under oxic conditions since it was observed that uncultured *Nitrospira* assimilate pyruvate in activated sludge when oxygen is present as revealed by MAR-FISH (Daims *et al.*, 2001).

D.2.2.3. Expression of the paralogous *nxrA* genes under oxic conditions with different nitrite concentrations

The main focus of the gene expression study was on the expression of the two different *nxrA* paralogs. The presence of more copies of paralogous genes in the genome of one organism is not unusual. In general, besides gene loss and horizontal gene transfer, such gene duplications are a very important tool for the adaptation of bacteria to new environmental conditions by functional diversification and specialization. A new function for one of the paralogs can evolve based on the assumption that one of the paralogous gene copies escapes the selection pressure for maintaining the specific function while the original function is maintained by the second copy (Gevers *et al.*, 2004; Koonin *et al.*, 2005). Such duplications are even known for enzymes involved in the microbial nitrogen-cycle. For example, the *nifH* gene in *Azorhizobium caulinodans* encoding the enzyme dinitrogen reductase and the *nirS* gene in one strain of *Thauera sp.* encoding the enzyme nitrite reductase are present in duplicate (Iki *et al.*, 2007; Etchebehere and Tiedje, 2005). In the latter example, different transcriptional activities suggest functional differences between the paralogs. A functional difference is also assumed for the two *nxrA* paralogs, also when having the same catalytical effect. Otherwise, one duplicate would be redundant and probably be lost from the genome.

The most interesting finding in this study was the differential expression of the *nxrA1* gene under different conditions. Under anoxic conditions and under oxic conditions with 0.3 mM nitrite as well as in one replicate with 15 mM nitrite, the expression of *nxrA1* was at the lower limit of detectability. Unfortunately, the expression of the *nxrA1* gene between the replicates in the 15 mM incubations differed enormously. This difference was unexpected, especially since the expression levels of all other examined genes matched quite well between the replicates. Taken together, these results allow two hypotheses.

One hypothesis is that the *nxrA1* gene is only expressed at a nitrite concentration near 3 mM. This is the concentration *Ca.* N. defluvii was shown to exhibit the highest nitrite oxidation rate (Spieck *et al.*, 2006). This would mean that both paralogous genes are expressed at optimal conditions to obtain maximal amounts of protein for the utilization of nitrite. However, this hy-

pothesis implies that the obtained result for the expression of the *nxrA1* gene in replicate I of the 15 mM nitrite incubations was wrong. An explanation for this could be DNA contamination since there was a weak band in the gel picture of the PCR with the DNase-treated RNA solution of this incubation. However, this explanation seems unlikely since the expression levels of the other examined genes matched quite well between the two replicates and the RT was performed as a multiplexed reaction - meaning that all transcripts were reverse transcribed in one reaction. Furthermore, a non-RT qPCR was conducted and showed no amplification and therefore confirms the obtained results. The possibility, that the reverse primer for the *nxrA1* gene was not added in the RT of replicate II of the 15 mM nitrite incubation was ruled out by repeating the RT-reaction and subsequent end-point PCR. In this experiment, a strong band was visible for replicate I while no band was obtained for replicate II (data not shown). This, again, confirms the obtained results.

The second hypothesis suggests an upregulation of the *nxrA1* gene with increasing nitrite concentrations. A similar nitrite-dependent upregulation of enzymes using nitrite as substrate has already been shown in former studies. Haveman and colleagues (2004) showed that the expression of the *nrfHA* gene encoding a cytochrome c nitrite reductase was upregulated in *Desulfovibrio vulgaris* with 5 mM nitrite compared to 0.1 mM nitrite. Another study on the Cyanobacterium *Synechococcus* sp. revealed a nitrite-dependent activation of the expression of a nitrate assimilation operon (Kikuchi *et al.*, 1996).

However, if an upregulation of *nxrA1* depending on increasing nitrite concentrations did occur, an explanation for the extremely low expression level of the *nxrA1* gene in replicate II of the 15 mM nitrite incubations is missing. Concerning this, the measurement of the nitrite concentrations after the incubations applying the Griess reaction (Griess, 1879) revealed not only fluctuations in the nitrite concentrations over the whole incubation time, but also differences between the two 15 mM nitrite replicates. Due to inaccuracy of the syringes the actual concentrations deviated by about 1.5 mM between the two replicates being higher in replicate II. One explanation derived from this finding could be that downregulation of the *nxrA1*-expression occurred due to a decrease in oxygen, which could have been caused by a higher oxidation-rate of nitrite in this incubation. Fresh supply of oxygen was avoided by using airtightly closed bottles.

A rough calculation challenges this hypothesis. A headspace of about 200 mL includes approximately 42 mL of molecular oxygen (O_2). Under standard conditions an ideal gas has a mo-

lar volume of 24 mL mmol^{-1}. Therefore, 42 mL pure O_2 have ~1.75 mmol of O_2 which is enough to oxidize 3.5 mmol of nitrite. During the experiment, 0.6 mmol nitrite were added and about the same amount was consumed. For this reason, the cells should not have experienced oxygen deficiency. Still, this cannot be ruled out since other processes consuming O_2 as well as contaminants respiring O_2 also have to be considered.

Another possible explanation for the differences in the expression of the *nxrA1* gene could be that the slightly higher nitrite-concentration in replicate II itself was inhibiting the expression of the *nxrA1* gene. The conditions were chosen close to the upper limit of nitrite *Ca*. N. defluvii can deal with, defined by 20-25 mM nitrite (Lebedeva *et al.*, 2008).

Taken together, there are many open questions to be answered concerning these experiments. To prove all the hypotheses mentioned, these experiments would have to be repeated in more replicates.

The expression of the *nxrA2* gene was similar in all incubations with a slightly reduced expression in the oxic 15 mM nitrite incubations. This similar expression level under different conditions suggests a constitutive expression of this gene. Results of a former study in the main WWTP of Vienna also support constitutive expression of the *nxrA2* gene (Koch, 2009, unpublished). The constitutive expression of the *nxrB* gene later was interpreted as an adaptation to enable the utilization of nitrite immediately after becoming available (Lücker *et al.*, 2010). This is likely since the concentrations of nitrite in natural habitats can change very quickly.

The combination of the assumed upregulation of the expression of the *nxrA1* gene with increasing nitrite concentrations with the constitutive expression of the *nxrA2* gene shows similarities to other organisms. For example, in *Methylocystis* sp., it was shown that two different particulate methane monooxygenase enzymes (pMMO) converting methane to methanol were expressed differently (Baani *et al.* 2008). There, one pMMO was constitutively expressed, whereas the second one was expressed only at high concentrations of methane. Another example for such an expression pattern was shown for one strain of *Thauera* sp. This strain has two copies of *nirS* encoding a nitrite reductase enzyme. There, again, one gene was expressed constitutively while the other one was upregulated at higher nitrate-concentrations (Etchebehere and Tiedje, 2005).

Therefore, referring to the obtained results, a similar expression pattern to the aforementioned examples could also be hypothesized for *Ca*. N. defluvii. If an upregulation of the *nxrA1* gene dependent on increasing nitrite concentrations really could be confirmed this could be interpreted as an adaptation to achieve higher growth yields at temporarily higher nitrite concentrations or a kind of defence mechanism to eliminate nitrite when exceeding a harmful concentration. However, the latter hypothesis is less likely since *Ca*. N. defluvii was shown to grow up to a nitrite concentration of 20-25 mM (Lebedeva *et al.*, 2008).

For further support of this hypothesis, a comparison of the two *nxrA* subunits of *Ca*. N. defluvii to the *nxrA* subunits of *Nitrospira moscoviensis* could be of interest. This organism was shown to grow best at a nitrite concentration of 0.35 mM (Ehrich *et al.*, 1995). Therefore, it would be of interest if there is a higher similarity of the *nxrA* genes of *Nitrospira moscoviensis* to the *nxrA2* gene of *Ca*. N. defluvii since the latter was also shown to be expressed at these low nitrite concentrations. However, this comparison is complicated by the fact that the sequences of the *nxrA* genes of *Nitrospira moscoviensis* are not complete due to gaps in the obtained genome sequences (Koch, unpublished). The available partial sequences of the *nxrA* genes of *N. moscoviensis* were compared to each other and showed a higher similarity to each other than to the *nxrA* copies of *Ca*. N. defluvii (Koch, 2009, unpublished; Koch, unpublished). However, for a reliable comparison between the Nxr's of *N. moscoviensis* and *Ca*. N. defluvii the whole sequences of the *nxrA* copies of *Nitrospira moscoviensis* must be available. Furthermore, to make valid statements concerning their potential substrates and substrate affinities, purified preparations of the encoded enzymes in their native conformation would be needed.

D.2.2.4. Expression of the paralogous *nxrA* genes under anoxic conditions with pyruvate and nitrate

This study was conducted to answer the question whether one of the two Nxr copies in *Ca*. N. defluvii could also play a role in denitrification. *Nitrobacter* and *Nitrospira moscoviensis* were shown to reduce nitrate to nitrite under anoxic conditions (Freitag *et al.*, 1987; Bock *et al.*, 1988; Ehrich *et al.*, 1995). To answer this question for *Ca*. N. defluvii, anoxic incubations were performed with nitrate as electron acceptor and pyruvate as possible electron donor. A significant change in the expression level of the two *nxrA* copies would be expected if one of the two Nxr's encoded in *Ca*. N. defluvii was able to perform nitrate reduction. However, the *nxrA2* gene was expressed at the same level as under nitrifying conditions which would be consistent with the proposed constitutive expression of this gene and no expression of the *nxrA1* gene was ob-

served. Therefore, a denitrifying role for *nxrA1* can be excluded, at least under the tested conditions. For the Nxr encoded by the *nxrA2* gene a denitrifying role is unlikely since there was no, at least visible, consumption of nitrate over the incubation time. However, there is no real evidence that the Nxr encoded by the *nxrA2* gene is not able to perform the reduction of nitrate to nitrite since this gene was clearly expressed under denitryfing conditions. The limiting factor in this experiment was the method for the measurement of the nitrate concentration. With the applied test strips a change in the nitrate concentration by half would not have been clearly detectable.

Additionally to all these hypotheses, however, also the prevalent pool of proteins has to be considered when examining the transcriptome of an organism. Proteins often have a much longer lifetime compared to transcripts and a sufficient pool of protein for the implementation of the protein's function can make it reduant and even detrimental in terms of energy costs to transcribe the respective gene. Consequently, the transcription of a certain gene can be repressed or downregulated due to the existing protein pool although the environmental conditions would ask for its expression. Therefore, the lack of detectability of a certain transcript does not mean absence and inactivity of the encoded protein. This also has to be considered in this study since the incubation times were very short. Consequently, for making reliable statements concerning changes in the transcriptional activity of certain genes the additional investigation of the proteom is indispensable.

Taken together, with all these results obtained, a first step in the uncovering of the functions of the Nxr paralogs has been made and a basis for further investigations was provided.

D.3. Investigation of the coexistence of three subpopulations of *Nitrospira* sublineage II in the wastewater treatment plant of the University of veterinary medicine Vienna applying quantitative FISH

D.3.1. Quantification of three subpopulations of *Nitrospira* sublineage II over a time period of six years

The aim of this study was to examine the abundances of different subpopulations of *Nitrospira* sublineage II in the WWTP of the University of Veterinary Medicine Vienna. In this WWTP, this genus represented up to 1/5 of the total bacterial biomass over the observation period of six years. Generally, in WWTPs the NOB-community is dominated by two sublineages of this genus, I and II. Sublineage I was shown to make up between 1 to 20 % of the bacterial biomass in many engineered systems (Müller, 2008; Daims *et al*., 2001a; Schramm *et al*., 1998; Juretschko *et al*., 1998; Dorninger *et al*., unpublished; this study). In this study examining the WWTP of the Vetmed, sublineage II was dominating very consistently over the whole observation period. However, the appearance of sublineage I and II has not yet been linked to specific environmental conditions with the exception of one study by Maixner and colleagues (2006). They could show that these two sublineages in principle can either outcompete each other or coexist stably depending on the nitrite concentration. Unfortunately, no data concerning the nitrite levels are available for the WWTP of the Vetmed. The stable coexistence there might also rely on a niche differentiation as mentioned in the study from Maixner and colleagues (2006). Thereby, two major kinds of niche differentiation are conceivable. A spatial niche differentiation would emerge when one sublineage with lower nitrite affinity is localized closer to ammonia-oxidizing bacteria (AOB) and the sublineage with higher nitrite-affinity lives farther from these substrate-supplying AOB. A chronological niche differentiation could be due to fluctuations in the nitrite-concentration based on irregular charging of the WWTP with sewage. Beside the nitrite concentration there are several other factors that can result in changes in the environmental conditions and therefore affect the community composition. Especially the presence of different carbon sources which could favor the growth of a certain subpopulation and differences in the oxygen concentration could affect the community composition. In respect to oxygen a different affinity to oxygen among the subpopulations could explain a stable coexistence due to changes in the oxygen concentration within the system during the processing of wastewater.

Another hypothesis that could explain the dominance of sublineage II in this WWTP is that the nitrite concentrations in this WWTP are rather low. This suggestion is based on the fact that the only cultured member of sublineage II, *Nitrospira moscoviensis*, grows best at a rather low concentration of 0.35 mM nitrite (Ehrich *et al.*, 1995) in comparison to *Ca.* N. defluvii representing sublineage I and growing best at a nitrite concentration of 3 mM (Spieck *et al.*, 2006). But still, there can be many other factors affecting the competitiveness of different sublineages, as for example organic compounds which could probably be used for mixotrophic lifestyles (Watson *et al.*, 1986; Lücker *et al.*, 2010).

The quantified abundances of the two examined subpopulations 195 and 256Cl2 were more or less consistent with the qualitative assessment by Christiane Dorninger. However, for cluster 2.4 a clearly increasing abundance was observed over time since the beginning of sampling in the year 2004. The cluster 2.5 did not show comparable abundance shifts and remained stable over time. But still, a stable coexistence of these subpopulations was clearly demonstrated in this study. To explain such a coexistence and also shifts in the abundances of these two subpopulations it would be of interest to have supplementary data about the wastewater composition in terms of concentrations of nitrite, ammonium, trace elements, urea, other organic compounds and potentially toxic substances like antibiotics as well as pH and temperature. Shifts in the wastewater composition could possibly be linked to shifts in the composition of these subpopulations and give hints to their physiological requirements. Probably they represent different ecotypes with different physiological requirements despite a close relation on the basis of 16S rRNA sequence analysis. This, for example, was shown for different populations of the genus *Prochlorococcus* which were adapted to high- and low-light conditions, respectively (Coleman and Chisholm, 2007).

Unfortunately, the abundance of the third subpopulation, cluster 2.2, could not be quantified due to the weak signal obtained from this probe which did not allow taking suitable pictures for quantification.

D.3.2. Limitations for the quantification of bacterial cells using fluorescence *in situ* hybridization (FISH)

As mentioned above, the quantification of cluster 2.2 was not possible due to the weak signal of the used probe. A reason for the weak signal of this probe as well as for the probe 256Cl2 could be low accessibility of the target region due to the secondary structure of the 16S rRNA. Low *in situ* accessibility was reported earlier for many regions of the 16S and 23S rRNA of *E.coli* (Fuchs *et al.*, 1998, 2000 and 2001). There, approximately 30% of the total 16S rRNA sequence showed a low accessibility (Fuchs *et al.,* 1998). A consensus 16S rRNA accessibility map for prokaryotes was created that should be considered during probe design (Behrens *et al.*, 2003).

For the design of probes targeting very closely related organisms whose variability of the 16S rRNA is only based on SNPs, the accessibility map cannot always be taken into account. Furthermore, the accessibility of certain rRNA regions varies among organisms. Therefore, even considering this consensus accessibility map does not guarantee a good FISH signal. One way to improve accessibility is to use unlabelled helper probes (Fuchs *et al.*, 2000). Other possible solutions would be to elongate the hybridization time up to 96 h or to design longer probes (Yilmaz *et al.*, 2006). Also the use of double-labelled FISH-probes was shown to increase the signal from labelled cells at least twice. Even for single-labelled probes which did not give any detectable signal, the identical, but double-labelled probe could be detected. Double-labelling has been supposed to open the secondary structure of the rRNA (Stoecker *et al.*, 2010). Nevertheless, all these techniques have specific limitations (Stoecker *et al.*, 2010).

In addition to problems with the signal intensity of probes, the so-called "autofluorescence" (AF) of sludges is an issue to consider, i.e. when organic compounds or minerals emit at the same wavelength as the applied fluorescence dye. In this context, the so-called signal-to-noise ratio should be mentioned. The signal-to-noise ratio (SNR) compares the intensity of a desired signal to the intensity level of the background noise. The higher the SNR, the easier it is to distinguish between labelled cells and the autofluorescence of activated slude - the background noise. In the case of probes giving low signal intensities, the SNR can be very low which in turn can make it unfeasible to quantify bacterial populations despite the use of suitable probes. This is especially problematic when using probes which give weak signals. For the probe Ntspa175 targeting cluster 2.2 of *Nitrospira* sublineage II the AF signal almost completely covered the

signal from labelled colonies in most of the cases when applying the Cy3 fluorescence dye. An alternative to this fluorescence dye would have been the use of Fluos-labelled probes. But also for this dye enormous AF was observed. Especially for probe Ntspa175 and probe Ntspa256Cl2 specific for *Nitrospira* cluster 2.5, Fluos-labelled probes gave weaker signals compared to Cy3-labelled probes and therefore images were even harder to take. The Fluos fluorochrome is only advantageous when using epifluorescence microscopy. Thereby, the application of this dye allows a differentiation between "real" and AF signal by eye since various shades are distinguishable. However, after digitalization of the original signal by taking images a differentiation of differently coloured shades is not possible anymore and therefore the application of the Fluos fluorochrome would not have been advantageous when quantifiying populations on basis of digitalized images.

For further studies the signal intensity of the probes must be improved to obtain more valid data for all known subpopulations. Some possible approaches to obtain enhanced signals from the targeted subpopulations for a more reliable image analysis were mentioned above. Further studies could then tackle to seasonal changes in the composition of nitrifying bacteria in this WWTP by seasonal sampling in equal time intervals. Additional analyses of the wastewater composition could give more detailed insights into shifts in the composition of the NOB. Changes in the wastewater composition could be linked to changes in feed composition and the keeping of animals at Vetmed during the year.

Summing up, the obtained results showed that a stable coexistence of very closely related organisms in the same habitat is possible at the level of sublineages as well as at the level of subpopulations. Which physiological differences between the different *Nitrospira* populations provide the basis of this coexistence needs to be explored further.

E. <u>Summary</u>

The biogeochemical nitrogen cycle is of paramount importance for the biosphere since nitrogen is essential to all organisms. Therefore, microbes participating in this cycle have been investigated for more than one century. But still, much is unknown. Especially the nitrification process - the transformation of ammonia/ammonium to nitrate - is of particular interest since many new aspects have been revealed in the last decade. This study focussed on the further investigation of the genus *Nitrospira* - a genus of nitrite-oxidizing bacteria (NOB) performing the oxidation of nitrite to nitrate - the second step in the nitrification process. This bacterial genus was investigated concerning its ecophysiology on the one hand and its distribution in the wastewater treatment plant of the University of Veterinary Medicine Vienna on the other hand.

The key enzyme for the oxidation of nitrite to nitrate is the membrane-associated nitrite-oxidoreductase (Nxr) which in "*Candidatus* Nitrospira defluvii" - a member of sublineage I of the genus *Nitrospira* - is present in two copies in the genome. The alpha-subunits of the encoded enzymes differ from each other indicating possible differences of their substrate-affinities. Therefore, the first part of this study focussed on the expression of these alpha-subunits with different nitrite concentrations to reveal a possible substrate-dependent regulation. For this purpose, qPCR assays specific for these genes were developed. First experiments supported the hypothesis that one of the Nxr's is constitutively expressed, whereas the second copy is upregulated at a nitrite-concentration of 3 mM - the optimal concentration for growth of *Ca*. N. defluvii. Furthermore, this enzyme was shown to be capable of performing the reverse step - the reduction of nitrate to nitrite - in other organisms. Therefore, the developed qPCR assays were also used to check for the expression of the two encoded Nxr enzymes under denitrifying conditions. First results, however, did not support this hypothesis.

Another part of this thesis tackled to a possible mixotrophic lifestyle of this organism by examining the expression of the enzyme citrate synthase. This enzyme is essential in the oxidative tricarboxylic acid cycle (oTCA), which is yet unknown to be functional in *Ca*. N. defluvii. To analyze its expression, a qPCR assay specific for the *gltA* gene encoding the citrate synthase was developed. This assay allows the investigation of *Ca*. N. defluvii with regard to the use of organic compounds with the oTCA cycle. Future experiments with cultures of *Ca*. N. defluvii should test the use of different organic compounds after incubating the cultures under oxic con-

ditions. Such data could explain the distribution of this sublineage as well as its dominance in some wastewater treatment plants (WWTPs).

Another part of this study dealt with the distribution of *Nitrospira* populations in the WWTP of the University of Veterinary Medicine Vienna. Different subpopulations of sublineage II of the genus *Nitrospira* were examined concerning their abundance in samples taken over six years. For this purpose, fluorescence *in situ* hybridization (FISH) in combination with confocal microscopy and the image analysis software daime was applied. This study showed that members of sublineage II of the genus *Nitrospira* are highly dominant in this WWTP. Furthermore, stable coexistence of different subpopulations over the whole sampling period was revealed. This likely is caused by differences in the ecophysiology of the subpopulations which may represent different ecotypes. Due to different physiological demands or capabilities they could inhabit different niches in WWTP.

Taken together, new insights into the ecophysiology and community structure of nitrite-oxidizing bacteria have been revealed and provide material for further investigations. Such information about the genus *Nitrospira* is important to better understand the nitrification process in WWTPs.

F. <u>Zusammenfassung</u>

Der biogeochemische Stickstoff-Kreislauf ist von enormer Bedeutung für die Biosphäre, da das Element Stickstoff für alle Organismen lebensnotwendig ist. Aus diesem Grund heraus wurde seit mehr als einem Jahrhundert intensiv an jenen Mikroorganismen geforscht, die für die Umwandlung von Stickstoffverbindungen veranwortlich sind. Doch bis heute gibt es noch viele zu klärende Fragen, was diese Prozesse betrifft. Diesbezüglich ist vor allem der Prozess der Nitrifikation von besonderem Interesse, da gerade in Bezug darauf innerhalb des letzten Jahrzehnts viele neue Erkenntnisse gewonnen wurden. Die Nitrifikation ist jener Teil des Stickstoff-Kreislaufes, in dem Ammonium/Ammoniak zu Nitrat oxidiert wird.

Diese Diplomarbeit fokussierte sich auf die weitere Erforschung der Gattung *Nitrospira*, einer Gattung von Nitrit-oxidierenden Bakterien (NOB), welche den zweiten Schritt der Nitrifikation – die Oxidation von Nitrit zu Nitrat - durchführen. Ziel dabei war es einerseits, mehr über die Ökophysiologie dieser Mikroorganismen sowie andererseits mehr über ihre temporäre Verteilung in der Kläranlage der Veterinärmedizinischen Universität Wien in Erfahrung zu bringen.

Das Schlüsselenzym für die Oxidation von Nitrit ist das membranassoziierte Enzym Nitrit-Oxidoreductase (Nxr). Jene Gene, welche dieses Enzym codieren, liegen im Genom von "*Candidatus* Nitrospira defluvii" (*Ca*. N. defluvii), einer Art der sublineage I der Gattung *Nitrospira*, in jeweils zwei paralogen Kopien vor. Jene beiden paralogen Gene, welche die alpha-Untereinheiten codieren, unterscheiden sich dabei deutlich voneinander. Da diese Untereinheiten für die Substratbindung verantwortlich sind, könnte dies auf unterschiedliche Substrat-Affinititäten hindeuten. Daher fokussierte sich der erste Teil dieser Studie darauf, die Expression dieser alpha-Untereinheiten unter unterschiedlichen Nitritkonzentrationen zu untersuchen, um so eine mögliche Substrat-abhängige Regulierung dieser Gene aufzeigen zu können. Dafür wurde eine qPCR-Methode entwickelt, welche spezifisch die Expression dieser beiden Gene detektieren kann. Erste Experimente stützen die Hypothese, dass eines der beiden Gene konstituitiv exprimiert wird, während die Expression des zweiten Gens bei einer Nitrit-Konzentration von 3 mM hochreguliert wird. Dies entspricht jener Konzentration, bei der *Ca*. N. defluvii die höchste Nitrit-Oxidationsrate aufweist. Weiters kann mit der entwickelten qPCR-Methode auch getestet werden, ob eines der beiden codierten Nxr-Enzyme auch den reversen

Schritt - die Reduktion von Nitrat zu Nitrit - katalysieren kann. Dies konnte zuvor schon für das Nxr-Enzym von anderen Organismen gezeigt werden. Erste Versuche konnten diese Hypothese jedoch nicht stützen.

Eine weitere Arbeit dieser Diplomarbeit beschäftigte sich mit der Untersuchung eines möglichen mixotrophen Lebensstils von *Ca*. N. defluvii. Um dies zu untersuchen sollte die Expression des Enzyms Citrat-Synthase untersucht werden. Dieses Enzym ist essentiell im oxidativen Tricarbonsäurezyklus (Krebs-Zyklus, Zitronensäurezyklus). Ob dieser in *Ca*. N. defluvii funktionell ist, konnte bislang noch nicht gezeigt werden. Deshalb wurde auch für das Gen *gltA*, welches die Citrat-Synthase codiert, eine qPCR-Methode entwickelt. Diese ermöglicht den Nachweis der Nutzung von organischen Verbindungen über den Tricarbonsäurezyklus, wenn eine erhöhte Expression dieses Gens nachgewiesen werden kann. Aufgrund von Biomasselimitierung konnten diesbezüglich jedoch keine spezifischen Untersuchungen durchgeführt werden. Diese könnten jedoch Gegenstand von zukünftigen Experimenten sein, bei denen Anreicherungskulturen von *Ca*. N. defluvii unter oxischen Bedingungen mit bestimmten organischen Verbindungen inkubiert werden könnten. Ergebnisse aus diesen Untersuchungen könnten Hinweise für die weite Verbreitung sowie die Dominanz der Gattung *Nitrospira* in Kläranlagen aufgrund von möglichen Präferenzen bezogen auf verschiedene organische Verbindungen liefern.

Ein weiterer Teil dieser Diplomarbeit befasste sich mit der Verbreitung von Populationen der Gattung *Nitrospira* in der Kläranlage der Veterinärmedizinischen Universität Wien. Dabei wurden die Häufigkeiten verschiedener nahverwandter Subpopulationen der sublineage II der Gattung *Nitrospira* basierend auf ihren Biomasseanteilen untersucht. Um diese zu erheben wurde die Methode Fluoreszenz *in situ* Hybridisierung (FISH) in Kombination mit Konfokalmikroskopie sowie der Quantifizierungssoftware daime eingesetzt. Die durchgeführten Erhebungen zeigten, dass sublineage II-angehörige Populationen der Gattung *Nitrospira* in dieser Kläranlage höchstabundant waren. Innerhalb dieser sublineage II konnte weiters eine stabile Koexistenz von zwei Subpopulationen über den gesamten Beprobungszeitraum nachgewiesen werden. Diese stabile Koexistenz könnte auf verschiedenen physiologischen Anforderungen oder Fähigkeiten dieser Subpopulationen basieren.

Zusammenfassend konnten neue Einblicke in die Ökophysiologie und die Gemeinschaftstruktur von Nitritoxidierenden Bakterien gewonnen werden, welche wiederum Grundlage für weitere

Experimente darstellen. Diese Informationen wiederum sind von enormer Bedeutung, um den Prozess der Nitrifikation in Kläranlagen besser verstehen zu können.

G. <u>Abbreviations</u>

%	percent
°C	degree Celsius
0.3 mM NO_2^- R1	*Ca*. N. defluvii incubation with 0.3 mM nitrite replicate 1
0.3 mM NO_2^- R2	*Ca*. N. defluvii incubation with 0.3 mM nitrite replicate 2
15 mM NO_2^- R1	*Ca*. N. defluvii incubation with 15 mM nitrite replicate 1
15 mM NO_2^- R2	*Ca*. N. defluvii incubation with 0.3 mM nitrite replicate 1
3 mM NO_2^- R1	*Ca*. N. defluvii incubation with 3 mM nitrite replicate 1
3 mM NO_2^- R2	*Ca*. N. defluvii incubation with 3 mM nitrite replicate 2
A	Adenine
abs	absolute
AOA	ammonia-oxidizing archaea
AOB	ammonia-oxidizing bacteria
BLAST	Basic Local Alignment Search Tool
bp	base pair(s)
C	Cytosine
Ca. N. defluvii	"*Candidatus* Nitrospira defluvii"
CLSM	Confocal laser scanning microscope
Cy3	5,5'-di-sulfo-1,1'-di-(X-carbopentynyl)-3,3,3',3'-tetra-methylindol-Cy3.18-derivative Nhydroxysuccimidester
Cy5	5,5'-di-sulfo-1,1'-di-(X-carbopentynyl)-3,3,3',3'-tetra-methylindol-Cy5.18-derivative Nhydroxysuccimidester
dd	double distilled and filtered
DNA	deoxy-ribonucleic acid
dNTP	desoxy-nucleotide-tri-phosphate
E. coli	*Escherichia coli*
EDTA	ethylene-di-amine-tetra-acetic acid
ERT	Eppendorf reaction tube
et al.	et alteri (lat., "and others")
EtBr	Ethidium bomide
FA	Formamide
FISH	Fluorescence *in situ* hybridisation
FLUOS	5,(6)-carboxfluorescein-N-hydroxysuccimidester
FW	forward (primer labelling)
g	gram(s)
G	Guanine
h	hour(s)

H_2O	water
HCl	Hydrochloric acid
k	kilo (10^3)
KBL	kilobase-ladder (DNA length standard)
L	liter(s)
LB	Luria Bertani
m	milli (10^{-3})
M	molar
min	minute(s)
mM	mili molar
mol	Mol
n	nano (10^{-9})
N_2	elemental nitrogen
N_2O	Nitrous oxide
NaCl	Sodium chloride
NCBI	National Center for Biotechnology Information
NH_3	Ammonia
NH_4^+	Ammonium
NirS, *nirS*	nitrite reductase and corresponding gene
NO	Nitric oxide
NO_2^-	Nitrite
NO_3^-	Nitrate
NOB	nitrite-oxidizing bacteria
Nxr, *nxr*	nitrite oxidoreductase and corresponding gene
o/n	over night
O_2	molecular oxygen
p	pico (10^{-12})
PBS	Phosphate buffered saline
PCR	Polymerase chain reaction
PFA	Paraformaldehyde
RNA	Ribonucleic acid
rpm	rotations per minute
rRNA	ribosomal RNA
RT	Room temperature or Reverse transcription
RV	reverse (primer labelling)
SDS	Sodium dodecyl sulphate
sec.	second(s)
STD	standard
Taq	thermostable DNA-polymerase from *Thermus aquaticus*

Abbreviations

TBE	Tris-boric acid-EDTA
U	Uracil
UV	Ultraviolet
Vetmed	University of Veterinary Medicine Vienna
w/v	weight per volume
λ	wavelength
μ	mikro (10^{-6})

H. <u>References</u>

Alawi, M., A. Lipski, T. Sanders, E.M. Pfeiffer and E. Spieck (2007). Cultivation of a novel cold-adapted nitrite oxidizing betaproteobacterium from the siberian arctic. *Isme J* **1**(3): 256-64.

Altschul, S.F., W. Gish, W. Miller, E.W. Myers and D.J. Lipman (1990). Basic local alignment search tool. *J Mol Biol* **215**(3): 403-10.

Amann, R.I., B.J. Binder, R.J. Olson, S.W. Chisholm, R. Devereux and D.A. Stahl (1990). Combination of 16s rRNA-targeted oligonucleotide probes with flow cytometry for analyzing mixed microbial populations. *Appl Environ Microbiol* **56**(6): 1919-25.

Andersson, A.F., M. Lundgren, S. Eriksson, M. Rosenlund, R. Bernander, P. Nilsson (2006). Global analysis of mRNA stability in the archaeon Sulfolobus. *Genome Biol* **7**:R99.

Andrews, J.H. and R.F. Harris (1986). R-selection and k-selection and microbial ecology. *Advances in Microbial Ecology* **9**: 99-147.

Baani, M. and W. Liesack (2008). Two isozymes of particulate methane monooxygenase with different methane oxidation kinetics are found in methylocystis sp. Strain sc2. *Proc Natl Acad Sci U S A* **105**(29): 10203-8.

Bartosch, S., C. Hartwig, E. Spieck and E. Bock (2002). Immunological detection of nitrospira-like bacteria in various soils. *Microb Ecol* **43**(1): 26-33.

Behrens, S., C. Ruhland, J. Inacio, H. Huber, A. Fonseca, I. Spencer-Martins, B. M. Fuchs, and R. Amann (2003). In situ accessibility of small-subunit rRNA of members of the domains Bacteria, Archaea, and Eucarya to Cy3-labeled oligonucleotide probes. *Appl Environ Microbiol* **69**:1748–1758.

Beijerinck, M.W. (1888) Die Bacterien der Papillionaceen Knoellchen. *Bot Zeitung* **46**: 797–804.

Bernard, P., P. Gabant, E. M. Bahassi and M. Couturier (1994). Positive-selection vectors using the F plasmid ccdB killer gene. *Gene* **148**: 71–74.

Bock, E. and M. Wagner (2006). Oxidation of inorganic nitrogen compounds as energy source. *The Prokaryotes* **2**: 457-495.

Bock, E., P. A. Wilderer, A. Freitag (1988). Growth of Nitrobacter in the absence of dissolved oxygen. *Water Res* **22**: 245-250.

Bothe, H., S.J. Ferguson, W.E. Newton (2007). Biology of the Nitrogen Cycle. Amsterdam: Elsevier

Brochier-Armanet, C., B. Boussau, S. Gribaldo, P. Forterre (2008). Mesophilic renarchaeota: proposal for a third archaeal phylum, the Thaumarchaeota. *Nat. Rev. Microbiol.* **6**(3): 245–52.

Broda, E. (1977) Two kinds of lithotrophs missing in nature. *Z. Allgem. Mikrobiol.* **17**, 491±493.

Brosius, J., T. Dull, D. Sleeter, and H. Noller (1981). Gene organization and primary structure of a ribosomal RNA operon from *Escherichia coli*. *J Mol Biol* **148**: 107-127.

Bustin, S. A. (2002). Quantification of mRNA using real-time reverse transcription PCR (RT-PCR): trends and problems. *J Mol Endocrinol* **29**: 23–39.

Bustin, S.A. (2000). Absolute quantification of mRNA using real-time reverse transcription polymerase chain reaction assays. *J Mol Endocrinol* **25**: 169-193.

Cabello, P., M.D. Roldan and C. Moreno-Vivian (2004). Nitrate reduction and the nitrogen cycle in archaea. *Microbiology* **150**(Pt 11): 3527-46.

Campbell, B.J., A.S. Engel, M.L. Porter, K. Takai (2006). The versatile ε -proteobacteria: Key players in sulphidic habitats. *Nat Rev Microbiol* **4**:458–468.

References

Coleman, M.L. and S.W. Chisholm (2007). Code and context: Prochlorococcus as a model for cross-scale biology. *Trends Microbiol* **15**(9): 398-407.

Coskuner, G. and T. P. Curtis (2002). In situ characterization of nitrifiers in an activated sludge plant: detection of *Nitrobacter* Spp. *J. Appl. Microbiol.* **93**:431-437.

Daims, H., J.L. Nielsen, P.H. Nielsen, K.H. Schleifer and M. Wagner (2001a). In situ characterization of nitrospira-like nitrite-oxidizing bacteria active in wastewater treatment plants. *Appl Environ Microbiol* **67**(11): 5273-84.

Daims, H., N.B. Ramsing, K.-H. Schleifer and M. Wagner (2001b) Cultivation-independent, semi-automatic determination of absolute bacterial cell numbers in environmental samples by fluorescence in situ hybridization. *Appl Environ Microbiol* **67:** 5810–5818.

Daims, H., S. Lücker, D. Le Paslier, M. Wagner (2010). Diversity, environmental genomics, and ecophysiology of nitrite-oxidizing bacteria. *In* Nitrification, pp. 295-322. (Ward BB, Arp DJ, Klotz MG, ed.). ASM Press, Washington, DC.

Daims, H., S. Lücker, M. Wagner (2006). *daime*, a novel image analysis program for microbial ecology and biofilm research. *Environ Microbiol* **8**: 200-213.

Dhanasekaran, S., T.M. Doherty, John Kenneth (2010). Comparison of different standards for real-time PCR-based absolute quantification. *J Immunol Methods.* **354**: 34–39

Dorak, M.T. (2006) Real-time PCR. New York: Taylor and Francis Group

Downing, L.S. and R. Nerenberg (2008). Effect of oxygen gradients on the activity and microbial community structure of a nitrifying, membrane-aerated biofilm. *Biotechnol Bioeng* **101**(6): 1193-204.

Ehrich, S., D. Behrens, E. Lebedeva, W. Ludwig and E. Bock (1995). A new obligately chemolithoautotrophic, nitrite-oxidizing bacterium, nitrospira moscoviensis sp. Nov. And its phylogenetic relationship. *Arch Microbiol* **164**(1): 16-23.

Erguder, T., N. Boon, L. Wittebolle, M. M., and W. Verstraete (2009). Environmental factors shaping the ecological niches of ammonia-oxidizing archaea. *FEMS Microbiol Rev* **33**, 855–869.

Etchebehere, C. and Tiedje, J.M. (2005). Presence of two different active *nirS* nitrite reductases genes in a denitrifying *Thauera* sp. from a high nitrate-removal-rate reactor. *Appl Environ Microbiol* **71:** 5642–5645.

Francis, C.A., K.J. Roberts, J.M. Beman, A.E. Santoro and B.B. Oakley (2005). Ubiquity and diversity of ammonia-oxidizing archaea in water columns and sediments of the ocean. *Proc NatlAcad Sci U S A* **102**(41): 14683-8.

Freitag, A., M. Rudert, and E. Bock (1987). Growth of Nitrobacter by dissimilatoric nitrate reduction. *FEMS Microbiol Lett* **48**: 105-109.

Fuchs, B. M., F. O. Glöckner, J. Wulf, and R. Amann (2000). Unlabeled helper oligonucleotides increase the in situ accessibility to 16S rRNA of fluorescently labeled oligonucleotide probes. *Appl Environ Microbiol* **66**: 3603–3607.

Fuchs, B. M., G. Wallner, W. Beisker, I. Schwippl, W. Ludwig, and R. Amann (1998). Flow cytometric analysis of the in situ accessibility of *Escherichia coli* 16S rRNA for fluorescently labeled oligonucleotide probes. *Appl Environ Microbiol* **64**: 4973–4982.

Fuchs, B. M., K. Syutsubo, W. Ludwig, and R. Amann (2001). In situ accessibility of *Escherichia coli* 23S rRNA to fluorescently labeled oligonucleotide probes. *Appl Environ Microbiol* **67**: 961–968.

Gayon, U., and Dupetit, G. (1886). Recherches sur la reduction des nitrates par les infiniment petits. *Mem Sot Sci Phys Nat Bordeaux Ser* **3**: 201–307.

Gevers, D., K. Vandepoele, C. Simillon and Y. Van de Peer (2004). Gene duplication and biased functional retention of paralogs in bacterial genomes. *Trends Microbiol* **12**(4): 148-54.

Griess, P. (1879). Bemerkungen zu der Abhandlung der H.N. Weselsky und Benedikt 'Über einige Azoverbindugnen'. *Ber. dt. chem. Ges.*, **Bd. 12:** 426-8.

Haveman, S.A., E.A. Greene, C.P. Stilwell, J.K. Voordouw, G. Voordouw (2004). Physiological and gene expression analysis of inhibition of *Desulfovibrio vulgaris* hildenborough by nitrite. *J Bacteriol* **186**: 7944–7950.

Hayatsu, M., K. Tago and M. Saito (2008). Various players in the nitrogen cycle: Diversity and functions of the microorganisms involved in nitrification and denitrification. *Soil Science and Plant Nutrition* **54**: 33–45.

Hentschel, U., J. Hopke, M. Horn, A. B. Friedrich, M. Wagner, J. Hacker, and B. S. Moore (2002). Molecular evidence for a uniform microbial community in sponges from different oceans. *Appl Environ Microbiol* **68**: 4431-4440.

Holland, P.M., R.D. Abramson, R. Watson, D.H. Gelfand (1991). Detection of specific polymerase chain reaction product by utilizing the 59-39 exonuclease activity of *Thermus aquaticus* DNA polymerase. *Proc Natl Acad Sci USA* **88**: 7276–7280.

Holmes, A.J., N.A. Tujula, M. Holley, A. Contos, J.M. James, P.Rogers, and M.R. Gillings (2001). Phylogenetic structure of unusual aquatic microbial formations in Nullarbor caves, Australia. *Environ Microbiol* **3**: 256-264.

Hunik, J.H., H.J.G. Meijer, and J. Tramper (1993). Kinetics of Nitrobacter agilis at extreme substrate, product and salt concentrations. *Appl Microbiol Biotech* **40**: 442-448.

Iki, T., T. Aono and H. Oyaizu (2007). Evidence for functional differentiation of duplicated nifh genes in azorhizobium caulinodans. *FEMS Microbiol Lett* **274**(2): 173-9.

Jetten, M.S. (2008). The microbial nitrogen cycle. *Environ Microbiol* **10**(11): 2903-9.

Jetten, M.S., M. Strous, K.T. van de Pas-Schoonen, J. Schalk, U. G. van Dongen, A.A. van de Graaf, S. Logemann, G. Muyzer, M.C. van Loosdrecht and J.G. Kuenen (1998). The anaerobic oxidation of ammonium. *FEMS Microbiol Rev* **22**(5): 421-37.

Juretschko, S., G. Timmermann, M. Schmid, K.H. Schleifer, A. Pommerening-Roser, H.P. Koops and M. Wagner (1998). Combined molecular and conventional analyses of nitrifying bacterium diversity in activated sludge: Nitrosococcus mobilis and nitrospira-like bacteria as dominant populations. *Appl Environ Microbiol* **64**(8): 3042-51.

Kibbe, W.A. (2007). 'OligoCalc: an online oligonucleotide properties calculator'. *Nucleic Acids Res* **35.**

Kikuchi, H., M. Aichi, I. Suzuki, and T. Omata (1996). Positive regulation by nitrite of the nitrate assimilation operon in the cyanobacteria *Synechococcus sp.* strain PCC 7942 and *Plectonema boryanum*. *J Bacteriol* **178**: 5822–5825.

Kirstein, K. and E. Bock (1993). Close genetic relationship between nitrobacter hamburgensis nitrite oxidoreductase and escherichia coli nitrate reductases. *Arch Microbiol* **160**(6): 447-53.

Kneip, C., P. Lockhart, C. Voss and U.G. Maier (2007). Nitrogen fixation in eukaryotes--new models for symbiosis. *BMC Evol Biol* **7**: 55.

Koch, H. (2009). Ecophysiological investigation of nitrite-oxidizing bacteria of the genus *Nitrospira*. Diploma thesis.

Könneke, M., A.E. Bernhard, J.R. de la Torre, C.B. Walker, J.B. Waterbury and D.A. Stahl (2005). Isolation of an autotrophic ammonia-oxidizing marine archaeon. *Nature* **437**(7058): 543-6.

Koonin, E.V. (2005). Orthologs, paralogs and evolutionary genomics. *Annu Rev Genet* **39**: 309–338.

Lebedeva, E.V., M. Alawi, C. Fiencke, B. Namsaraev, E. Bock and E. Spieck (2005). Moderately thermophilic nitrifying bacteria from a hot spring of the baikal rift zone. *FEMS Microbiol Ecol* **54**(2): 297-306.

References

Lebedeva, E.V., M. Alawi, F. Maixner, P.G. Jozsa, H. Daims and E. Spieck (2008). Physiological and phylogenetic characterization of a novel lithoautotrophic nitrite-oxidizing bacterium, 'candidatus nitrospira bockiana'. *Int J Syst Evol Microbiol* **58**(Pt 1): 242-50.

Lebedeva, E.V., S. Off, S. Zumbrägel, M. Kruse, A. Shagzhina, S. Lücker, F. Maixner, A. Lipski, H. Daims, E. Spieck (2011). Isolation and characterization of a moderately thermophilic nitrite-oxidizing bacterium from a geothermal spring. *FEMS Microbiol Ecol* **75**(2): 195-204.

Leininger, S., T. Urich, M. Schloter, L. Schwark, J. Qi, G. W. Nicol, J. I. Prosser, S. C. Schuster, C. Schleper (2006). Archaea predominate among ammonia-oxidizing prokaryotes in soils. *Nature* **442**:806-809.

Loy, A., F. Maixner, M. Wagner, M. Horn (2007). probeBase - an online resource for rRNA-targeted oligonucleotide probes: new features 2007. *Nucleic Acids Res* **35**: D800-D804.

Loy, A., R. Arnold, P. Tischler, T. Rattei, M. Wagner and M. Horn (2008). Probecheck--a central resource for evaluating oligonucleotide probe coverage and specificity. *Environ Microbiol* **10**(10): 2894-8.

Lücker, S., M. Wagner, F. Maixner, E. Pelletier, H. Koch, B. Vacherie, T. Rattei, J. S. Sinninghe Damsté, E. Spieck, D. Le Paslier, and H. Daims (2010). A *Nitrospira* metagenome illuminates the physiology and evolution of globally important nitrite-oxidizing bacteria. *Proc Natl Acad Sci U S A* **107**: 13479–13484.

Madigan, M.T., J.M. Martinko, J. Parker (1996). *Brock Biology of Microorganisms.* Prentice-Hall, Upper Saddle River, NJ, ed. 8.

Maixner, F., D.R. Noguera, B. Anneser, K. Stoecker, G. Wegl, M. Wagner and H. Daims (2006). Nitrite concentration influences the population structure of nitrospira-like bacteria. *Environ Microbiol* **8**(8): 1487-95.

Markham, N.R. and M. Zuker (2005). DINAMelt web server for nucleic acid melting prediction. *Nucleic Acids Res* **33**: 577–*W581*

Meincke, M., E. Bock, D. Kastrau and P.M.H. Kroneck (1992). Nitrite oxidoreductase from nitrobacter hamburgensis: Redox centers and their catalytic role. *Arch Microbiol* **158**: 127-131.

Monis, P.T., S. Giglio, and C.P. Saint (2004). Comparison of SYTO9 and SYBR Green I for real-time polymerase chain reaction and investigation of the effect of dye concentration on amplifcation and DNA melting curve analysis. *Analytical Biochemistry* **340**: 24–34.

Morgenroth, E., A. Obermayer, E. Arnold, A. Brühl, M. Wagner, and P.A. Wilderer (2000). Effect of long-term idle periods on the performance of sequencing batch reactors. *Water Sci Technol* **41**: 105–113.

Mulder, A., A.A. van de Graaf, L.A. Robertson, and J.G. Kuenen (1995). Anaerobic ammonium oxidation discovered in a denitrifying fluidized bed reactor. *FEMS Microbiol Ecol* **16**: 177–184.

Müller, A. (2008). Influence of wastewater composition and operational mode on the community structure of nitrifying bacteria in wastewater treatment plants. Diploma thesis.

Nelson, D. L., M. M. Cox (2005). Principles of biochemistry. 4th ed. New York: W.H. Freeman & Co

Nicol, G., S. Leininger, C. Schleper, and J. Prosser (2008). The influence of soil pH on the diversity, abundance and transcriptional activity of ammonia-oxidising archaea and bacteria. *Environ Microbiol* **10:** 2966–2978.

Nogueira, R. and L.F. Melo (2006). Competition between *Nitrospira* spp. and *Nitrobacter* spp. in nitrite-oxidizing bioreactors. *Biotechnol Bioeng* **95**(1): 169-75.

Nolan, T., R.E. Hands, S.A. Bustin (2006). Quantification of mRNA using real-time RT-PCR. *Nat Protoc* **1**: 1559–1582.

Okabe, S., H. Satoh, and Y. Watanabe (1999). *In situ* analysis of nitrifying biofilms as determined by *in situ* hybridization and the use of microelectrodes. *Appl Environ Microbiol* **65**: 3182-3191.

Olson, T. and A. Hooper (1983). Energy coupling in the bacterial oxidation of small molecules: An extracytoplasmic dehydrogenase in Nitrosomonas. *FEMS Microbiol* **19**: 47–50.

Park, H.D. and D.R. Noguera (2008). *Nitrospira* community composition in nitrifying reactors operated with two different dissolved oxygen levels. *J Microbiol Biotechnol* **18**: 1470-1474.

Prohl, C., B. Wackwitz, D. Vlad, and G. Unden (1998). Functional citric acid cycle in an arcA mutant of Escherichia coli during growth with nitrate under anoxic conditions. *Arch Microbiol* **170**: 1–7.

Prosser, J. I. (1989). Autotrophic nitrification in bacteria. *Adv Microb Physiol* **30**: 125-81.

Purkhold, U., A. Pommerening-Roser, S. Juretschko, M. C. Schmid, H. P. Koops and M. Wagner (2000). Phylogeny of all recognized species of ammonia oxidizers based on comparative 16S rRNA and amoA sequence analysis: Implications for molecular diversity surveys. *Appl Environ Microbiol* **66: 5368–5382**.

Radstrom, P., R. Knutsson, P. Wolffs, M. Lovenklev and C. Lofstrom (2004). Pre-PCR processing: strategies to generate PCR-compatible samples. *Mol Biotechnol* **26**: 133–146.

Rozen, S. and H.J. Skaletsky (2000). Primer3 on the WWW for general users and for biologist programmers. *Bioinformatics Methods and Protocols: Methods in Molecular Biology.* Humana Press, Totowa, NJ, 365-386

Saiki, R.K., D.H. Gelfand, S. Stoffel, S.J. Scharf, R. Higuchi, G.T. Horn, K.B. Mullis and H.A. Erlich (1988). Primer-directed enzymatic amplification of DNA with a thermostable DNA polymerase. *Science* **239**: 487-91.

Sanger, F., S. Nicklen and A.R. Coulson (1977). DNA sequencing with chain-terminating inhibitors. *Proc Natl Acad Sci U S A* **74**(12): 5463-7.

Santoro, A., C. Francis, N. de Sieyes, and A. Boehm (2008). Shifts in the relative abundance of ammonia-oxidizing bacteria and archaea across physicochemical gradients in a subterranean estuary. *Environ Microbiol* **10**: 1068–1079.

Schmittgen, T.D. and B.A. Zakrajsek (2000). Effect of experimental treatment on housekeeping gene expression: validation by real-time, quantitative RT-PCR. *J Biochem Biophys Methods* **46**: 69-81.

Schramm, A., D. De Beer, A. Gieseke and R. Amann (2000). Microenvironments and distribution of nitrifying bacteria in a membrane-bound biofilm. *Environ Microbiol* **2**(6): 680-6.

Schramm, A., D. de Beer, J.C. van den Heuvel, S. Ottengraf and R. Amann (1999). Microscale distribution of populations and activities of nitrosospira and nitrospira spp. Along a macroscale gradient in a nitrifying bioreactor: Quantification by in situ hybridization and the use of microsensors. *Appl Environ Microbiol* **65**(8): 3690-6.

Schramm, A., D. De Beer, M. Wagner and R. Amann (1998). Identification and activities in situ of nitrosospira and nitrospira spp. As dominant populations in a nitrifying fluidized bed reactor. *Appl Environ Microbiol* **64**(9): 3480-5.

Selinger, D.W., R.M. Saxena, K.J. Cheung, G.M. Church, C. Rosenow (2003). Global RNA half-life analysis in *Escherichia coli* reveals positional patterns of transcript degradation. *Genome Res* **13**: 216–223.

Shiba, H., T. Kawasumi, Y. Igarashi, T. Kodama, Y. Minoda (1985). The CO2 assimilation via the reductive tricarboxylic-acid cycle in an obligately autotrophic, aerobic hydrogenoxidizing bacterium, *Hydrogenobacter thermophilus*. *Arch Microbiol* **141**: 198–203.

Spang, A., R. Hatzenpichler, C. Brochier-Armanet, T. Rattei, P. Tischler, E. Spieck, W. Streit, D.A. Stahl, M. Wagner, and C. Schleper (2010). Distinct gene set in two different lineages of ammonia oxidizing archaea supports the phylum Thaumarchaeota. *Trends Microbiol* **18**: 331–340.

Spieck, E., C. Hartwig, I. McCormack, F. Maixner, M. Wagner, A. Lipski and H. Daims (2006). Selective enrichment and molecular characterization of a previously uncultured nitrospira-like bacterium from activated sludge. *Environ Microbiol* **8**(3): 405-15.

Spieck, E., J. Aamand, S. Bartosch and E. Bock (1996). Immunocytochemical detection and localization of the membrane-bound nitrite oxidoreductase in cells of nitrobacter and nitrospira. *FEMS Microbiol Lett* **139**: 71-76.

Spieck, E., S. Ehrich, J. Aamand and E. Bock (1998). Isolation and immunocytochemical location of the nitrite-oxidizing system in nitrospira moscoviensis. *Arch Microbiol* **169**(3): 225-30.

Starkenburg, S.R., P.S. Chain, L.A. Sayavedra-Soto, L. Hauser, M.L. Land, F.W. Larimer, S.A. Malfatti, M.G. Klotz, P.J. Bottomley, D.J. Arp and W.J. Hickey (2006). Genome sequence of the chemolithoautotrophic nitrite-oxidizing bacterium nitrobacter winogradskyi nb-255. *Appl Environ Microbiol* **72**(3): 2050-63.

Stöcker, K., C. Dorninger, H. Daims, and M. Wagner (2010). Double labeling of oligonucleotide probes for fluorescence *in situ* hybridization (DOPE–FISH) improves signal intensity and increases rRNA accessibility. *Appl Environ Microb* **76***: 922–926.

Strous, M., and M.S.M. Jetten (2004). Anaerobic oxidation of methane and ammonium. *Ann Rev Microbiol* **58**: 99–117.

Strous, M., J.A. Fuerst, E.H.M. Kramer, S. Logemann, G. Muyzer, K.T. van de Pas-Schoonen (1999). Missing lithotroph identified as new planctomycete. *Nature* **400**: 446–449.

Sundermeyer-Klinger, H., V. Meyer, B. Warninghoff, and E. Bock (1984). Membrane-bound nitrite oxidoreductase of Nitrobacter: evidence for a nitrate reductase system. *Arch Microbiol* **140**: 153–158.

Suzuki, M. T., L. T. Taylor and E. F. DeLong (2000). Quantitative analysis of small-subunit rRNA genes in mixed microbial populations via 5'-nuclease assays. *Appl Environ Microbiol* 66(11): 4605-4614.

Szymanski, M., M. Z. Barciszewska, V. A. Erdmann, J. Barciszewski (2002). 5S ribosomal RNA database. *Nucleic Acids Res* **30:** 176–178.

Teske, A., E. Alm, J. M. Regan, T. S., B. E. Rittmann, and D. A. Stahl (1994). Evolutionary relationships among ammonia- and nitrite-oxidizing bacteria. *J Bacteriol* **176**: 6623-6630.

Tourna, M., M. Stieglmeier, A. Spang, M. Könneke, A. Schintlmeister, T. Urich, M. Engel, M. Schloter, M. Wagner, A. Richter, C. Schleper (2011). *Nitrososphaera viennensis*, an ammonia oxidizing archaeon from soil. *Proc Natl Acad Sci U S A.* **108**(20):8420-5.

Vandesompele, J., K. De Preter, F. Pattyn, B. Poppe, N. Van Roy, A. De Paepe, and F. Speleman (2002). Accurate normalization of real-time quantitative RT-PCR data by geometric averaging of multiple internal control genes. *Genome Biol* **3**

von Wintzingerode, F., U. B. Gobel and E. Stackebrandt (1997). Determination of microbial diversity in environmental samples: pitfalls of PCR-based rRNA analysis. *FEMS Microbiol Rev* **21**(3):213-29.

Wagner, M., G. Rath, R. Amann, H.-P. Koops, and K.-H. Schleifer (1995). *In situ* identification of ammonia-oxidizing bacteria. *Syst Appl Microbiol* **18**: 251–264.

Wagner, M., M. Horn, and H. Daims (2003). Fluorescence *in situ* hybridisation for the identification and characterisation of prokaryotes. *Curr Opin Microbiol* **6**:302–309.

Watson, S.W., E. Bock, F.W. Valois, J.B. Waterbury and U. Schlosser (1986). *Nitrospira marina* gen. Nov. Sp. Nov.: A chemolithotrophic nitrite-oxidizing bacterium. *Arch of Microbiology* **144**: 1-7.

Winogradsky, S. (1890). Recherches sur les Organismes de la Nitrification. *Comp Rendu* **110**: 1013–1016.

Witter, C.T., M.G. Herrmann, A.A. Moss, and R.P. Rasmussen (1997). Continuous fluorescence monitoring of rapid cycle DNA amplification. *Biotechniques* **22:** 130–138.

Wong, M.L. and J.F. Medrano (2005). Real-time PCR for mRNA quantitation. *Biotechniques* **39**: 75–85

Wu, D.Y., L. Ugozzoli, B.K. Pal, J. Qian, and R.B. Wallace (1991). The effect of temperature and oligonucleotide primer length on the specificity and efficiency of amplification by the polymerase chain reaction. *DNA and Cell Biology* **10:** 233–238.

Yamamoto, M., H. Arai, M. Ishii, Y. Igarashi (2006). Role of two 2-oxoglutarate:ferredoxin oxidoreductases in *Hydrogenobacter thermophilus* under aerobic and anaerobic conditions. *FEMS Microbiol Lett* **263**: 189–193.

Yilmaz, L.S., H.E. Okten, and D.R. Noguera (2006). Making all parts of the 16S rRNA of *Escherichia coli* accessible in situ to single DNA oligonucleotides. *Appl Environ Microbiol* **72**: 733–744.

Zehr, J.P., E.J. Carpenter and T.A. Villareal (2000). New perspectives on nitrogen-fixing microorganisms in tropical and subtropical oceans. *Trends Microbiol* **8**: 68-73.

Zhang, C. L., Q. Ye, Z. Y. Huang, W. J. Li, J. Q. Chen, Z. Q. Song, W. D. Zhao, C. Bagwell, W. P. Inskeep, C. Ross (2008). Global occurrenceof archaeal *amoA* genes in terrestrial hot springs. *Appl Environ Microbiol* **74**: 6417-6426.

I. <u>Acknowledgements</u>

Finally, I want to thank the following people:

Univ.-Prof. Mag. Dr. Michael Wagner for awaking my interest in microbial ecology and giving me the opportunity to write my diploma thesis in his department.

Univ.-Ass. Dipl.-Biol. Dr. Holger Daims for all the lectures, seminars and other courses awaking my interest for this subject during the last years and for making me a member of his working group.

Chrissy and **Hanna** for being my supervisors during my diploma thesis and previously during my "Großpraktikum", for taking time for all of my questions, for patiently discussing my issues and for all the fun we had.

Sascha Galushko for the great help with the incubations and calculations.

Karin for being my "third" supervisor

Roland, **Faris** and **Jan** for answering all my questions.

All DOME-members for a great working atmosphere, the interesting discussions and all the fun.

Mariella and Max for sharing with me the ups and downs of my diploma thesis.

Katrin and Steffi for the funny and instructive time during the last six years.

And most of all I want to thank **my parents** and **family** for supporting me all the time and giving me the opportunity to make my first steps in the big wide world of biology.

J. <u>Curriculum vitae</u>

Domenico Franco Savio

Personal data

Date of birth	April 21, 1986
Place of birth	Steyr, Austria
Citizenship	Austria

Education

1992-1996	Volksschule Tabor, 4400 Steyr, Austria
1996-2000	Bundesrealgymnasium Steyr, 4400 Steyr, Austria
2000-2005	Handelsakademie Steyr, 4400 Steyr, Austria
since 2005	Study of biology with focus on ecology at the University of Vienna
since May 2010	Diploma thesis at the Department of Microbial Ecology, Vienna Ecology Center, University of Vienna.